



Westinghouse Electric Corporation

Power Systems

PWR Systems Division

Box 355
Pittsburgh Pennsylvania 15230

August 26, 1977

NS-CE-1532

Mr. John F. Stoltz, Chief
Light Water Reactors Branch No. 1
Division of Project Management
Office of Nuclear Reactor Regulation
U. S. Nuclear Regulatory Commission
Washington, D.C. 20555

Dear Mr. Stoltz:

Enclosed are twenty (20) copies of Westinghouse Nuclear Energy Systems Class 3 Report WCAP-9130 entitled, "Analysis of Reactor Coolant System for Postulated Loss-of-Coolant Accident: Indian Point 3 Nuclear Power Plant".

This report is the Westinghouse Proprietary Class 3 version of the Class 2 WCAP-9117 of the same title, which was transmitted to Mr. Victor Stello by Westinghouse letter NS-CE-1460, June 15, 1977.

This information is being submitted in response to the request of the Commission in connection with the Commission's review of the reactor pressure vessel supports analysis for Indian Point 3.

In accordance with your policy relating to Westinghouse reports, the enclosed report may receive unlimited distribution. We expect that this non-proprietary report will be placed in the Public Document Room and identified as a Westinghouse Topical Report.

Very truly yours,

WESTINGHOUSE ELECTRIC CORPORATION

C. Eicheldinger

C. Eicheldinger, Manager
Nuclear Safety Department

J.P. Bandstra/jm

8110300153 770630
PDR ADOCK 05000286
B PDR

WESTINGHOUSE CLASS 3

WCAP-9130

ANALYSIS OF REACTOR COOLANT SYSTEM FOR
POSTULATED LOSS-OF-COOLANT ACCIDENT:
INDIAN POINT 3 NUCLEAR POWER PLANT

June 1977

Prepared for:

Consolidated Edison Company of New York, Inc.
and
The Power Authority of the State of New York

This entire report is CONFIDENTIAL in Accordance with
Article 18, Paragraph B of the 1971 Reformulated Contract
between Westinghouse and Consolidated Edison of New York, Inc.

APPROVED:



R. L. Cloud, Manager
Mechanics & Materials Technology

APPROVED:



C. Eicheldinger, Manager
Nuclear Safety Department

WESTINGHOUSE ELECTRIC CORPORATION
Nuclear Energy Systems
P. O. Box 355
Pittsburgh, Pennsylvania 15230

PROP

TABLE OF CONTENTS

Section	Title	Page
1	INTRODUCTION	1-1
	1-1. General Description of the System	1-2
2	SUMMARY AND CONCLUSIONS	2-1
3	REACTOR PRESSURE VESSEL LOCA ANALYSIS	3-1
	3-1. Loads Applied to Reactor Vessel	3-1
	3-2. Reactor Coolant Loop Mechanical Loads	3-3
	3-3. Reactor Pressure Vessel Internal Hydraulic Loads	3-5
	3-4. Vertical Loads	3-9
	3-5. Horizontal Loads	3-9
	3-6. Reactor Cavity Pressurization Loads	3-17
	3-7. Method of Determining the Reactor Cavity Loads	3-17
	3-8. Reactor Coolant Loop Piping and Supports Static Analysis	3-60
	3-9. Purpose of Analysis	3-60
	3-10. General Description of Method	3-60
	3-11. Description of Model	3-60
	3-12. Results	3-81
	3-13. Test Results — Reactor Support Shoes	3-82
	3-14. Reactor Pressure Vessel Dynamic Analysis	3-82
	3-15. Mathematical Model and Method	3-82
	3-16. Reactor Pressure Vessel LOCA Analysis	3-88
	3-17. Displacements and Loads	3-89
	3-18. Postulated RPV Inlet Nozzle Break	3-89

WESTINGHOUSE PROPRIETARY CLASS 2

TABLE OF CONTENTS (cont)

Section	Title	Page
	3-19. Postulated RPV Outlet Nozzle Break	3-97
	3-20. Postulated RCP Outlet Nozzle Break	3-97
4	EVALUATION OF SYSTEM	4-1
	4-1. Evaluation Criteria	4-1
	4-2. Reactor Core	4-1
	4-3. Internals	4-1
	4-4. Piping	4-2
	4-5. Components	4-2
	4-6. Component Supports	4-2
	4-7. Concrete	4-2
	4-8. Reactor Coolant Loop Piping Evaluation	4-2
	4-9. Support Structure Evaluation	4-4
	4-10. Auxiliary Branch Lines	4-7
	4-11. Loads on Reactor Coolant System Components	4-10
	4-12. Control Rod Drive Mechanism	4-13
	4-13. Reactor Core	4-19
	4-14. Reactor Internals	4-23
	4-15. Primary Shield Wall Evaluation	4-24
5	PLANT MODIFICATION	5-1
	5-1. Plant Modification	5-1
	5-2. Primary Shield Wall Pipe Restraints	5-1
	5-3. Reactor Vessel Nozzle Inspection Openings	5-1
6	REFERENCES	6-1
Appendix A	Break Opening Area Calculation	A-1
Appendix B	Indian Point Reactor Support Shoe Test	B-1
Appendix C	Plant General Arrangement Drawings	C-1
Appendix D	Discussion of Procedure used for Reactor Coolant Loop Evaluation	D-1

WESTINGHOUSE PROPRIETARY CLASS 2

LIST OF ILLUSTRATIONS

Figure	Title	Page
1-1	Indian Point 3 Reactor Coolant System	1-3
1-2	Reactor Vessel and Internal Components	1-4
1-3	Schematic of Reactor Vessel Support Mechanism	1-5
1-4	Flow Diagram of Analysis Interfaces	1-6
3-1	Summary of Postulated Breaks	3-2
3-2	Coordinate Systems for Postulated Breaks	3-4
3-3	Wave Path for Depressurization Waves Entering RPV Inlet Nozzle (Cold Leg)	3-6
3-4	Wave Path for Depressurization Waves Entering RPV Outlet Nozzle (Hot Leg)	3-7
3-5	RPV Inlet Nozzle Safe End Break Horizontal Internal Hydraulic Force Applied to Reactor Core Barrel	3-10
3-6	RPV Inlet Nozzle Safe End Break Horizontal Internal Hydraulic Force Applied to Reactor Vessel	3-11
3-7	RPV Inlet Nozzle Safe End Break Vertical Internal Hydraulic Force Applied to Reactor Vessel	3-12
3-8	RPV Outlet Nozzle Safe End Break Horizontal Internal Hydraulic Force Applied to Reactor Core Barrel	3-13
3-9	RPV Outlet Nozzle Safe End Break Horizontal Hydraulic Force Applied to Reactor Vessel	3-14
3-10	RPV Outlet Nozzle Safe End Break Vertical Internal Hydraulic Force Applied to Reactor Vessel	3-15
3-11	Horizontal Force Calculation	3-16
3-12	RPV Inlet Nozzle Safe End Break Reactor Cavity Pressure Horizontal Force	3-18
3-13	RPV Inlet Nozzle Safe End Break Reactor Cavity Pressure Vertical Force	3-19
3-14	RPV Inlet Nozzle Safe End Break Reactor Cavity Pressure Moment	3-20

WESTINGHOUSE PROPRIETARY CLASS 2

LIST OF ILLUSTRATIONS (cont)

Figure	Title	Page
3-15	RPV Outlet Nozzle Safe End Break Reactor Cavity Pressure Horizontal Force	3-21
3-16	RPV Outlet Nozzle Safe End Break Reactor Cavity Pressure Vertical Force	3-22
3-17	RPV Outlet Nozzle Safe End Break Reactor Cavity Pressure Moment	3-23
3-18	Reactor Vessel Annulus Elements (Top View)	3-49
3-19	Reactor Vessel Annulus Elements	3-50
3-20	Reactor Vessel Annulus Elements (Side View)	3-51
3-21	Flow Path Network	3-52
3-22a	Pressure Time History for the Break Element (#1) 110 in ² Cold Leg Break	3-56
3-22b	Pressure Time History for a Reactor Vessel Annulus Element (#3) 110 in ² Cold Leg Break	3-57
3-23a	Pressure Time History for the Break Element (#1) 110 in ² Hot Leg Break	3-58
3-23b	Pressure Time History for a Reactor Vessel Annulus Element (#3) 110 in ² Hot Leg Break	3-59
3-24	Plan View of Steam Generator and Pump Support Model with Numbered Loops and Nodes	3-62
3-25	Plan View of Reactor Coolant Loop Model Showing Break Location	3-63
3-26	Reactor Coolant Loop Support Model (View A)	3-64
3-27	Reactor Coolant Loop Support Model (View B)	3-65
3-28	Reactor Coolant Loop Support Model (View C)	3-66
3-29	Model of RPV Outlet Nozzle Break Model Showing Break Location	3-67
3-30	Overall View of RPV Outlet Nozzle Break Model	3-68
3-31	Steam Generator and Reactor Coolant Pump Support Model (View A)	3-69
3-32	Steam Generator and Reactor Coolant Pump Support Model (View B)	3-70
3-33a	RCL Load vs. Deflection – RCL Cold Leg Break without Pipe Displacement Restraints	3-72
3-33b	RCL Load vs. Deflection – RCL Cold Leg Break with Pipe Displacement Restraints	3-73
3-34	RCL Load vs. Deflection – RCL Hot Leg Break with Pipe Displacement Restraints	3-74

WESTINGHOUSE PROPRIETARY CLASS 2

LIST OF ILLUSTRATIONS (cont)

Figure	Title	Page
3-35	Steam Generator Support Model	3-76
3-36	Steam Generator Shell/Upper Support Model	3-78
3-37	Reactor Coolant Pump Support Model	3-79
3-38	Vessel Support Test Load vs. Deflection	3-83
3-39	DARI Reactor Internals Model	3-85
3-40	Reactor Internals Mathematical Model for WOSTAS Variables	3-86
3-41	Displacement Coordinates and Support Pad Numbering Scheme	3-91
3-42	Nozzle/Vessel Centerline Horizontal Displacement: RPV Inlet Nozzle Break	3-92
3-43	Nozzle/Vessel Centerline Vertical Displacement: RPV Inlet Nozzle Break	3-93
3-44	Nozzle/Vessel Centerline Rotation: RPV Inlet Nozzle Break	3-94
3-45	Upper Core Plate Horizontal Motion: RPV Inlet Nozzle Break	3-95
3-46	Lower Core Plate Horizontal Motion: RPV Inlet Nozzle Break	3-96
3-47	Nozzle/Vessel Centerline Horizontal Displacement: RPV Outlet Nozzle Break	3-98
3-48	Nozzle/Vessel Centerline Vertical Displacement: RPV Outlet Nozzle Break	3-99
3-49	Nozzle/Vessel Centerline Rotation: RPV Outlet Nozzle Break	3-100
3-50	Upper Core Plate Horizontal Motion: RPV Outlet Nozzle Break	3-101
3-51	Lower Core Plate Horizontal Motion: RPV Outlet Nozzle Break	3-102
3-52	Nozzle/Vessel Centerline Horizontal Displacement: RCP Outlet Nozzle Break	3-103
3-53	Nozzle/Vessel Centerline Vertical Displacement: RCP Outlet Nozzle Break	3-104
3-54	Nozzle/Vessel Centerline Rotation: RCP Outlet Nozzle Break	3-105
3-55	Upper Core Plate Horizontal Motion: RCP Outlet Nozzle Break	3-106
3-56	Lower Core Plate Horizontal Motion: RCP Outlet Nozzle Break	3-107

LIST OF ILLUSTRATIONS (cont)

Figure	Title	Page
4-1	Accumulator Line Model X-Z Plane	4-8
4-2	Accumulator Line Model X-Y Plane	4-9
4-3	RHR Line Model X-Z Plane	4-11
4-4	RHR Line Model	4-12
4-5	Detail of Control Rod Drive Mechanism	4-14
4-6	Non-linear Model of the CRDM's, Support Platform, Reactor Vessel, and Internals	4-15
4-7	Non-linear Model of the CRDM's, Support Platform, Reactor Vessel, and Internals	4-16
4-8	Schematic Representation of Reactor Core Model	4-20
4-9	Deformed Grid	4-22
4-10	Primary Shield Wall Structural Model	4-25
5-1	Pipe Displacement Restraints	5-2
B-1	Test Support Structure	B-4
B-2	Horizontal Load – Horizontal Displacement Curve (LVDT No. 3) RVSS Test of B-7 Specimen with Vertical Preload of 20,000 lbs. at 550°F Pad Temperature	B-5
B-3	Fracture of Shoe – Test B-8	B-6

WESTINGHOUSE PROPRIETARY CLASS 2

LIST OF TABLES

Table	Title	Page
3-1	RCL Mechanical Loads	3-3
3-2	Volumes – Cold Leg	3-25
3-3	Flow Path Data – Cold Leg Break	3-27
3-4	Volumes – Hot Leg Break	3-31
3-5	Flow Path Data – Hot Leg Break	3-33
3-6	Mass and Energy Release Rates – 110-Square-inch Cold Leg Break	3-37
3-7	Mass and Energy Release Rates – 110-Square-inch Hot Leg Break	3-43
3-8	Peak Pressure and Time of Peak Pressures – 110-Square-inch Cold Leg Break	3-54
3-9	Peak Pressures and Time of Peak Pressure – 110-Square-inch Hot Leg Break	3-55
3-10	Maximum RPV Displacements	3-90
3-11	Maximum RPV Support Loads	3-90
4-1	Summary of Maximum Steam Generator Support Stresses	4-5
4-2	Summary of Maximum RCP Support Stresses	4-6
4-3	Head Adapter Moment Loads	4-19
B-1	Test Conditions and Results	B-3
B-2	Horizontal Load – Horizontal Displacement Curve (LVDT No. 3) RVSS Test of B-7 Specimen with Vertical Preload of 20,000 lbs. at 550°F Pad Temperature	B-5

ABSTRACT

During a postulated pipe rupture in the reactor coolant system of a nuclear power plant, various forces are applied to the reactor coolant system components. The applied forces produce loads and displacements in the components which must be analyzed to verify the capability of the plant to attain a safe and orderly shutdown from its normal operating condition. Pipe rupture analyses are presented in this report for the reactor coolant system of Indian Point 3 Nuclear Power Plant. Three pipe rupture locations were considered: 1) reactor pressure vessel inlet nozzle terminal end; 2) reactor pressure vessel outlet nozzle terminal end; and 3) reactor coolant pump outlet nozzle terminal end. The analyses include all the loads which result from the postulated ruptures. Specifically, cavity pressurization loads, internals reaction forces, and loop mechanical loads are included. The effect of proposed plant modifications which significantly reduce the severity of the pipe ruptures are included. The methods and results of the structural analyses of the reactor coolant system are presented, as are the evaluations of the components required to assure a safe shutdown of the plant.

The reactor coolant loop was analyzed for the combined effect of vessel motion and loop depressurization forces. An analysis was performed that included evaluation of the piping stresses, component support loads, and component nozzle loads. The piping stresses were shown to be acceptable. The loads on the reactor coolant pump and steam generator supports were used to calculate stresses in the support members. The stresses were all found to be acceptable. The loads and deformation induced in the reactor vessel supports were compared to results of scale model tests on the vessel supports and were shown not to cause support failure. The loads on the component nozzles and support attachment points, specifically on the steam generator, reactor coolant pump, and vessel, were evaluated and the resulting stresses are acceptable. The motion of the reactor coolant loop piping was used in an evaluation of the most highly stressed ECCS lines attached to the loop. The stresses are all acceptable. The CRDMs, internals, and the fuel were all analyzed in a time history manner using the motion of the reactor vessel and the internals. The stresses in the CRDMs and internals were shown to be acceptable. The reactor core evaluation indicated that fuel grids in the periphery of the core may experience permanent deformation, but the localized deformation does not affect the ability of the core to be cooled.

The conclusion of the analyses performed for Indian Point 3 Nuclear Power Plant is that the plant with the proposed modifications can be safely shutdown and maintained in a safe condition in the unlikely event the postulated pipe ruptures.

ACKNOWLEDGMENTS

This work was performed by Westinghouse under the direction of T. C. Esselman and D. F. Miller. The following persons were instrumental in the completion of the analysis and the report: J. P. Bandstra, L. C. Smith, H. L. Ott, W. T. Bogard, L. R. Wood, K. E. Juell, M. R. Patel, R. E. Kelly, G. R. Ellis, C. W. Gay, F. Loceff, A. J. Kuenzel, L. T. Gesinski, V. J. Esposito, R. J. Skwarek, A. J. Burnett, D. S. Nixdorf. The effort of C. E. Brown in the final issuance of the report is appreciated. The effort and coordination by E. Burke and D. Gaynor of Consolidated Edison was important in the completion of the task. United Engineers and Constructors performed the evaluation of the concrete structures.

SECTION 1

INTRODUCTION

The original evaluations of the reactor coolant system (RCS) of Indian Point 3 had demonstrated the safe shutdown capability of the plant with margin remaining. The analyses, however, did not include the effect of loads from asymmetric reactor pressurization. This loading condition has recently been found to be a significant loading on the reactor pressure vessel (RPV), and occurs for pipe ruptures postulated at the RPV nozzle safe end location. The additional loads lead to increased reactor vessel displacements which affect the entire reactor coolant system evaluation. To assure the safety of the plant, LOCA analyses of the reactor coolant system were begun to verify that the plant could attain a safe shutdown condition following a pipe rupture postulated at the most severe locations: RPV inlet nozzle, RPV outlet nozzle and pump outlet nozzle.

This report presents the evaluation of the reactor coolant system (RCS) for the loads induced by a loss-of-coolant accident (LOCA) which results from the unlikely event of a pipe rupture within that system. The objective of the evaluation is to verify the capability of the plant to reach and maintain a safe shutdown condition following the event. As a result of the postulated pipe rupture, the reactor coolant system depressurizes and thermal-hydraulic loads are applied to the system piping and components. The analyses include all loads in the system among which are the asymmetric loads in the reactor internals and the reactor cavity pressurization loads for the RPV nozzle break locations, and the effect of any inelastic structural response.

[] b,c

The results and conclusions from the analyses are presented in section 2. The methods used in the RPV blowdown analysis are described in section 3. The evaluations of the reactor coolant system components which insure the plant's safe shutdown capability are presented in section 4. Plant modifications which will be implemented to reduce the severity of the postulated pipe ruptures and thereby provide additional margin in plant safety are discussed in section 5. The modifications include the addition of pipe displacement restraints and alterations in the RPV nozzle inspection opening design. Changes in the RPV nozzle inspection opening design provide earlier venting of the reactor cavity which reduces the magnitude of the cavity pressure loads. Pipe displacement restraints limit the break opening area for postulated pipe ruptures at the reactor vessel safe end locations and significantly reduces the loads applied to the

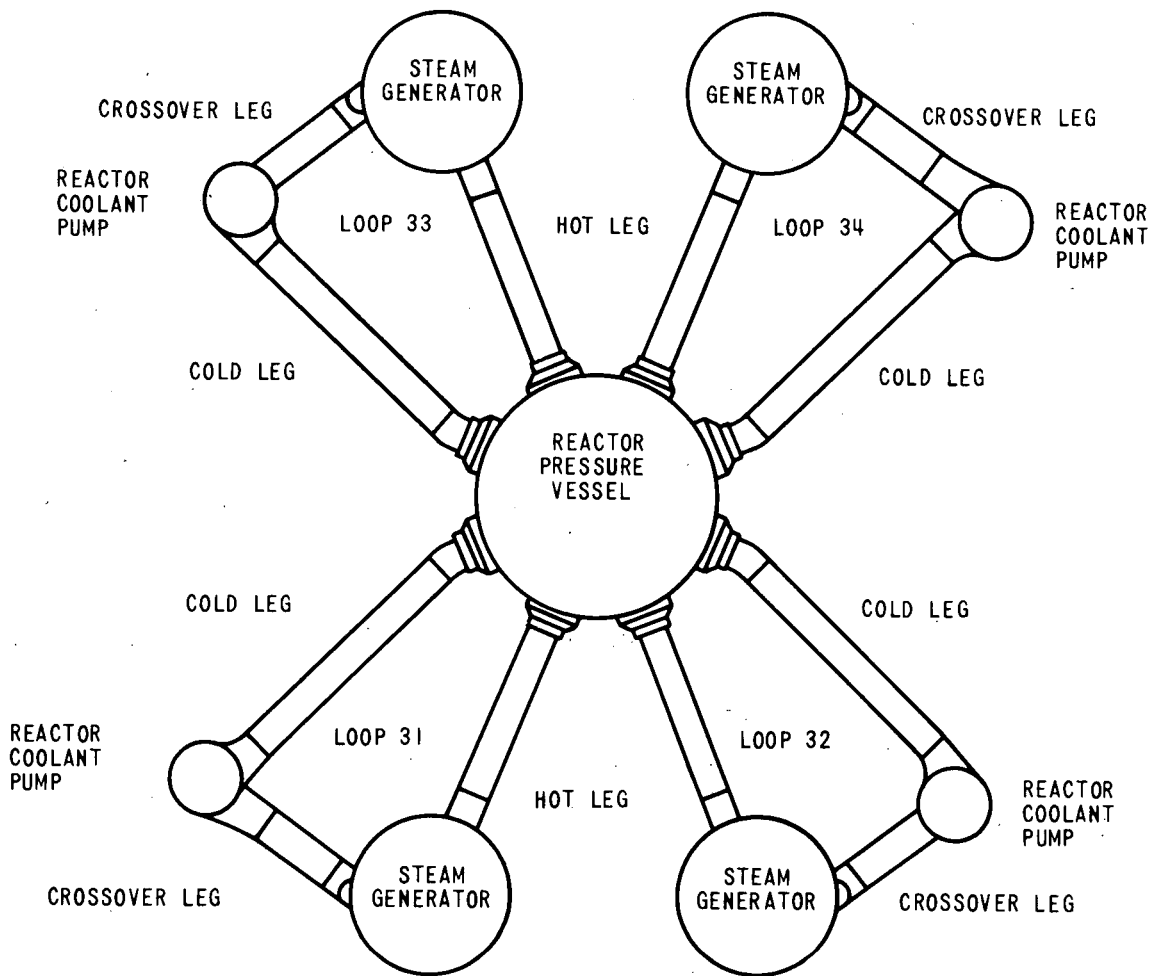
reactor pressure vessel (RPV). In addition, the restraints around the unbroken RPV nozzles constrain RPV motion. The analyses presented in this report include these plant modifications.

To understand the response of the reactor coolant system (RCS) during a postulated LOCA, one must have a general knowledge of the configuration and function of the system components. A brief discussion of the RCS follows.

1-1. GENERAL DESCRIPTION OF THE SYSTEM

The physical system for which the evaluation is performed is called the reactor coolant system (figure 1-1). This general term includes the components, piping, and supports necessary to operate and cool the reactor pressure vessel (RPV). The reactor pressure vessel contains the reactor core and internals needed to direct flow and structurally support the core. The general configuration of the reactor pressure vessel is shown in figure 1-2. Control rod drive mechanisms are attached to the upper vessel head and control the motion of the control rods and thus the reactor power level. Four reactor coolant loops, each consisting of large diameter stainless steel piping, a steam generator, a reactor coolant pump, and attached auxiliary piping are attached to the reactor vessel. The reactor coolant flows up through the middle of the vessel (inside the barrel), out to the hot leg piping, up and down the steam generator, through the crossover leg piping, through the pump and cold leg, and finally down the vessel between the vessel and barrel (downcomer annulus). Each steam generator and reactor coolant pump is supported by a redundant system of welded columns and beams. The steam generator is attached to the support at the bottom of the generator feet and at the top below the transition cone region. Snubbers connect the support structure to the concrete. In addition to the box-like support, the reactor coolant pump is restrained by tie rods. All the supports allow for unrestricted thermal expansion and are designed to take load if motion occurs in addition to the thermal growth. The reactor vessel is supported by four vessel supports beneath alternate reactor vessel nozzles. These supports allow for radial expansion, but resist any tangential motion and provide non-linear resistance in the vertical direction in that they resist downward but not upward motion. The support shoe is bolted to a water cooled plate and welded to a ring girder which is embedded in the shield wall concrete (figure 1-3). The pipe displacement restraints to be added in each shield wall penetration are cylindrical steel plates which surround the primary pipe and have longitudinal bars attached. The bars, after closing a gap, butt up against the shield wall pipe sleeve and restrict RPV motion. For pipe rupture postulated at the RPV safe end locations, the restraints limit the displacements of the broken pipe ends and, thus reduce the break opening area available for release of primary coolant fluid.

The following section presents a summary of the analysis results. Figure 1-4 presents a flow diagram of the analysis interface arrangements.



Note: RPV supports are situated beneath the cold leg nozzles of Loops 31 and 34 and beneath the hot leg nozzles of Loops 32 and 33.

Figure 1-1. Indian Point 3 Reactor Coolant System

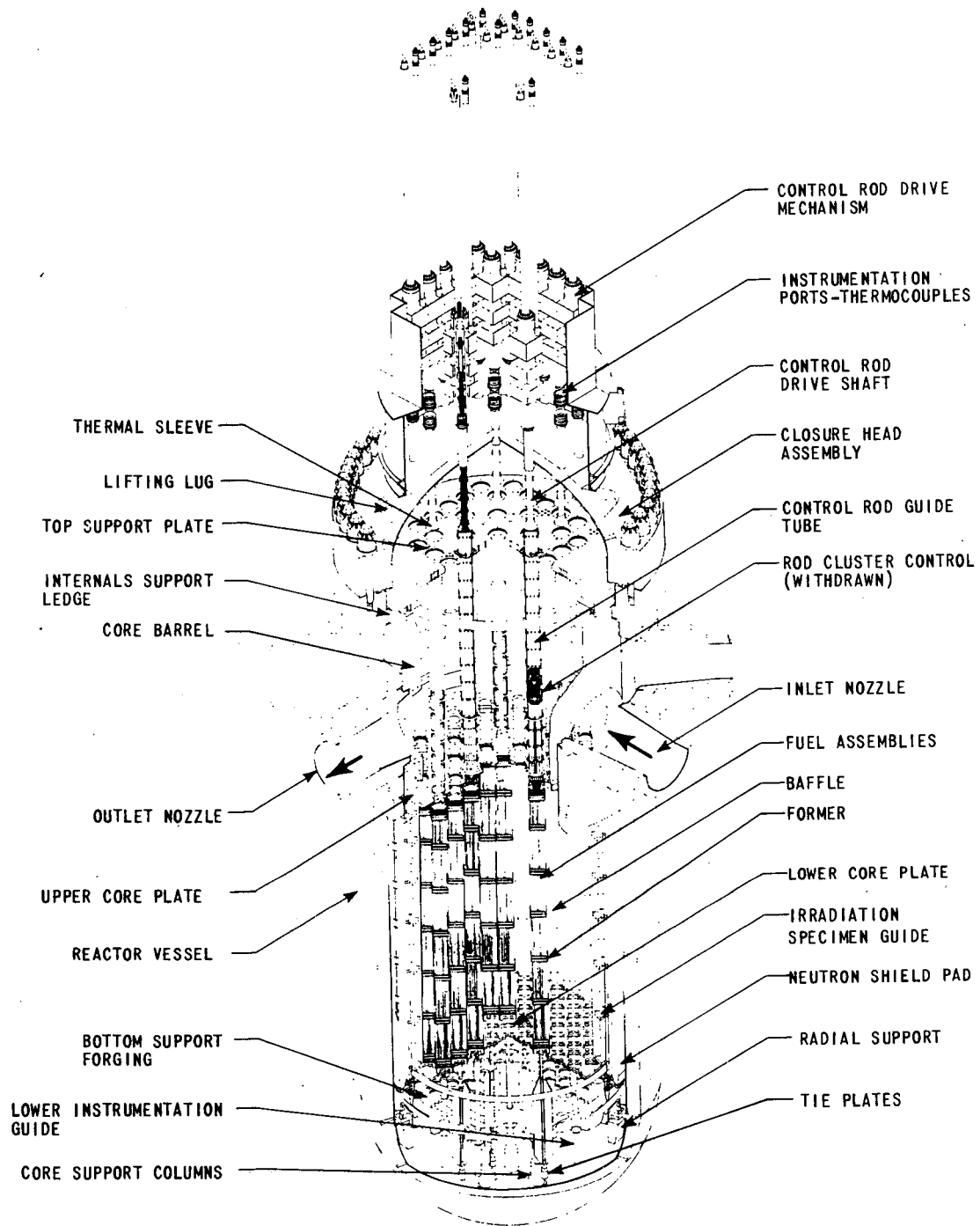


Figure 1-2. Reactor Vessel and Internal Components

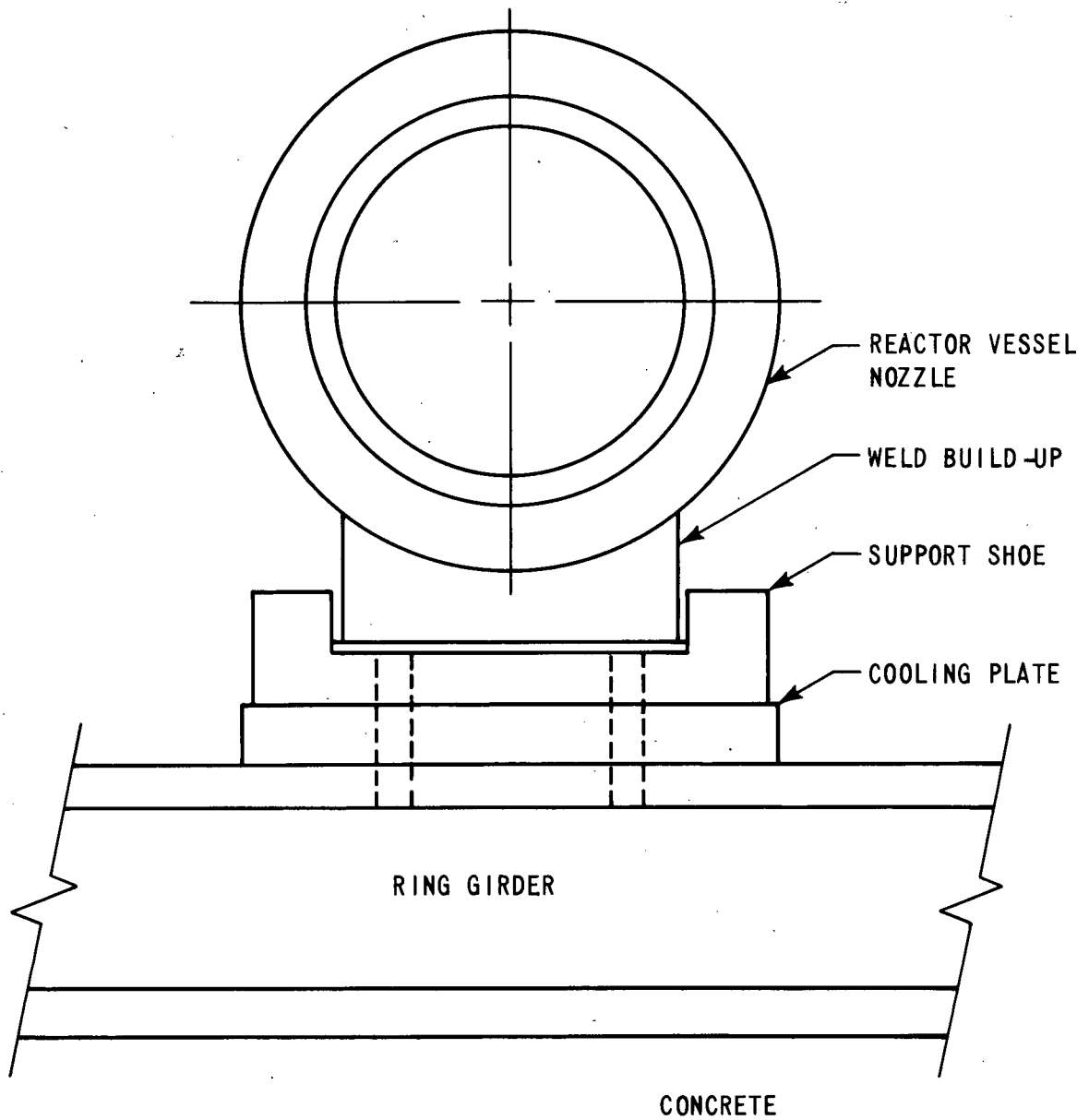


Figure 1-3. Schematic of Reactor Vessel Support Mechanism

Figure 1-4. Flow Diagram of Analysis Interfaces



SECTION 2

SUMMARY AND CONCLUSIONS

The reactor coolant system of Indian Point 3 Nuclear Power Plant was analyzed for postulated pipe ruptures at the following locations: 1) RPV inlet nozzle safe end; 2) RPV outlet nozzle safe end; and 3) RCP outlet nozzle terminal end. These pipe rupture locations produced the most severe loadings on the reactor pressure vessel and have the most severe consequences upon the structures required to assure plant safety. Thus, verifying the plant safety for these pipe ruptures assures that pipe rupture at other locations will cause no safety problems. The analyses described in this report include the effect of modifications to the plant which reduce the severity of the postulated event. The most significant change is the addition of pipe displacement restraints in each primary shield wall pipe annulus. These restraints limit the break opening area for pipe ruptures postulated at the reactor vessel safe end locations and provide resistance to RPV motion. Modifications to the RPV nozzle inspection openings design provide earlier venting of the reactor cavity and thus reduce the reactor cavity pressurization loads.

All the loads that would be applied to the reactor coolant system as a result of the accident were included in the analysis.

The break area considered in calculating the transient responses was 110 square inches for the vessel safe end locations. This area was determined to be the maximum possible and is conservative. The maximum possible break opening area at the pump outlet nozzle is twice the cross-sectional flow area of the primary piping. These areas were used to generate the applied loads. Loads were calculated using various computer codes. The cavity pressure loads were calculated using the TMD code,¹ the internals hydraulic loads were calculated using the MULTIFLEX code,² and the loop mechanical loads were calculated with the piping code WEST-DYN7.³ The MULTIFLEX code included the effects of fluid-solid interaction by consideration of the flexibility of the core barrel.

The loads or forcing functions were applied simultaneously in a time-history manner to a mathematical model of the reactor vessel and internals. The model of the reactor vessel and internals was formulated using DARIWOSTAS⁴ computer code and consists of beam elements, springs, masses, dampers, gap elements for non-linear modeling, sliders, and other specialized elements. The vessel restraints, coming from the reactor vessel supports and the attached reactor coolant loops, were represented as non-linear stiffnesses at the proper location on the vessel. The reactor vessel support stiffnesses included the results of tests performed on scale

models of the support mechanism. The reactor coolant loop stiffness matrices were obtained from a detailed finite element model of the loop components. A time-history analysis was performed with DARIWOSTAS code, which resulted in a determination of the motion of the vessel, motion of the internals, and loads in the vessel supports. The loads in the supports were used directly to analyze the adequacy of support. The displacements of the vessel and internals were subsequently used in more detailed analyses of the various components of the reactor coolant system.

[] b,c

The reactor coolant loop was analyzed for the combined effect of vessel motion and loop depressurization forces using the WECAN code.⁵ An analysis was performed that included evaluation of the piping stresses, component support loads, and component nozzle loads. The piping stresses were shown to be acceptable. The loads on the reactor coolant pump and steam generator supports were used to calculate stresses in the support members. The stresses were all found to be acceptable. The loads and deformation induced in the reactor vessel supports were compared to results of scale model tests on the vessel supports and were shown not to cause support failure. The loads on the component nozzles and support attachment points, specifically on the steam generator, reactor coolant pump, and vessel, were evaluated and the resulting stresses are acceptable. The motion of the reactor coolant loop piping was used in an evaluation of the most highly stressed ECCS lines attached to the loop. The stresses were all acceptable. The CRDMs, internals, and the fuel were all analyzed in a time history manner using the motion of the reactor vessel and the internals. The stresses in the CRDMs and internals were shown to be acceptable. The reactor core evaluation indicated that fuel grids in the periphery of the core may experience permanent deformation, and it is shown that this localized deformation does not affect the ability of the core to be cooled.

The conclusion of the analyses performed for Indian Point 3 Nuclear Power Plant is that the plant with the proposed modifications can be safely shutdown and maintained in a safe condition in the unlikely event the postulated pipe ruptures.

SECTION 3

REACTOR PRESSURE VESSEL LOCA ANALYSIS

Figure 3-1 shows the three postulated breaks considered in the evaluation of the reactor coolant system. They are, specifically, the pipe break at the vessel inlet nozzle, the vessel outlet nozzle and the reactor coolant pump discharge nozzle.

Time history loads are exerted on the reactor coolant system due to the hydraulic pressure transients which accompany a Loss of Coolant Accident (LOCA). Since RPV displacements are caused by these pressure transients, and the transients vary with the size of a pipe break, the pipe break opening area must be calculated to determine RPV displacements. This is done by using conservative approximations for primary equipment motion to determine relative axial and lateral displacements of the broken pipe ends. Worst case primary equipment motions are used in the calculations, as well as the influence of pipe displacement restraints on pipe motions. Using geometrical relationships, the relative pipe end motions are used to calculate a break opening area for the postulated RPV safe end break locations. The methods used to calculate break opening area are presented in Appendix A. The break size calculated for RPV nozzle break locations is 110 square inches, which takes into account the size-limiting effect of pipe restraints (see section 5) in the primary shield wall annulus around the primary coolant piping. The postulated break at the RCP outlet nozzle is assumed to have a break opening area equivalent to twice the pipe cross-sectional flow area.

3-1. LOADS APPLIED TO REACTOR VESSEL

Following a postulated pipe rupture, forces are imposed on the reactor vessel and its internals. These forces result from the release of the pressurized primary system's coolant and, for guillotine pipe breaks, from the disturbance of the mechanical equilibrium in the piping system prior to the rupture. The release of pressurized coolant results in travelling depressurization waves in the primary system. These depressurization waves are characterized by a wavefront with high pressure on the leading side of the wavefront and lower pressure on the following side. The wavefront translates and reflects throughout the primary system until the system is completely depressurized. The rapid depressurization results in transient hydraulic loads on the mechanical equipment of the system.

The release of coolant resulting from a postulated RPV nozzle break also results in a pressure increase in the region surrounding the postulated break. Pressurization occurs rapidly in the cavity around the reactor vessel; this can exert an asymmetric force on the outside of the vessel.

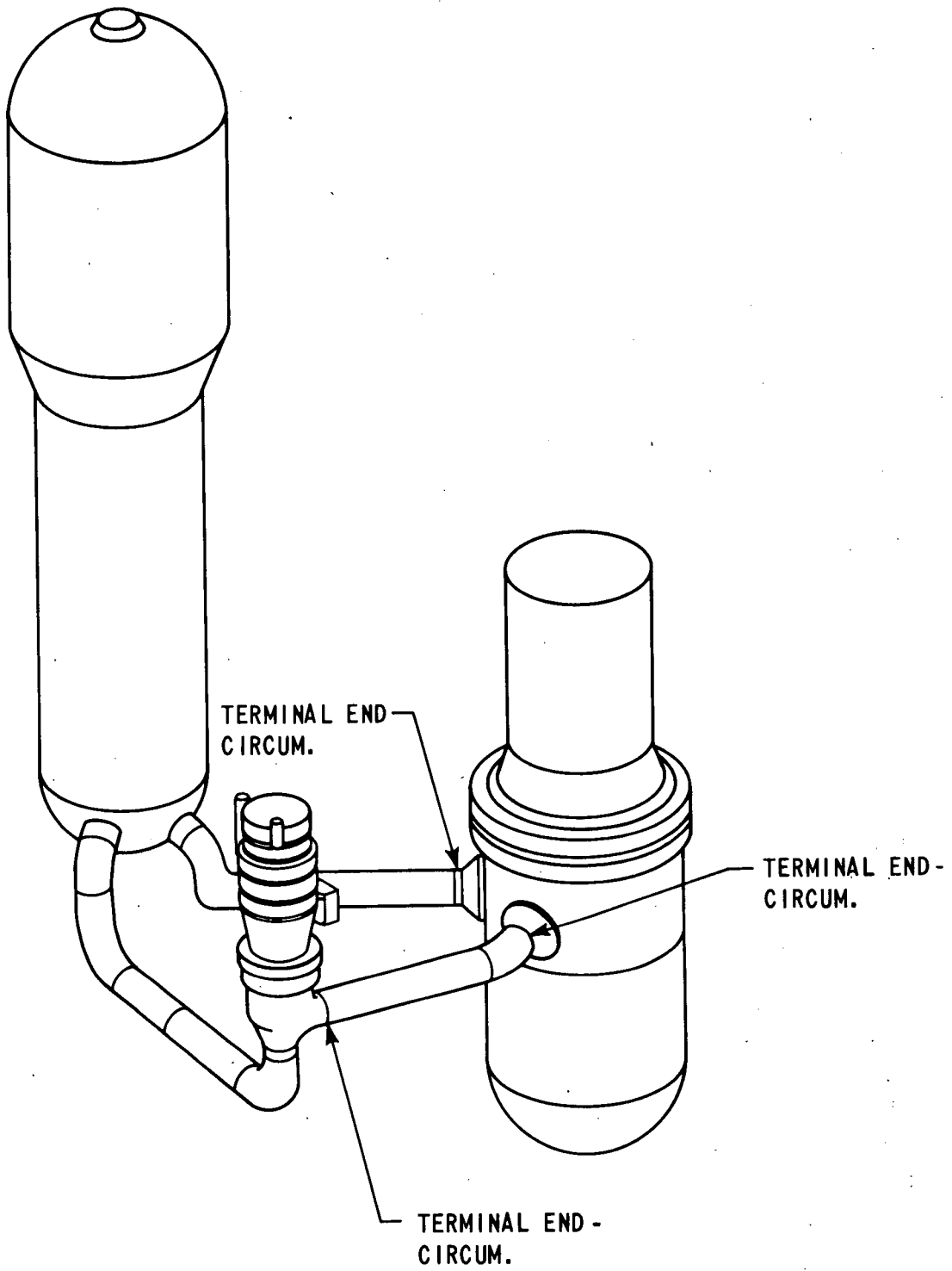


Figure 3-1. Summary of Postulated Breaks

The loads on the RPV and internals that result from the depressurization of the system and from the pressurization of the area around the break may be characterized as (1) reactor coolant loop mechanical loads, (2) reactor internal hydraulic loads (vertical and horizontal), and (3) RPV cavity pressurization loads (only for breaks at the reactor vessel safe end locations).

All the loads are calculated individually and combined in a time history manner. The analytical methods used for the calculations are discussed in the following paragraphs.

3-2. Reactor Coolant Loop Mechanical Loads

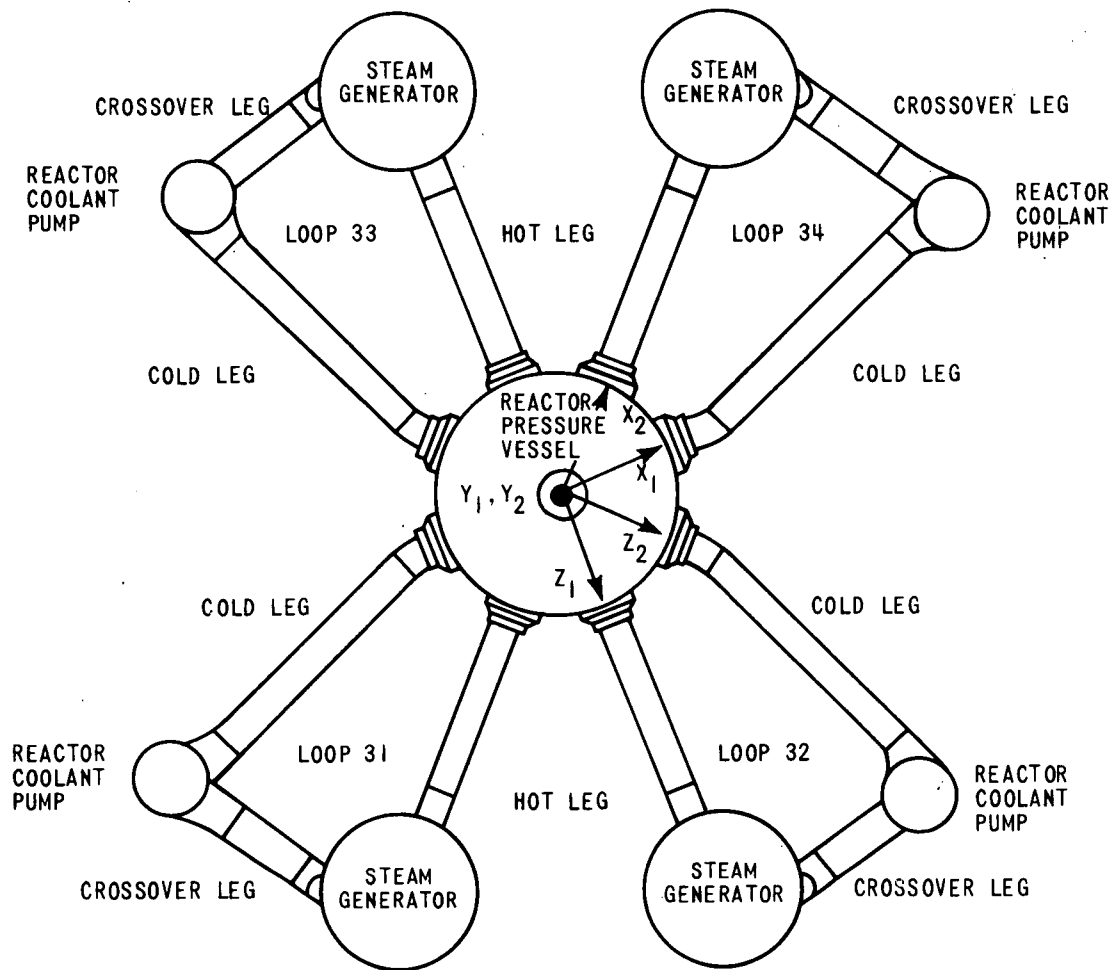
The reactor coolant loop mechanical loads are applied to the RPV nozzles by the reactor coolant loop piping. For guillotine pipe separations, the loop mechanical loads result from the release of normal operating forces present in the pipe prior to the separation as well as from transient hydraulic forces in the reactor coolant system. The magnitudes of the loop release forces are determined by performing a reactor coolant loop analysis for normal operating loads (pressure, thermal, and deadweight). The loads existing in the pipe at the postulated break location are calculated and are "released" at the initiation of the LOCA transient by application of the loads to the broken piping ends. These forces are applied with a ramp time of 1 millisecond due to the assumed instantaneous break opening time.

The magnitudes of the loop release loads for a postulated RPV inlet nozzle break, RPV outlet nozzle break, and RCP outlet nozzle break are given in table 3-1, in the coordinate systems shown in figure 3-2. These loads are applied to the DARIWOSTAS model, described in section 3-4, at the intersection of the RPV and nozzle centerlines.

[] a,b,c

**TABLE 3-1
RCL MECHANICAL LOADS**

Load Component \ Break Location	RPV Inlet Nozzle	RPV Outlet Nozzle	RCP Outlet Nozzle
Axial Load (Fx) kips	[] a,b,c		
Vertical Load (Fy) kips			
Moment (Mz) in-kips			



X_1, Y_1, Z_1 - COORDINATE SYSTEM FOR BREAK POSTULATED TO OCCUR IN COLD LEG, LOOP 31

X_2, Y_2, Z_2 - COORDINATE SYSTEM FOR BREAK POSTULATED TO OCCUR IN HOT LEG, LOOP 31

Figure 3-2. Coordinate Systems for Postulated Breaks

3-3. Reactor Pressure Vessel Internal Hydraulic Loads

Depressurization waves propagate from the postulated break location into the reactor vessel through either a hot leg or a cold leg nozzle. Figures 3-3 and 3-4 depict the possible wave propagation paths for waves entering the RPV cold leg and hot leg, respectively.

After a postulated break at the RPV inlet nozzle or at the RCP outlet nozzle, the depressurization path for waves entering the reactor vessel is through the nozzle which contains the broken pipe and into the downcomer annulus which is the region between the core barrel and reactor vessel (figure 3-3). The initial waves propagate up, around, and down the downcomer annulus, then up through the region circumferentially enclosed by the core barrel; that is, the fuel region. As a result, the region of the downcomer annulus close to the break depressurizes rapidly but, because of restricted flow areas and finite wave speed (approximately 3500 feet per second), the opposite side of the core barrel remains at a high pressure. This results in a net horizontal force on the core barrel and RPV. As the depressurization wave propagates around the downcomer annulus and up through the core, the barrel differential pressure reduces, and similarly, the resulting hydraulic forces drop. In the case of a postulated RPV outlet rupture, the waves follow a dissimilar depressurization path, passing through the outlet nozzle and directly into the upper internals region, depressurizing the core, and entering the downcomer annulus from the bottom exit of the core barrel, as shown in figure 3-4. Since the depressurization wave travels directly to the inside of the core barrel (so that the downcomer annulus is not directly involved), the internal differential pressures are not as large as for the RPV inlet nozzle break, and therefore, the horizontal force applied to the core barrel is less for the hot leg break than for a cold leg RPV inlet nozzle break. For breaks in either the hot leg or cold leg, the depressurization waves would continue to propagate by reflection and translation through the reactor vessel and loops. The reactor coolant pump outlet nozzle and reactor pressure vessel inlet nozzle pipe rupture locations have similar vessel internal hydraulic loads, but due to the influence of reactor cavity pressure loads, the vessel inlet nozzle break generates larger forces applied to the reactor vessel.

The MULTIFLEX computer code² calculates the hydraulic transients within the entire reactor coolant system. It considers subcooled, transition, and two-phase (saturated) blowdown regimes. The MULTIFLEX program employs the method of characteristics to solve the conservation laws, and assumes one-dimensionality of flow and homogeneity of the liquid-vapor mixture. The MULTIFLEX code considers a coupled fluid-structure interaction by accounting for the deflection of constraining boundaries, which are represented by separate spring-mass oscillator systems. A beam model of the core support barrel has been developed from the structural properties of the core barrel. In this model, the cylindrical barrel is vertically divided

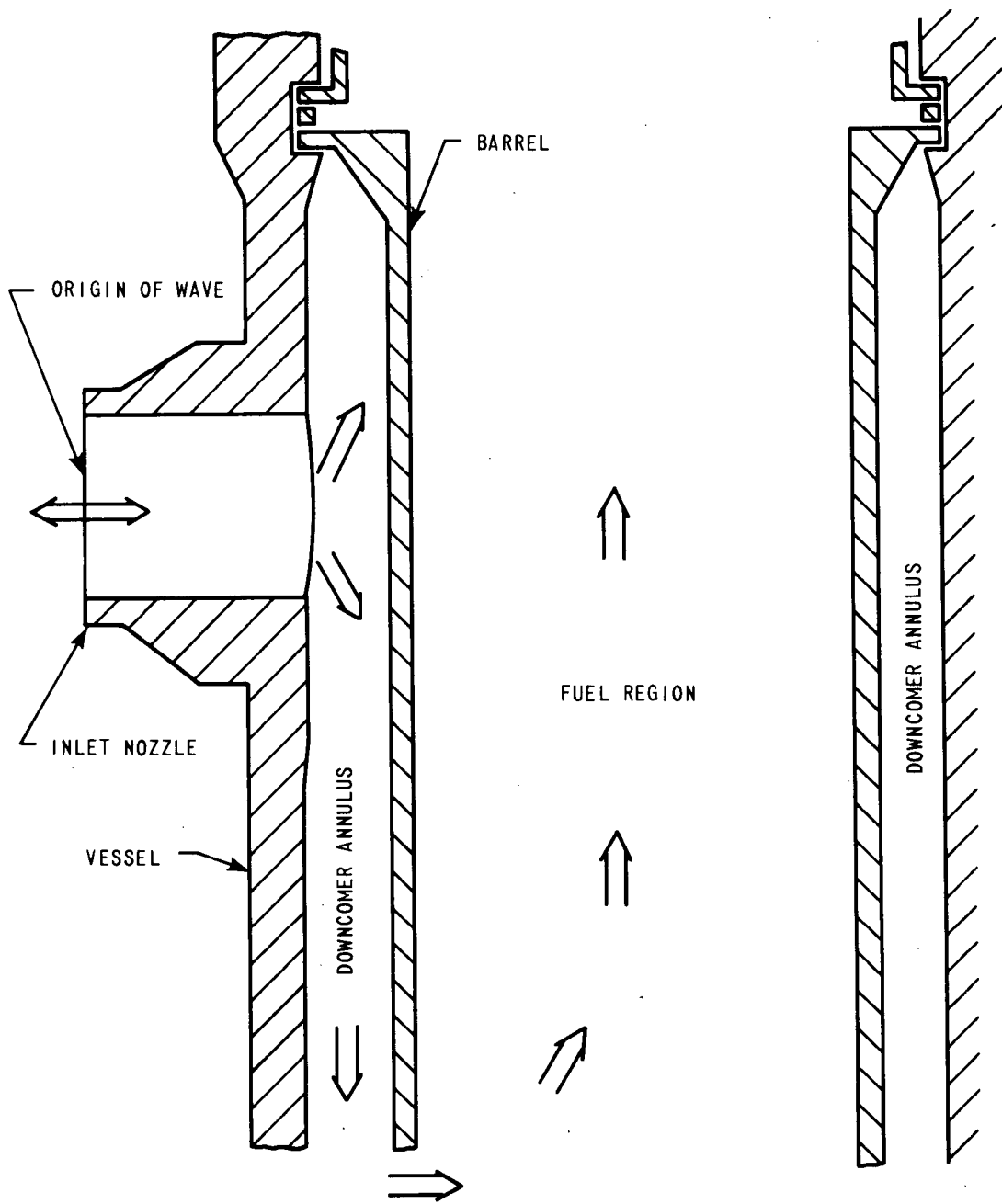


Figure 3-3. Wave Path for Depressurization Waves Entering RPV Inlet Nozzle (Cold Leg)

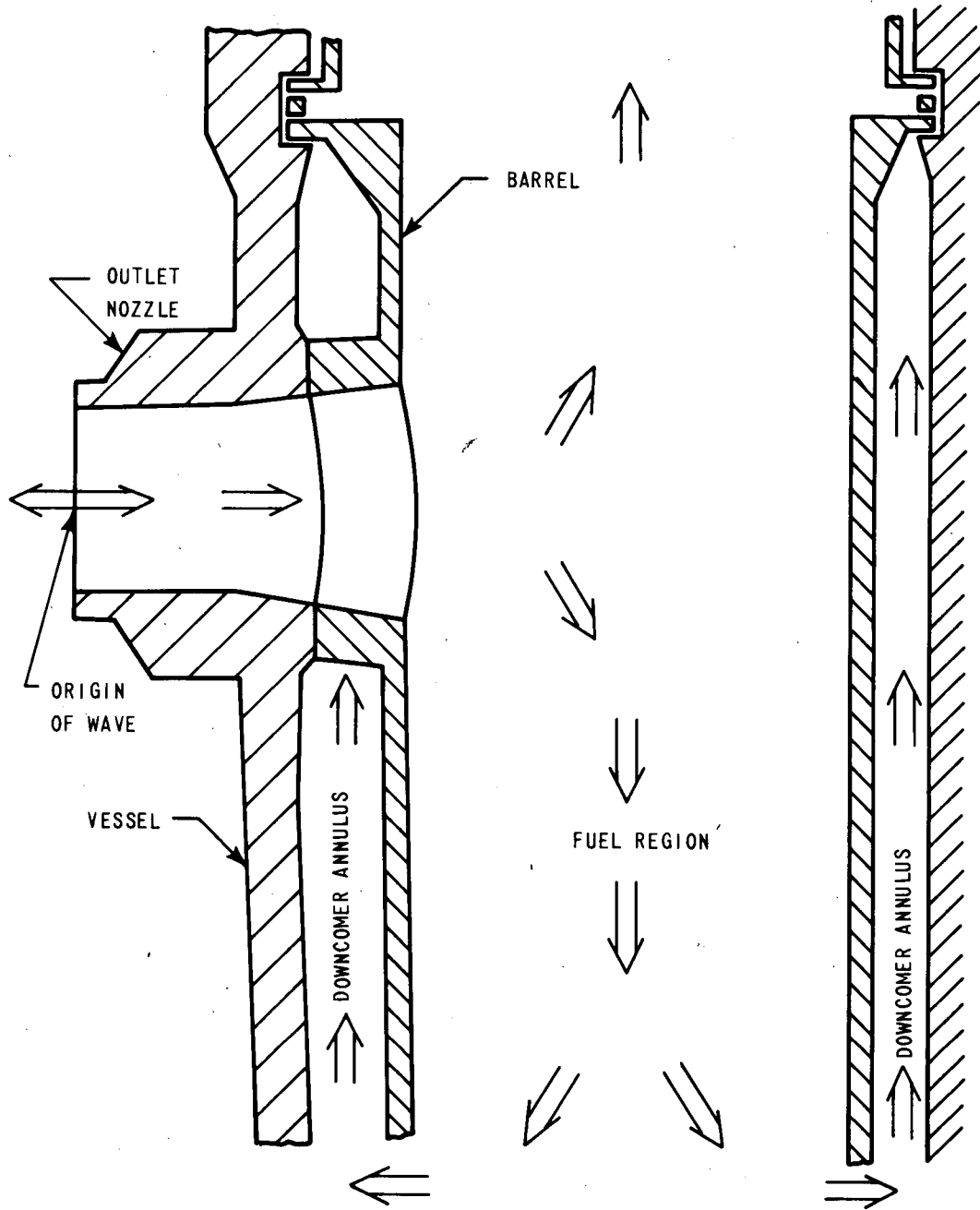


Figure 3-4. Wave Path for Depressurization Waves Entering RPV Outlet Nozzle (Hot Leg)

into [] segments and the pressure as well as the wall motions are projected onto the plane parallel to the broken inlet nozzle. Horizontally, the barrel is divided into [] segments, each consisting of [] separate walls. The spatial pressure variation at each time step is transformed into [] horizontal forces, which act on the [] mass points of the beam model. Each flexible wall is bounded on either side by a hydraulic flow path. a,c

The motion of the flexible walls is determined by solving the global equations of motion for the masses representing the forced vibration of an undamped beam:

$$[M] \{\ddot{x}\} + [K] \{x\} = \{F\} \quad (3-1)$$

where

- [M] = Generalized mass matrix
- [K] = Generalized stiffness matrix
- { \ddot{x} } = Acceleration matrix for mass points on the core barrel
- {x} = Displacement matrix for mass points on the core barrel

The force matrix {F} is obtained by multiplying hydraulic pressures and the areas on which they act. The mass and stiffness matrices are obtained from independent modal analyses of the core barrel. This barrel motion is translated into an equivalent rate of flow area in each downcomer annulus channel. At every time increment, [] are introduced between the structural and the hydraulic sections of the program for each location confined by a flexible wall. a,c

Its ability to treat multiple flow branches and a large number of mesh points gives the MULTIFLEX code the required flexibility to represent the various flow passages within the primary reactor coolant system. The RCS is divided into subregions in which the fluid flows mainly along their longitudinal axes; each subregion may then be regarded as an equivalent pipe. The entire primary RCS is thus represented by a complex network of equivalent pipes.

Time history values of the pressure, mass velocity, density, and other thermodynamic properties within the RPV (all of which are computed by the MULTIFLEX code), are utilized in the determination of the applied vertical and lateral loads on the reactor vessel internals.

The RPV internal hydraulic loads for pipe ruptures postulated at the vessel safe end locations were based upon a 110 square-inch break opening area. This limited area was verified to be conservative upon completion of the reactor coolant system blowdown analysis by using the

actual broken pipe displacements and geometrical relationships. Internal hydraulic loads for a break postulated at the reactor coolant pump outlet nozzle safe end location were calculated for the maximum value, that is, a full doubled-ended break opening area. Typical internal hydraulic loads are shown in figures 3-5 through 3-10.

3-4. Vertical Loads – The FORCE 2 computer code determines the vertical hydraulic loads on the reactor vessel internals during blowdown. FORCE 2 utilizes a detailed geometric description of the vessel components, transient pressures, and mass velocities computed by the MULTIFLEX code. The FORCE 2 code is applicable for all pressure and mass velocity transients arising from a postulated loss-of-coolant accident. Each reactor vessel component for which force calculations are required is designated as an element. If the flow region associated with an element in FORCE 2 is divided into more than one flow path in the MULTIFLEX hydraulic model, then the element in FORCE 2 is subdivided into a corresponding number of divisions.

The analytical basis for the derivation of the mathematical equations utilized in the FORCE 2 code is the conservation of momentum. In evaluating the vertical hydraulic loads on the reactor vessel internals, the following types of transient forces are considered:

- Pressure differential acting across the element
- Flow stagnation on the element and unrecovered orifice losses across the element.
- Friction losses along the element

These three types of forces are summed together to give the total force on each element. Individual forces on elements are further combined, depending upon what particular RV internal component is being considered, to yield the resultant vertical hydraulic load on that component.

3-5. Horizontal Loads – Variations in the fluid pressure distribution in the downcomer annulus region during the subcooled operation of the blowdown transient produce pressure loadings on the reactor vessel internals. The transient pressures computed by the MULTIFLEX code are used to calculate the lateral hydraulic loads on the reactor vessel wall, core barrel, and thermal shield.

The annular region between the reactor vessel wall and the core barrel (that is, the downcomer annulus) is modeled as cylindrical segments formed by dividing this region into circumferential and axial zones. Figure 3-11 shows a representation of the calculation of the horizontal force on a cylindrical segment. The x-component of the hydraulic force acting on a segment equals the x-projected area times the mean pressure acting over the segment. Similarly, the y-component of the hydraulic force acting on this segment equals the y-projected area times the mean pressure acting over the segment.

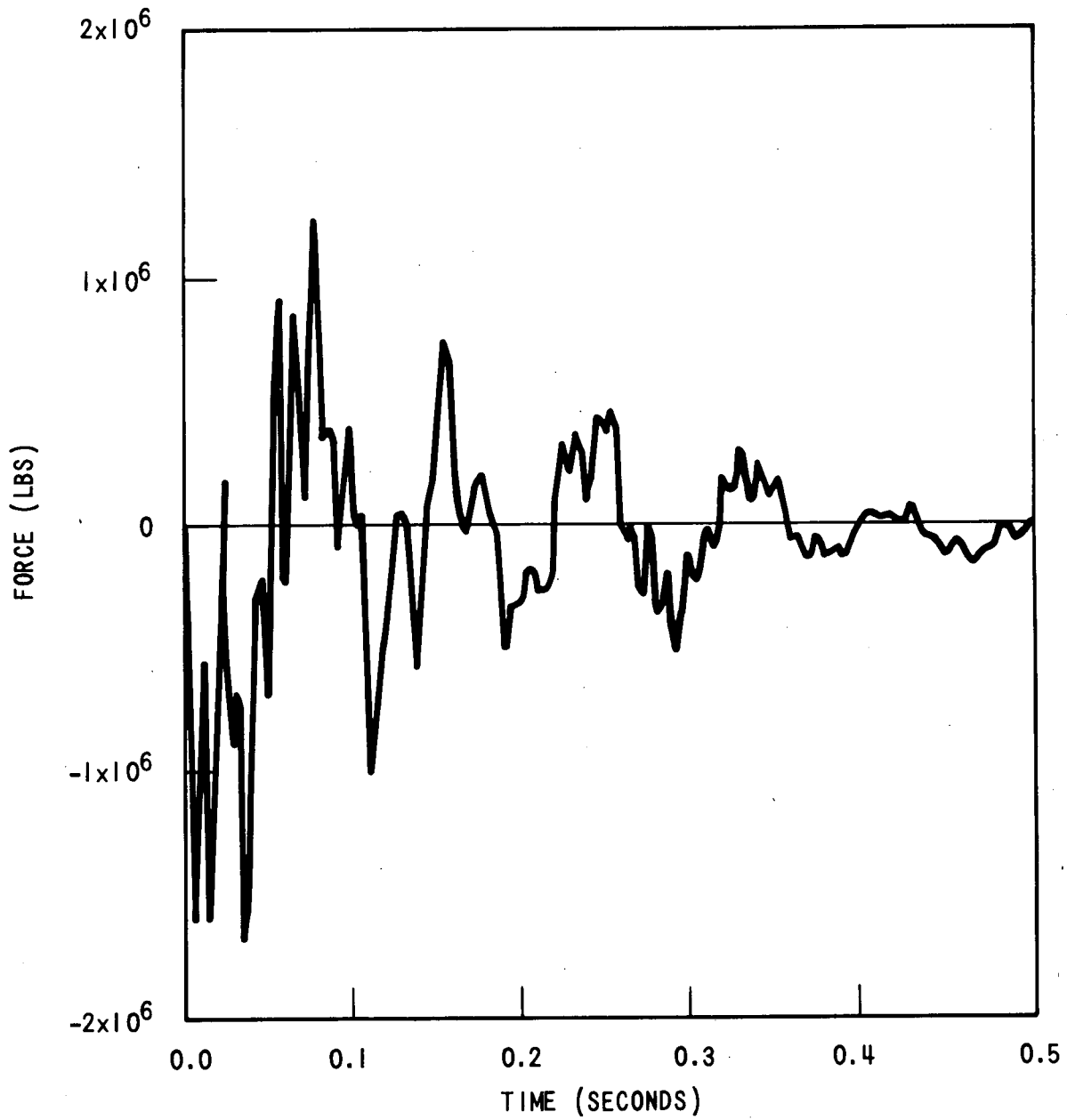


Figure 3-5. RPV Inlet Nozzle Safe End Break Horizontal Internal Hydraulic Force Applied to Reactor Core Barrel

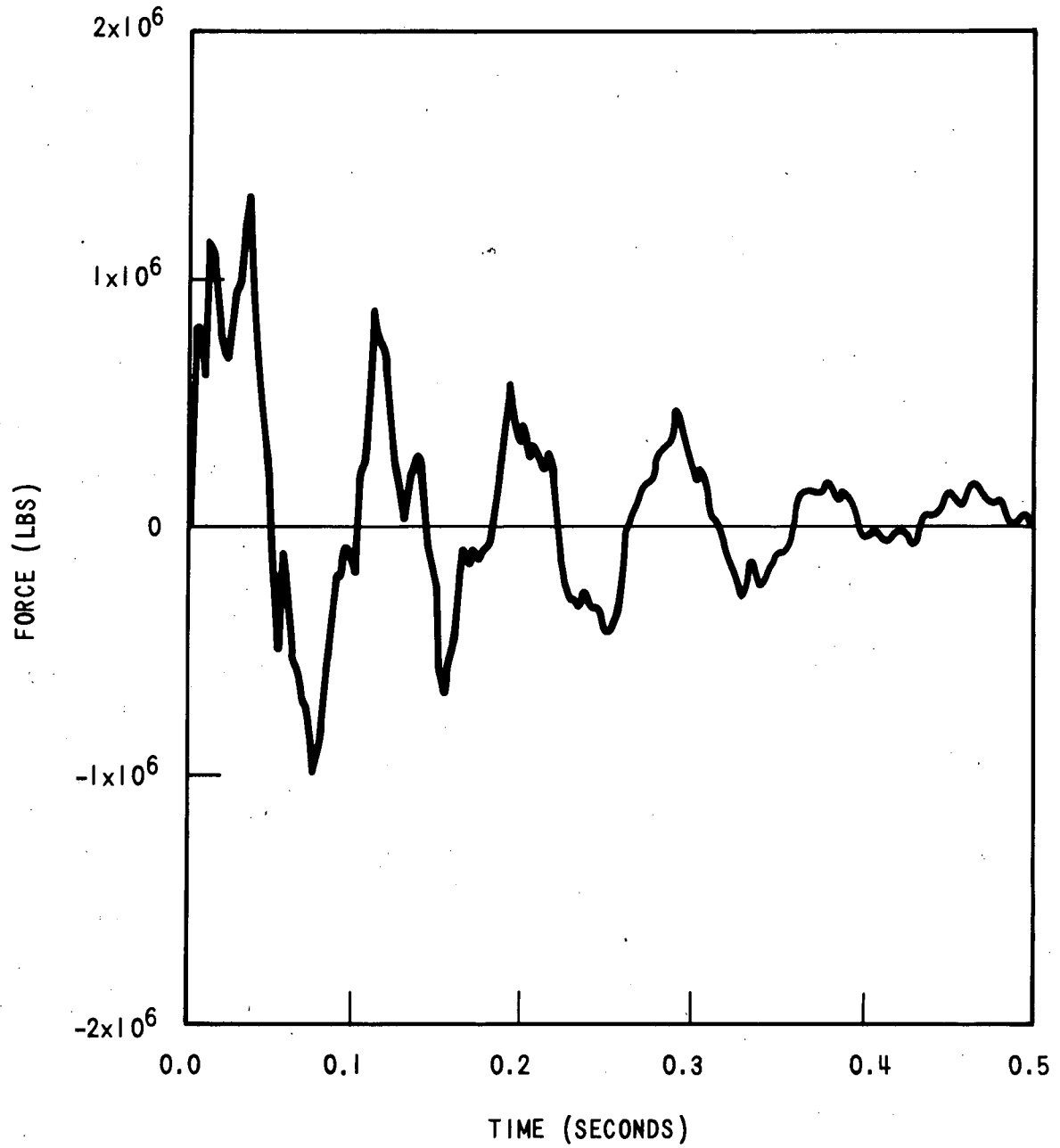


Figure 3-6. RPV Inlet Nozzle Safe End Break Horizontal Internal Hydraulic Force Applied to Reactor Vessel

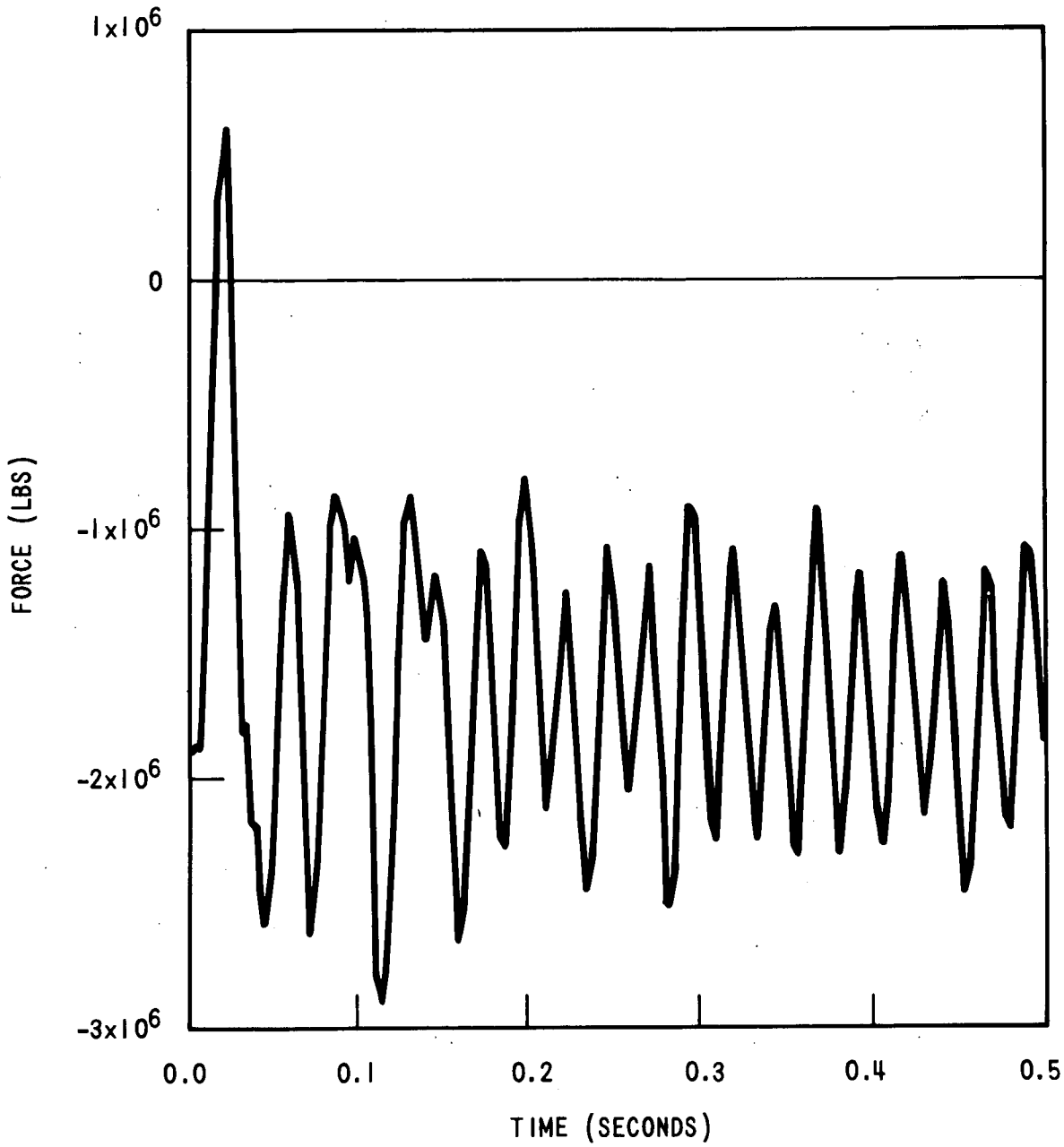


Figure 3-7. RPV Inlet Nozzle Safe End Break Vertical Internal Hydraulic Force Applied to Reactor Vessel

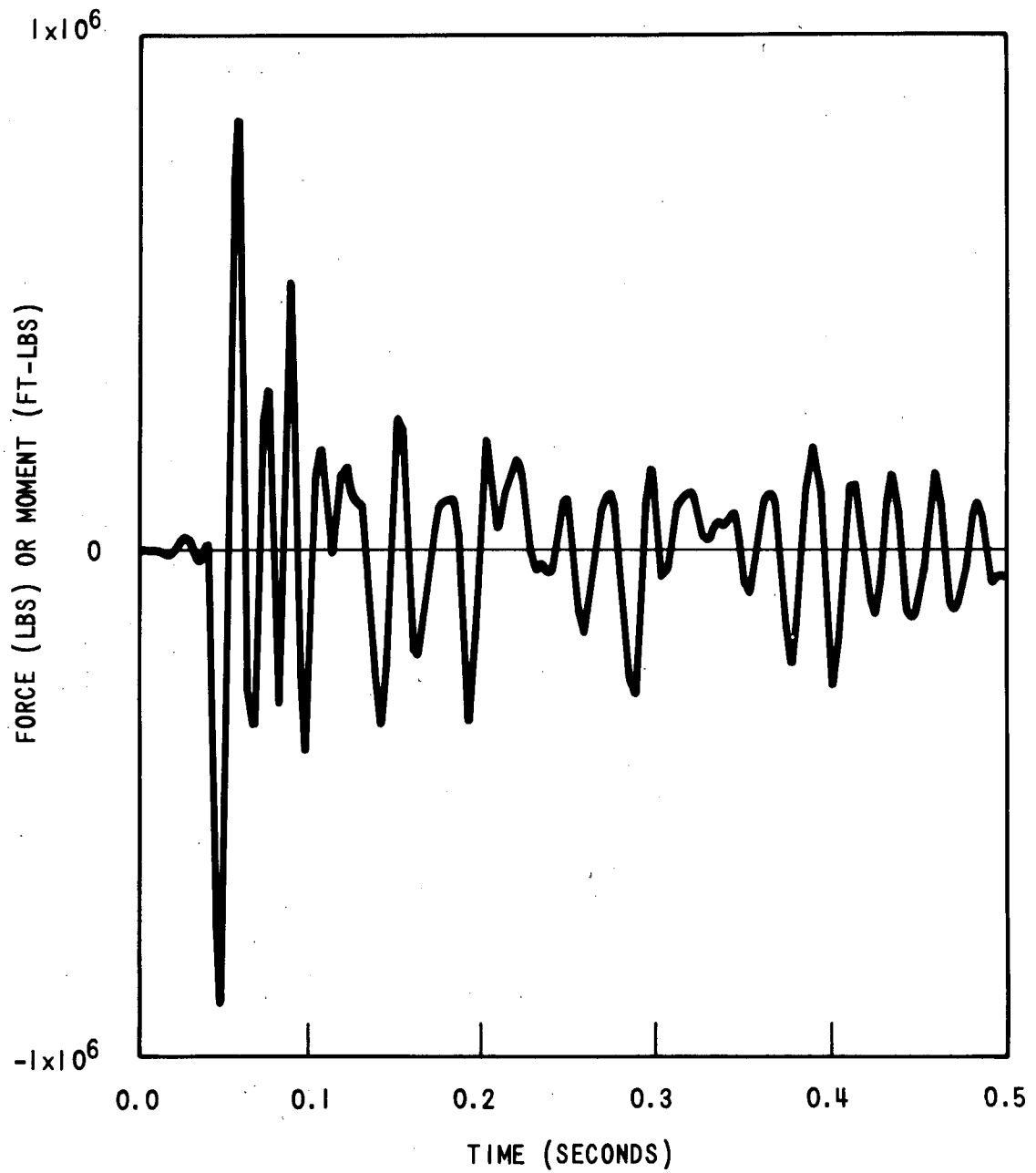


Figure 3-8. RPV Outlet Nozzle Safe End Break Horizontal Internal Hydraulic Force Applied to Reactor Core Barrel

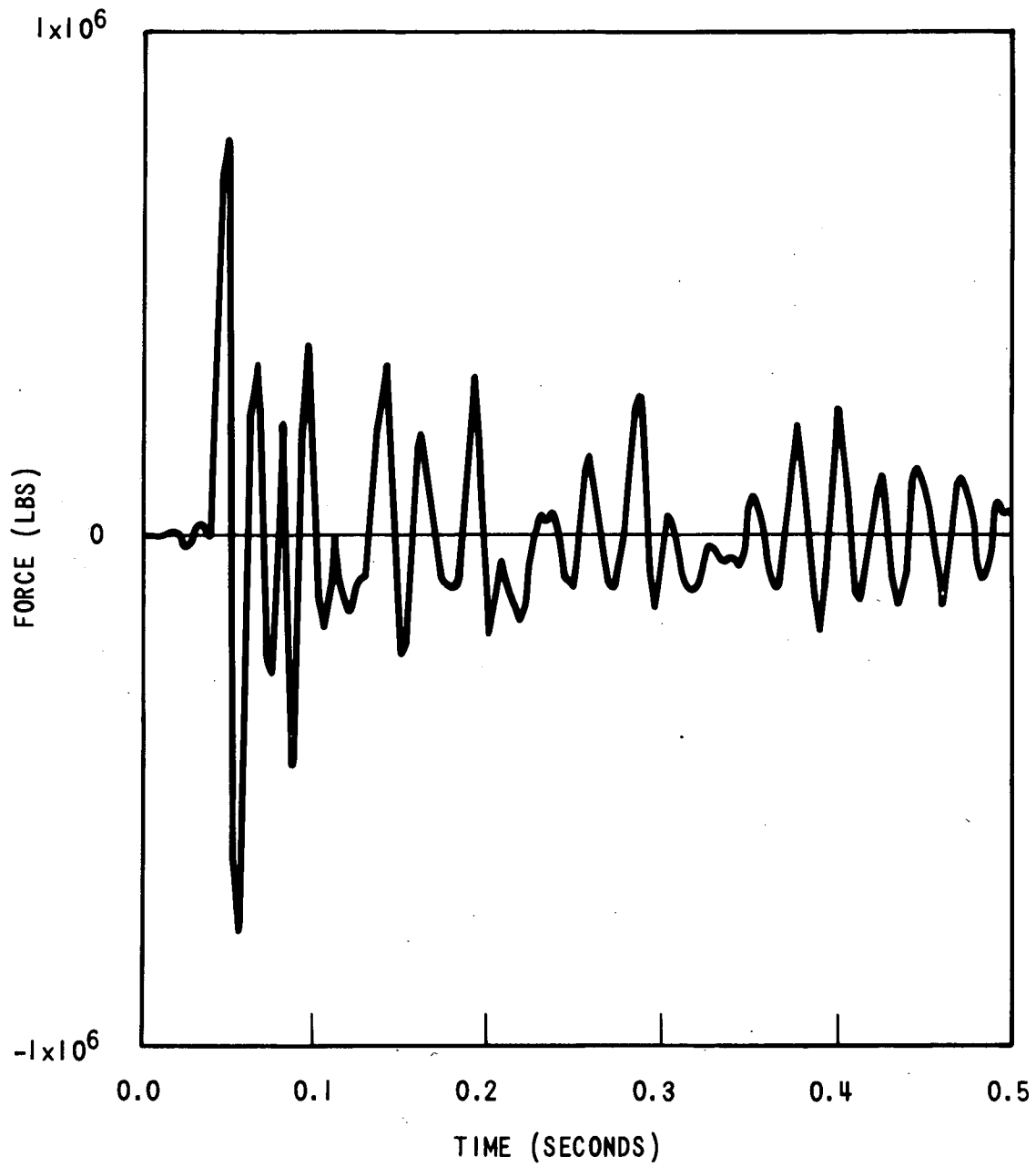


Figure 3-9. RPV Outlet Nozzle Safe End Break Horizontal Internal Hydraulic Force Applied to Reactor Vessel

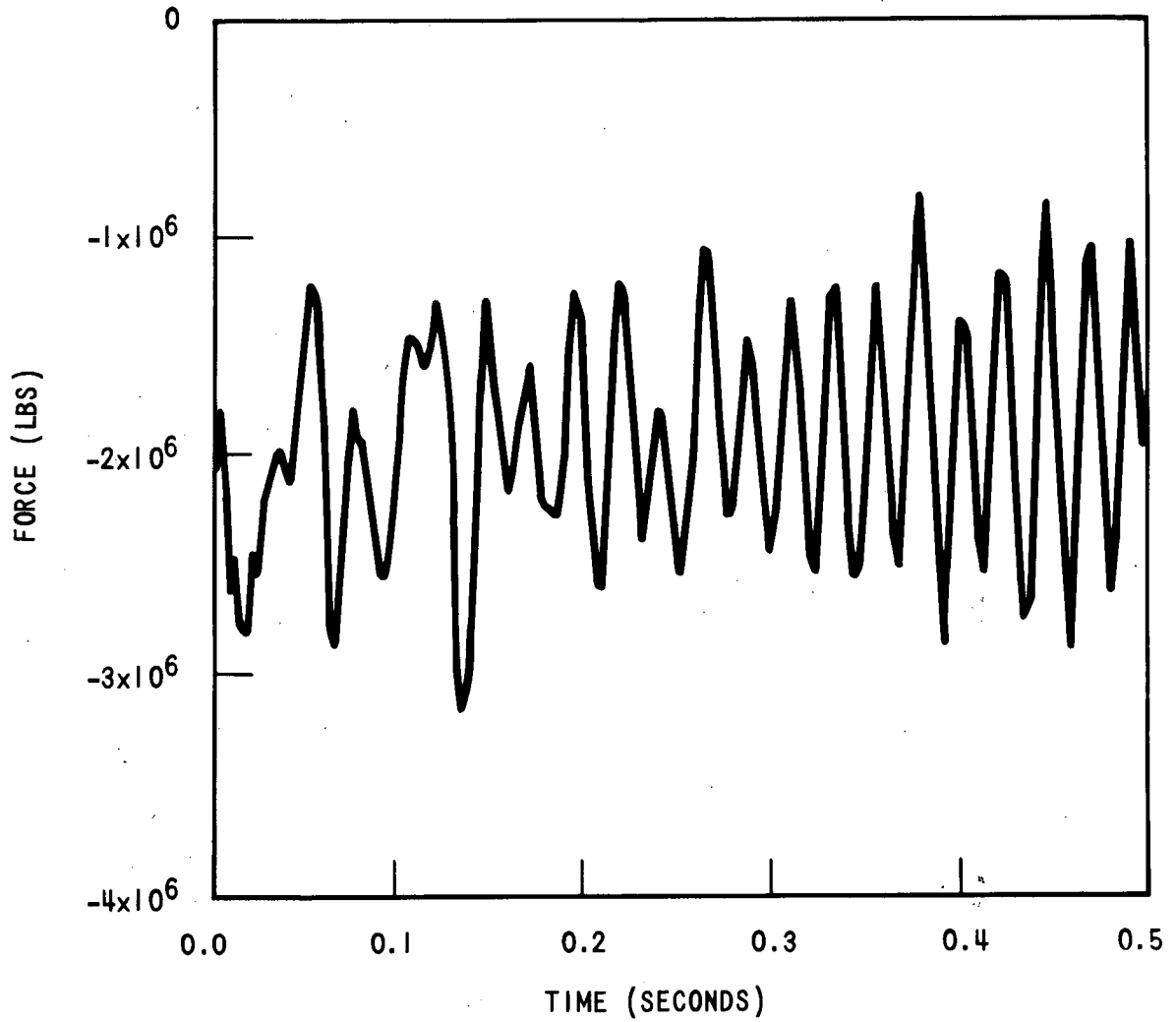


Figure 3-10. RPV Outlet Nozzle Safe End Break Vertical Internal Hydraulic Force Applied to Reactor Vessel

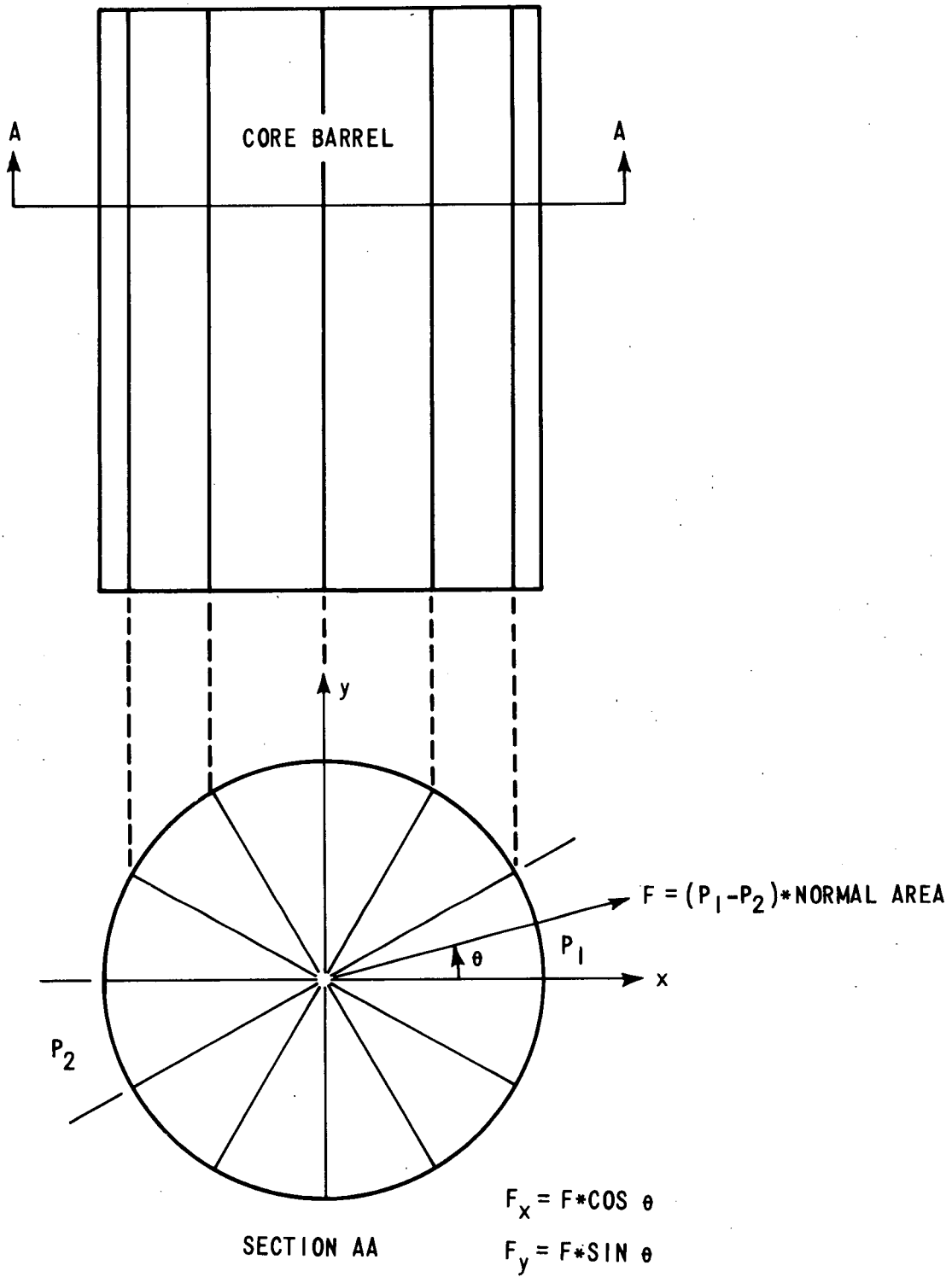


Figure 3-11. Horizontal Force Calculation

3-6. Reactor Cavity Pressurization Loads

Reactor cavity forces arise from the steam and water which are released into the reactor cavity through the annulus around the broken pipe. These forces occur only for postulated breaks at the RPV nozzle safe end locations. The reactor cavity is pressurized asymmetrically, with higher pressure on the side adjacent to the break. The horizontal differences in pressure across the reactor cavity result in horizontal forces on the reactor vessel. Vertical forces on the reactor vessel arise from similar variations in pressure on the upper and lower head and the tapered parts of the reactor vessel.

Reactor cavity loads were calculated for a 110 square-inch guillotine break opening at the cold leg and hot leg nozzle safe ends. This break area has been verified to be the maximum possible opening area due to the placement of pipe restraints in the primary shield wall. The reactor cavity loads applied to the DARIWOSTAS model for the vessel inlet nozzle safe end break are shown in figures 3-12, 3-13, and 3-14. Similarly, the reactor cavity loads for a break postulated at the reactor vessel outlet nozzle safe end are depicted in figures 3-15, 3-16, and 3-17. Vertical, horizontal, and moment loads applied at the intersection of the vessel vertical and broken nozzle centerlines are shown using the coordinate system shown in figure 3-2.

3-7. Method of Determining the Reactor Cavity Loads

The TMD computer code¹ with the unaugmented homogeneous critical flow correlation and the isentropic compressible subsonic flow correlation was used to calculate pressure transients in the reactor cavity region.

Nodalization sensitivity studies were performed before the analysis was begun. In the earlier models, no detail of the reactor vessel annulus was involved. Subsequent model changes primarily involved greater detail in the immediate vicinity of the break and in the reactor vessel annulus. The total integrated pressure in the reactor cavity changed only slightly between the later versions and final model.

All real area changes in the immediate vicinity of the broken loop nozzle were modeled. Consequently, any further nodalization in this region would introduce fictitious boundaries between elements.

[] a,c

b,c

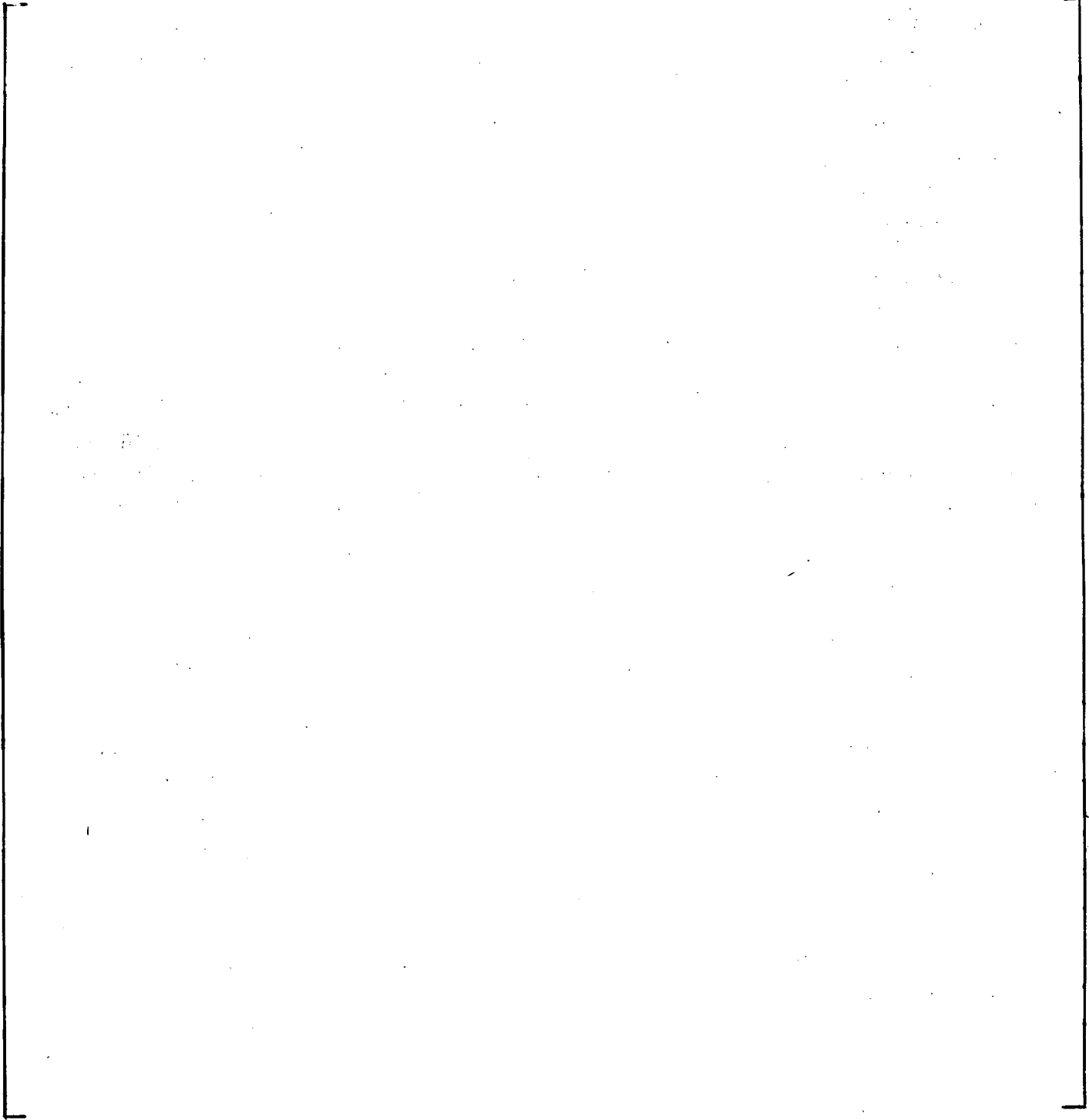


Figure 3-12. RPV Inlet Nozzle Safe End Break Reactor Cavity Pressure Horizontal Force

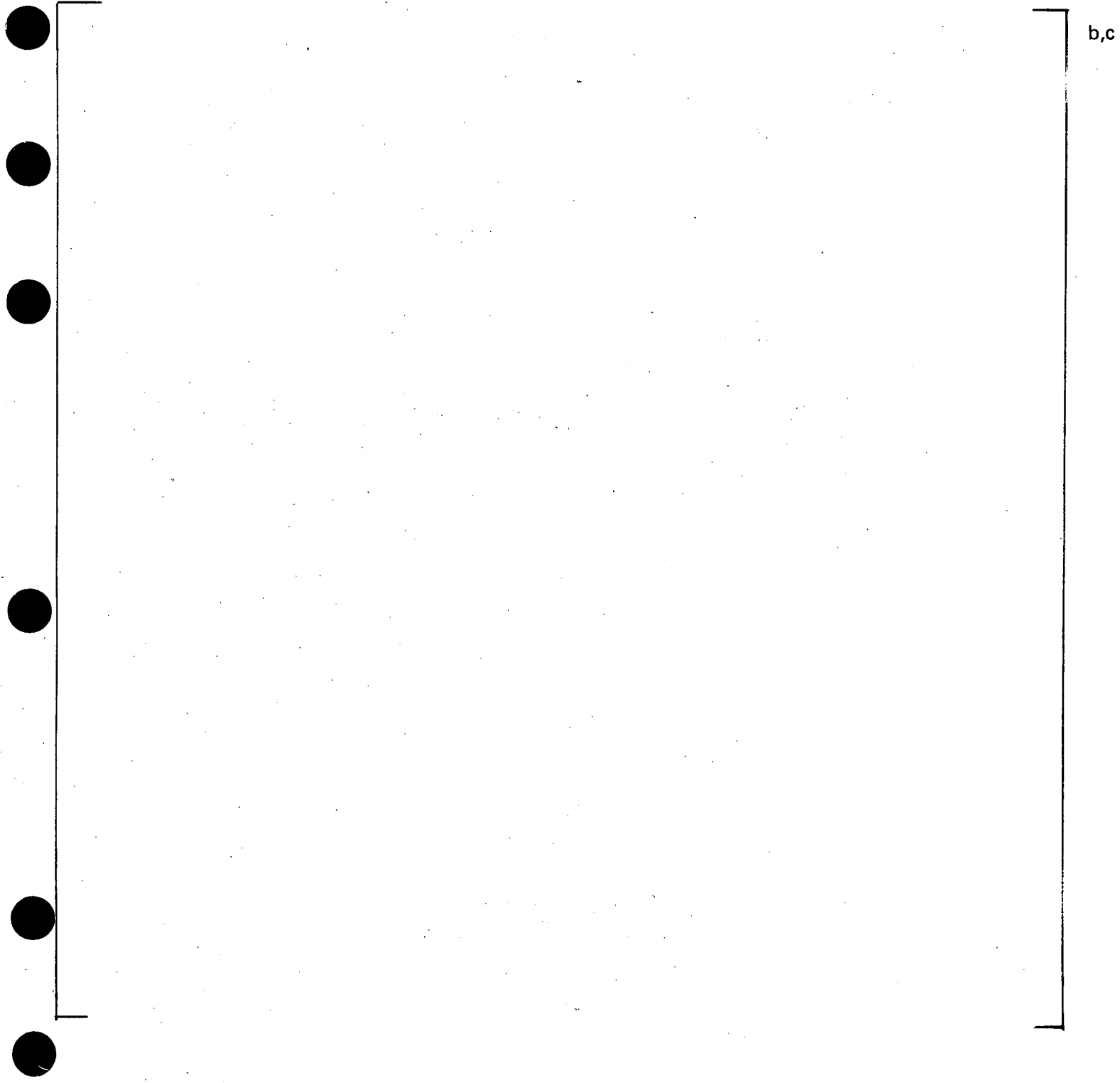


Figure 3-13. RPV Inlet Nozzle Safe End Break Reactor Cavity Pressure Vertical Force

b,c

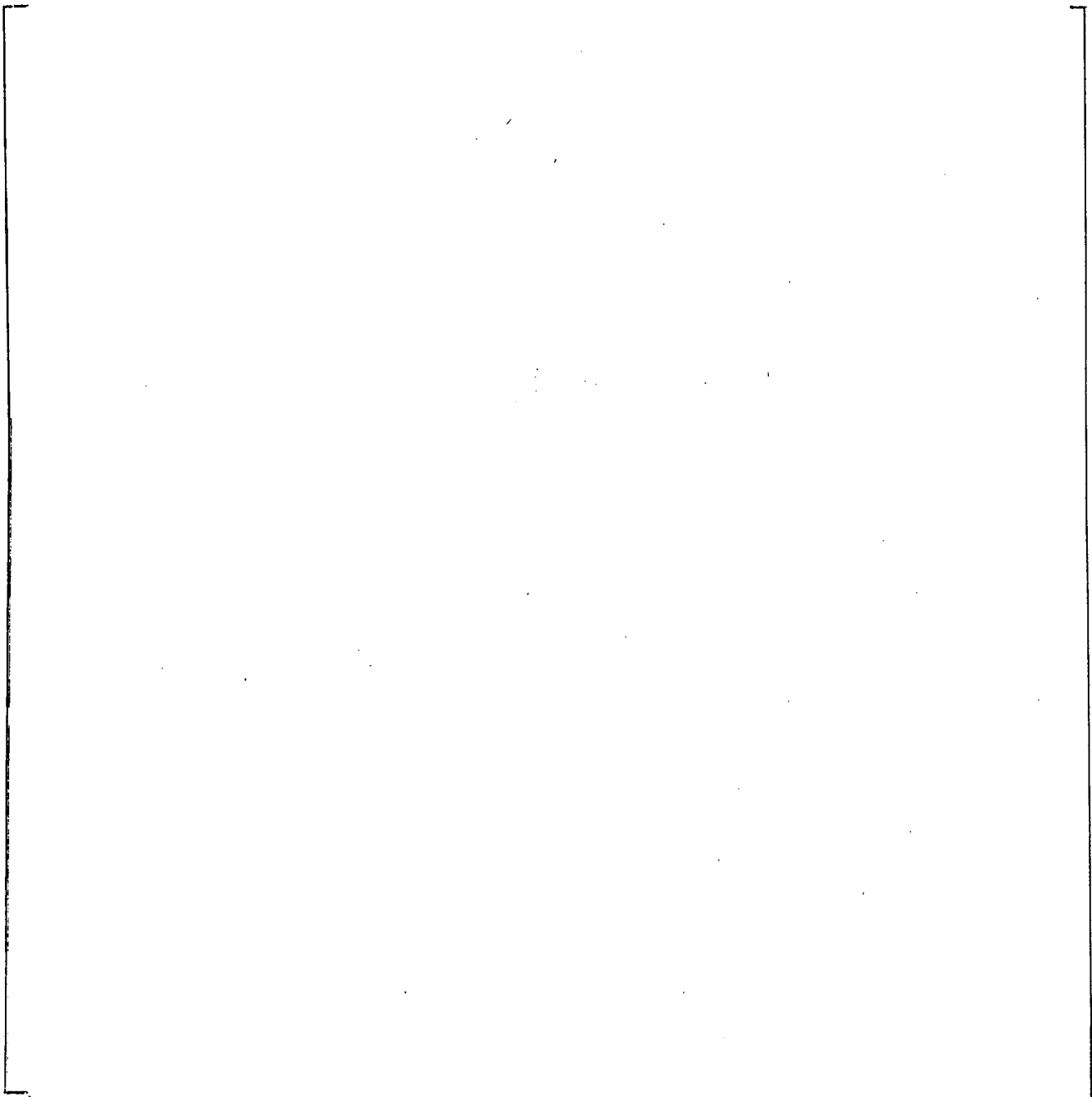


Figure 3-14. RPV Inlet Nozzle Safe End Break Reactor Cavity Pressure Moment

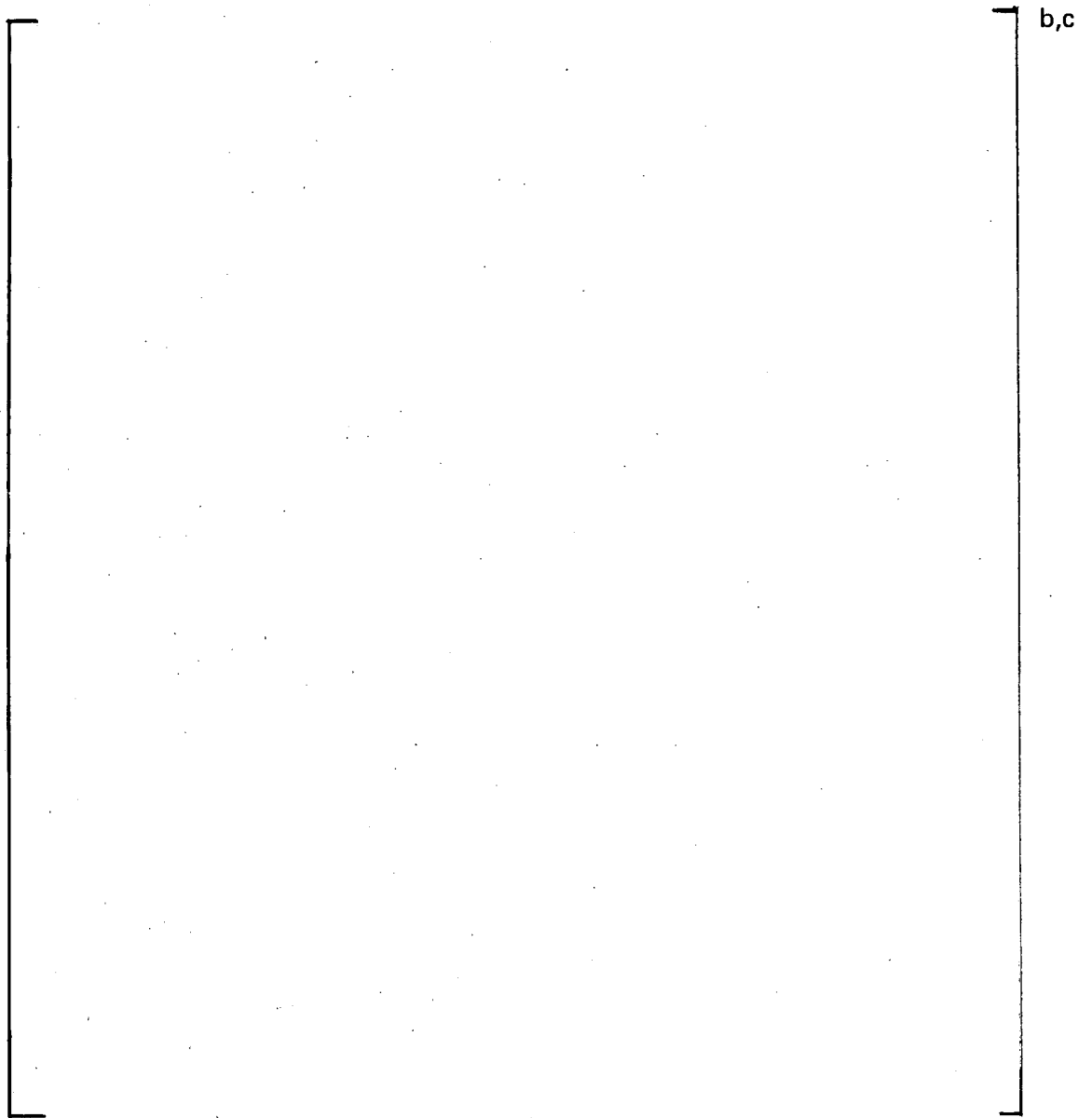


Figure 3-15. RPV Outlet Nozzle Safe End Break Reactor Cavity Pressure Horizontal Force

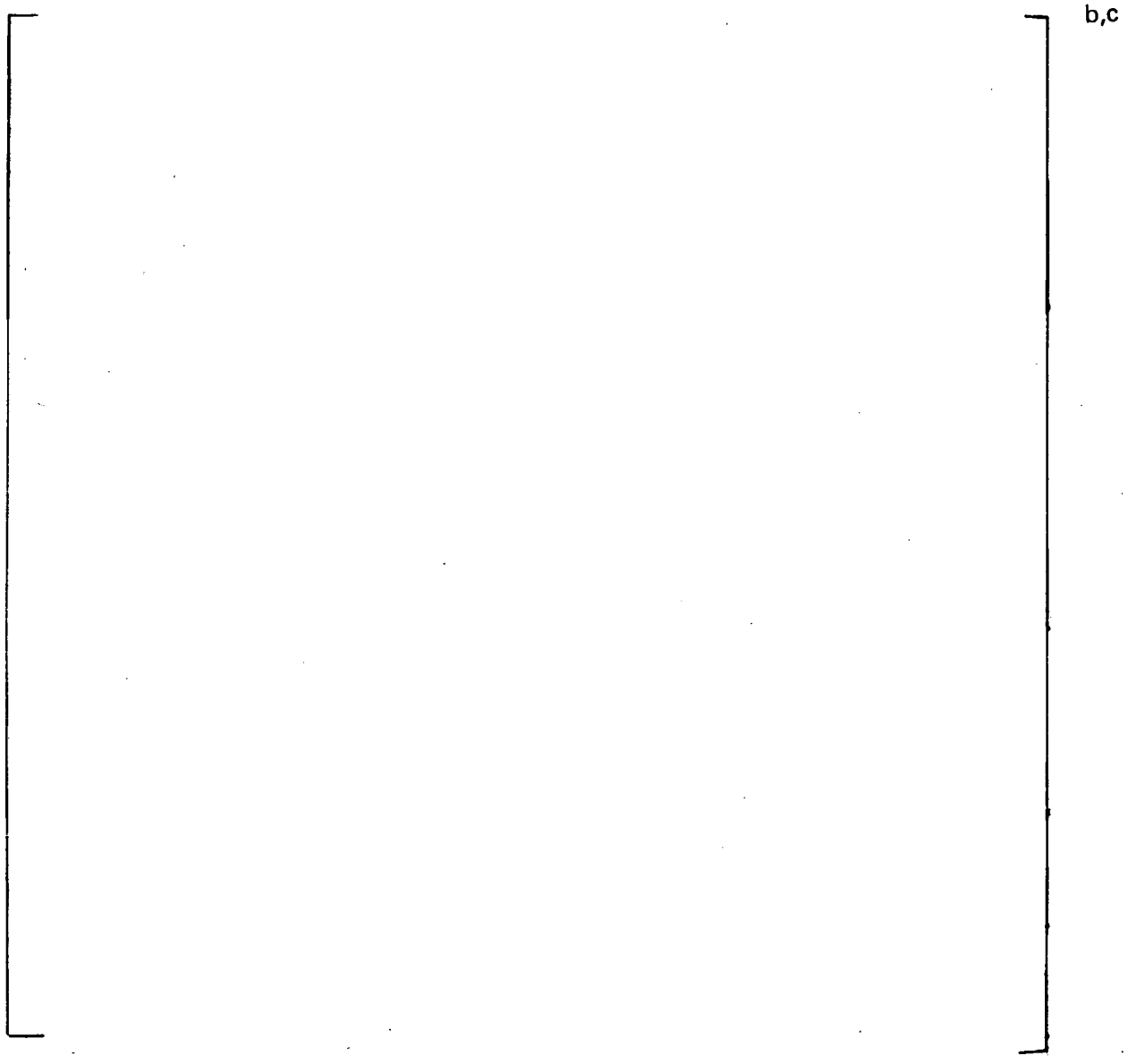


Figure 3-16. RPV Outlet Nozzle Safe End Break Reactor
Cavity Pressure Vertical Force

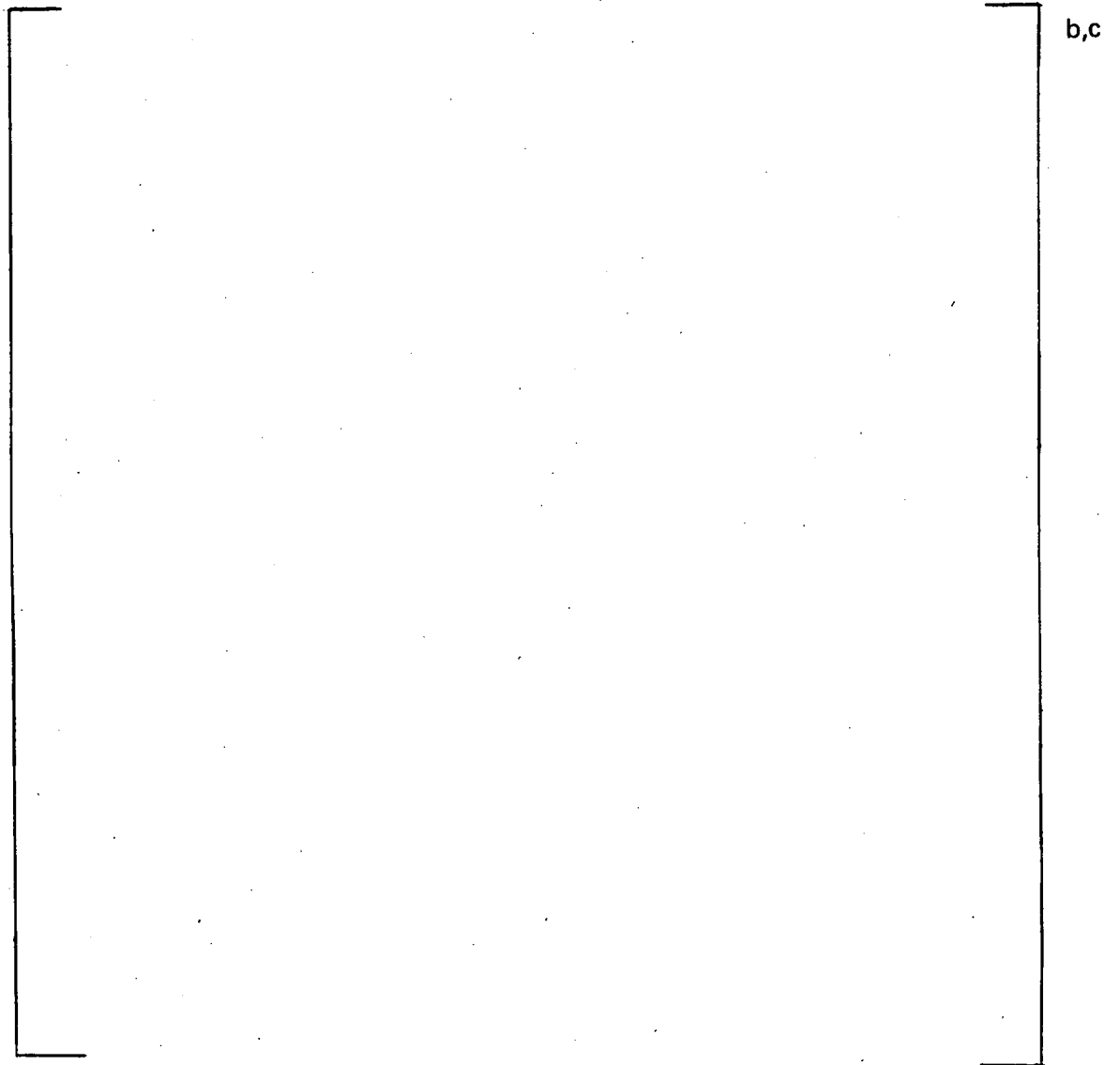


Figure 3-17. RPV Outlet Nozzle Safe End Break Reactor Cavity Pressure Moment

The inspection port plugs are in place during normal operation and were assumed to blow out



a,c

The loss coefficient (k) values were determined by changes in flow area and by turns the flow makes in traveling from the centroid of the upstream node to the centroid of the downstream node. The k and f factors for each path were determined using methods from such references as FLOW OF FLUIDS THROUGH VALVES, FITTINGS AND PIPES by the Crane Company and CHEMICAL ENGINEERING by J. M. Coulson and J. F. Richardson.

Tables 3-2, 3-3, 3-4, and 3-5 provide the volumes and flow path data for the elements and their connections. A break limiting restraint restricts the vessel inlet and outlet break sizes to 110 in². The mass and energy release rates for both breaks are presented in tables 3-6 and 3-7 respectively.

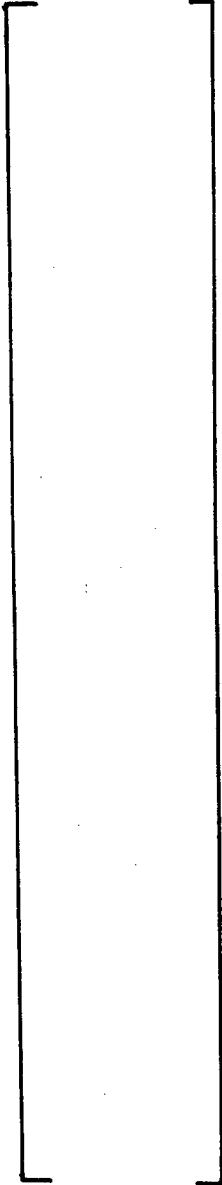
Figures 3-18, 3-19, and 3-20 illustrate the general configuration of the reactor vessel annulus nodalization for the cold leg break. The outlet break is similar. Figure 3-21 shows the flow path connections for the 61 element model. In the model, the lower containment is divided into two loop compartments (51-52). The upper containment is represented by compartment 38. The break occurs in element 1, immediately surrounding the nozzle. The corresponding broken loop pipe annulus is represented by element 46. The lower reactor cavity is modeled by element 2 and the remainder of the elements, as shown in figure 3-19, model the reactor vessel annulus. Compartments 28 and 29 adjoin compartments 30, 31 and 32.

**TABLE 3-2
VOLUMES – COLD LEG BREAK**

Element	Element Description	Volume (Ft ³)
1	Break Location	
2	Lower Reactor Cavity	
3	Reactor Vessel Annulus	
4		
5		
6		
7		
8		
9		
10		
11		
12		
13		
14		
15		
16		
17		
18		
19		
20		
21		
22		
23		
24		
25		
26		
27		
28		
29		
30		
31		

a,b,c

TABLE 3-2 (cont)
VOLUMES – COLD LEG BREAK

Element	Element Description	Volume (Ft ³)
32	Reactor Vessel Annulus	
33		
34		
35		
36	↓	
37	Reactor Vessel Annulus	
38	Upper Containment	
39	Inspection Volume	
40	Inspection Volume	
41	Inspection Volume, Port & Pipe Sleeve	
42	Inspection Volume, Port & Pipe Sleeve	
43	Inspection Volume, Port & Pipe Sleeve	
44	Inspection Volume	
45	Inspection Volume	
46	Broken Loop Pipe Sleeve	
47	Unbroken Loop Pipe Sleeve	
48	Unbroken Loop Pipe Sleeve	
49	Unbroken Loop Pipe Sleeve	
50	Unbroken Loop Pipe Sleeve	
51	Loop Compartment	
52	Loop Compartment	
53	Broken Loop Inspection Port	
54	Unbroken Loop Inspection Port	
55	Unbroken Loop Inspection Port	
56	Unbroken Loop Inspection Port	
57	Unbroken Loop Inspection Port	
58	Truncated Toroid	
59	Truncated Toroid	
60	Truncated Toroid	
61	Truncated Toroid	

a,b,c

**TABLE 3-3
FLOW PATH DATA
Cold Leg Break**

FLOW PATH FROM--TO	K FACTOR	F FACTOR	INERTIA LENGTH (FT.)	HYDRAULIC DIAMETER (FT.)	FLOW AREA (SQ.-FT.)	EQUIVALENT LENGTH (FT.)	AREA RATIO
1--3							
2--25							
3--5							
4--3A							
5--10							
6--11							
7--12							
8--13							
9--3A							
10--15							
11--16							
12--17							
13--1A							
14--3A							
15--20							
16--21							
17--21							
18--21							
19--3A							
20--22							
21--23							
22--40							
23--25							
24--3A							
25--27							
26--3A							
27--29							
28--3A							
29--32							
30--3A							
31--30							
32--35							
33--3A							
34--5							
35--6							
36--7							
37--A							
39--47							

a,b,c

3-27

TABLE 3-3 (cont)
FLOW PATH DATA
Cold Leg Break

FLOW PATH FROM--TO	K FACTOR	F FACTOR	INERTIA LENGTH (FT.)	HYDRAULIC DIAMETER (FT.)	FLOW AREA (SQ.-FT.)	EQUIVALENT LENGTH (FT.)	AREA RATIO
40--20	[]
41--22							
42--24							
43--26							
44--28							
45--31							
46--51							
47--51							
48--40							
49--44							
50--51							
51--52							
52--41							
56--44							
57--45							
58--45							
59--32							
60--11							
61--21							
1--53							
2--32							
3-- 6							
4-- 9							
5-- 6							
6-- 7							
7-- 8							
8-- 2							
9--14							
10--11							
11--12							
12--13							
13-- 2							
14--19							
15--16							
16--17							
17--18							
18-- 2							
19--22							
20--21							
21-- 2							

a,b,c

TABLE 3-3 (cont)
 FLOW PATH DATA
 Cold Leg Break

FLOW PATH FROM--TO	K FACTOR	F FACTOR	INERTIA LENGTH (FT.)	HYDRAULIC DIAMETER (FT.)	FLOW AREA (SQ.-FT.)	EQUIVALENT LENGTH (FT.)	AREA RATIO
22--24							
23--2							
24--26							
25--42							
26--28							
27--2							
28--43							
29--2							
30--33							
31--32							
32--44							
33--4							
34--35							
35--45							
36--37							
37--2							
38--52							
39--54							
40--55							
41--23							
42--26							
43--27							
44--29							
45--32							
48--51							
49--52							
50--45							
51--38							
52--42							
53--38							
54--38							
55--38							
56--38							
57--38							
58--1							
59--45							
60--1							
61--30							
1--46							
2--38							

a,b,c

TABLE 3-3 (cont)
 FLOW PATH DATA
 Cold Leg Break

FLOW PATH FROM--TO	K FACTOR	F FACTOR	INERTIA LENGTH (FT.)	HYDRAULIC DIAMETER (FT.)	FLOW AREA (SQ.-FT.)	EQUIVALENT LENGTH (FT.)	AREA RATIO
3--10							
4--5							
6--5A							
9--10							
11--3							
14--15							
15--39							
16--30							
19--20							
20--39							
21--39							
22--23							
23--40							
24--25							
25--41							
26--27							
27--42							
28--29							
29--43							
30--2A							
31--2B							
32--37							
33--34							
34--31							
35--36							
36--32							
38--22							
39--60							
40--21							
41--24							
44--31							
45--34							
52--43							
58--35							
59--44							
60--16							
61--40							

a,b,c

3-30

**TABLE 3-4
VOLUMES – HOT LEG BREAK**

<u>Element</u>	<u>Element Description</u>	<u>Volume (Ft³)</u>
1	Break Location	
2	Lower Reactor Cavity	
3	Reactor Vessel Annulus	
4		
5		
6		
7		
8		
9		
10		
11		
12		
13		
14		
15		
16		
17		
18		
19		
20		
21		
22		
23		
24		
25		
26		
27		
28		
29		
30		
31		

a,b,c

TABLE 3-4 (cont)
VOLUMES — HOT LEG BREAK

<u>Element</u>	<u>Element Description</u>	<u>Volume (Ft³)</u>
32	Reactor Vessel Annulus	
33		
34		
35		
36		
37	Reactor Vessel Annulus	
38	Upper Containment	
39	Inspection Volume	
40	Inspection Volume	
41	Inspection Volume, Port & Pipe Sleeve	
42	Inspection Volume, Port & Pipe Sleeve	
43	Inspection Volume, Port & Pipe Sleeve	
44	Inspection Volume	
45	Inspection Volume	
46	Broken Loop Pipe Sleeve	
47	Unbroken Loop Pipe Sleeve	
48	Unbroken Loop Pipe Sleeve	
49	Unbroken Loop Pipe Sleeve	
50	Unbroken Loop Pipe Sleeve	
51	Loop Compartment	
52	Loop Compartment	
53	Broken Loop Inspection Port	
54	Unbroken Loop Inspection Port	
55	Unbroken Loop Inspection Port	
56	Unbroken Loop Inspection Port	
57	Unbroken Loop Inspection Port	
58	Truncated Toroid	
59	Truncated Toroid	
60	Truncated Toroid	
61	Truncated Toroid	

a,b,c

**TABLE 3-5
FLOW PATH DATA
Hot Leg Break**

FLOW PATH FROM--TO	K FACTOR	F FACTOR	INERTIA LENGTH (FT.)	HYDRAULIC DIAMETER (FT.)	FLOW AREA (SQ.-FT.)	EQUIVALENT LENGTH (FT.)	AREA RATIO
1-- 3							
2--25							
3-- 5							
4--3A							
5--10							
6--11							
7--12							
8--13							
9--3A							
10--15							
11--16							
12--17							
13--18							
14--3A							
15--20							
16--21							
17--21							
18--21							
19--3A							
20--22							
21--23							
22--40							
23--25							
24--3A							
25--27							
26--3A							
27--29							
28--3A							
29--32							
30--3A							
31--30							
32--35							
33--3A							
34-- 5							
35-- 6							
36-- 7							
37-- 8							
38--41							

b,c

333

TABLE 3-5 (cont)
 FLOW PATH DATA
 Hot Leg Break

FLOW PATH FROM--TO	K FACTOR	F FACTOR	INERTIA LENGTH (FT.)	HYDRAULIC DIAMETER (FT.)	FLOW AREA (SQ. FT.)	EQUIVALENT LENGTH (FT.)	AREA RATIO
39--47							
40--20							
41--22							
42--24							
43--26							
44--28							
45--31							
46--51							
47--51							
48--40							
49--44							
50--51							
51--52							
52--41							
56--44							
57--45							
58--45							
59--32							
60--11							
61--21							
1--53							
2--32							
3-- 6							
4-- 0							
5-- 6							
6-- 7							
7-- 8							
8-- 2							
9--14							
10--11							
11--12							
12--13							
13-- 2							
14--10							
15--16							
16--17							
17--18							
18-- 2							
19--22							
20--21							

b,c

3-34

TABLE 3-5 (cont)
 FLOW PATH DATA
 Hot Leg Break

FLOW PATH FROM--TO	K FACTOR	F FACTOR	INERTIA LENGTH (FT.)	HYDRAULIC DIAMETER (FT.)	FLOW AREA (SQ.-FT.)	EQUIVALENT LENGTH (FT.)	AREA RATIO
21-- 2							
22--24							
23-- 2							
24--26							
25--42							
26--28							
27-- 2							
28--43							
29-- 2							
30--33							
31--32							
32--44							
33-- 4							
34--35							
35--45							
36--37							
37-- 2							
38--52							
39--54							
40--55							
41--23							
42--26							
43--27							
44--29							
45--32							
48--51							
49--52							
50--45							
51--38							
52--42							
53--38							
54--38							
55--38							
56--38							
57--38							
58-- 1							
59--45							
60-- 1							
61--39							
1--46							

b,c

TABLE 3-5 (cont)
 FLOW PATH DATA
 Hot Leg Break

FLOW PATH FROM--TO	K FACTOR	F FACTOR	INERTIA LENGTH (FT.)	HYDRAULIC DIAMETER (FT.)	FLOW AREA (SQ. FT.)	EQUIVALENT LENGTH (FT.)	AREA RATIO
2--3A							
3--10							
4--5							
6--5A							
9--10							
11--3							
14--15							
15--39							
16--39							
19--20							
20--39							
21--39							
22--23							
23--40							
24--25							
25--41							
26--27							
27--42							
28--29							
29--43							
30--2A							
31--2A							
32--37							
33--34							
34--31							
35--36							
36--32							
38--22							
39--60							
40--21							
41--24							
42--3A							
43--3A							
44--31							
45--34							
52--43							
58--35							
59--40							
60--16							
61--40							

b,c

3-36

TABLE 3-6
 MASS AND ENERGY RELEASE RATES
 110 SQUARE INCH COLD LEG BREAK

TIME (SEC)	MASS RATE (LB/S)	ENERGY RATE (BTU/S)
.00000		
.00100		
.00200		
.00305		
.00405		
.00505		
.00605		
.00704		
.00810		
.00910		
.01010		
.01106		
.01209		
.01311		
.01404		
.01503		
.01605		
.01701		
.01800		
.01903		
.02017		
.02112		
.02207		
.02321		
.02413		
.02501		
.02609		
.02702		
.02800		
.02913		
.03014		
.03102		
.03210		
.03307		
.03406		
.03520		
.03617		

b,c

TABLE 3-6 (cont)
 MASS AND ENERGY RELEASE RATES
 110 SQUARE INCH COLD LEG BREAK

TIME (SEC)	MASS RATE (LB/S)	ENERGY RATE (BTU/S)
.03702		
.03805		
.03905		
.04013		
.04120		
.04207		
.04303		
.04401		
.04513		
.04610		
.04707		
.04807		
.04910		
.05003		
.05112		
.05208		
.05308		
.05403		
.05505		
.05606		
.05707		
.05810		
.05907		
.06006		
.06112		
.06207		
.06311		
.06403		
.06514		
.06608		
.06705		
.06804		
.06908		
.07007		
.07105		
.07207		
.07307		
.07405		
.07505		
.07607		
.07711		

b,c

TABLE 3-6 (cont)
 MASS AND ENERGY RELEASE RATES
 110 SQUARE INCH COLD LEG BREAK

TIME (SEC)	MASS RATE (LB/S)	ENERGY RATE (BTU/S)
.07804		
.07908		
.08001		
.08108		
.08207		
.08310		
.08403		
.08511		
.08600		
.08705		
.08810		
.08909		
.09005		
.09111		
.09208		
.09310		
.09418		
.09511		
.09607		
.09701		
.09813		
.09904		
.10010		
.10501		
.11001		
.11506		
.12007		
.12509		
.13002		
.13509		
.14003		
.14505		
.15004		
.15506		
.16000		
.16515		
.17020		
.17500		
.18006		
.18506		
.19004		

b,c

TABLE 3-6 (cont)
 MASS AND ENERGY RELEASE RATES
 110 SQUARE INCH COLD LEG BREAK

TIME (SEC)	MASS RATE (LB/S)	ENERGY RATE (BTU/S)
.19505		
.20007		
.21006		
.22003		
.23004		
.24002		
.25016		
.26006		
.27002		
.28001		
.29026		
.30000		
.31013		
.32015		
.33009		
.34001		
.35002		
.36015		
.37004		
.38013		
.39007		
.40007		
.41009		
.42006		
.43011		
.44007		
.45006		
.46006		
.47009		
.48006		
.49008		
.50014		
.51005		
.52010		
.53007		
.54000		
.55003		
.56002		
.57004		
.58007		
.59010		

b,c

TABLE 3-6 (cont)
MASS AND ENERGY RELEASE RATES
110 SQUARE INCH COLD LEG BREAK

TIME (SEC)

.60052
.61003
.62001
.63041
.64006
.65012
.66003
.67008
.68006
.69001
.70012
.71003
.72026
.73003
.74004
.75010
.76004
.77000
.78002
.79021
.80001
.81026
.82006
.83005
.84003
.85000
.86010
.87013
.88024
.89002
.90023
.91000
.92002
.93001
.94015
.95011
.96008
.97002
.98012
.99010
1.00008

b,c

TABLE 3-6 (cont)
MASS AND ENERGY RELEASE RATES
110 SQUARE INCH COLD LEG BREAK

TIME (SFC)	MASS RATE (LB/S)	ENERGY RATE (BTU/S)
1.10006	[]
1.20002		
1.30011		
1.40013		
1.50005		
1.60018		
1.70003		
1.80003		
1.90011		
1.98286		

b,c

3-42

MASS AND ENERGY RELEASE RATES
110 SQUARE INCH COLD LEG BREAK

TABLE 3-7
MASS AND ENERGY RELEASE RATES
110 SQUARE INCH HOT LEG BREAK

TIME (SEC)	MASS RATE (LB/S)	ENERGY RATE (BTU/S)
-----	-----	-----
.00000	[]
.00100		
.00205		
.00303		
.00407		
.00501		
.00603		
.00703		
.00801		
.00910		
.01003		
.01100		
.01200		
.01307		
.01412		
.01503		
.01603		
.01707		
.01803		
.01912		
.02015		
.02109		
.02209		
.02313		
.02403		
.02510		
.02610		
.02721		
.02800		
.02906		
.03004		
.03105		
.03201		
.03304		
.03405		
.03502		
.03606		

b,c

TABLE 3-7 (cont)
 MASS AND ENERGY RELEASE RATES
 110 SQUARE INCH HOT LEG BREAK

TIME (SEC)	MASS RATE (LB/S)	ENERGY RATE (BTU/S)
.03711		
.03810		
.03909		
.04008		
.04107		
.04206		
.04305		
.04405		
.04507		
.04601		
.04711		
.04809		
.04903		
.05010		
.05122		
.05205		
.05301		
.05415		
.05502		
.05605		
.05710		
.05804		
.05916		
.06008		
.06102		
.06203		
.06301		
.06407		
.06532		
.06610		
.06706		
.06806		
.06901		
.07011		
.07106		
.07208		
.07312		
.07401		
.07512		
.07616		
.07708		

b,c

TABLE 3-7 (cont)
 MASS AND ENERGY RELEASE RATES
 110 SQUARE INCH HOT LEG BREAK

TIME (SEC.)	MASS RATE (LB/S)	ENERGY RATE (BTU/S)
.07813		
.07913		
.08008		
.08110		
.08225		
.08305		
.08412		
.08505		
.08611		
.08709		
.08815		
.08901		
.09002		
.09109		
.09205		
.09309		
.09406		
.09513		
.09609		
.09711		
.09815		
.09901		
.10000		
.10506		
.11019		
.11500		
.12000		
.12501		
.13004		
.13506		
.14026		
.14500		
.15002		
.15513		
.16005		
.16518		
.17008		
.17521		
.18001		
.18503		
.19010		

b,c

TABLE 3-7 (cont)
 MASS AND ENERGY RELEASE RATES
 110 SQUARE INCH HOT LEG BREAK

TIME (SEC)	MASS RATE (LB/S)	ENERGY RATE (BTU/S)
.1950A		
.20011		
.21009		
.22002		
.23017		
.24009		
.25016		
.26001		
.27005		
.28009		
.2900A		
.30013		
.31006		
.32003		
.33002		
.34013		
.35007		
.36009		
.37006		
.38016		
.39002		
.40002		
.41001		
.42010		
.4300A		
.44007		
.4500A		
.46002		
.4701A		
.48004		
.49007		
.50011		
.51002		
.52010		
.53012		
.54004		
.55019		
.56007		
.57005		
.58003		
.59002		

b,c

TABLE 3-7 (cont)
 MASS AND ENERGY RELEASE RATES
 110 SQUARE INCH HOT LEG BREAK

TIME (SEC)	MASS RATE (LB/S)	ENERGY RATE (BTU/S)
.60006		
.61010		
.62013		
.63010		
.64007		
.65009		
.66018		
.67002		
.68002		
.69015		
.70008		
.71001		
.72008		
.73010		
.74001		
.75006		
.76002		
.77001		
.78008		
.79011		
.80012		
.81010		
.82001		
.83006		
.84031		
.85020		
.86005		
.87008		
.88004		
.89014		
.90008		
.91003		
.92008		
.93010		
.94012		
.95002		
.96001		
.97021		
.98003		
.99007		
1.00002		

b,c

TABLE 3-7 (cont)
 MASS AND ENERGY RELEASE RATES
 110 SQUARE INCH HOT LEG BREAK

<u>TIME (SEC)</u>	<u>MASS RATE (LB/S)</u>	<u>ENERGY RATE (BTU/S)</u>
1.10006	[]
1.20007		
1.30000		
1.40012		
1.50015		
1.60013		
1.70011		
1.80002		
1.90009		
2.00001		
2.01325		

b,c

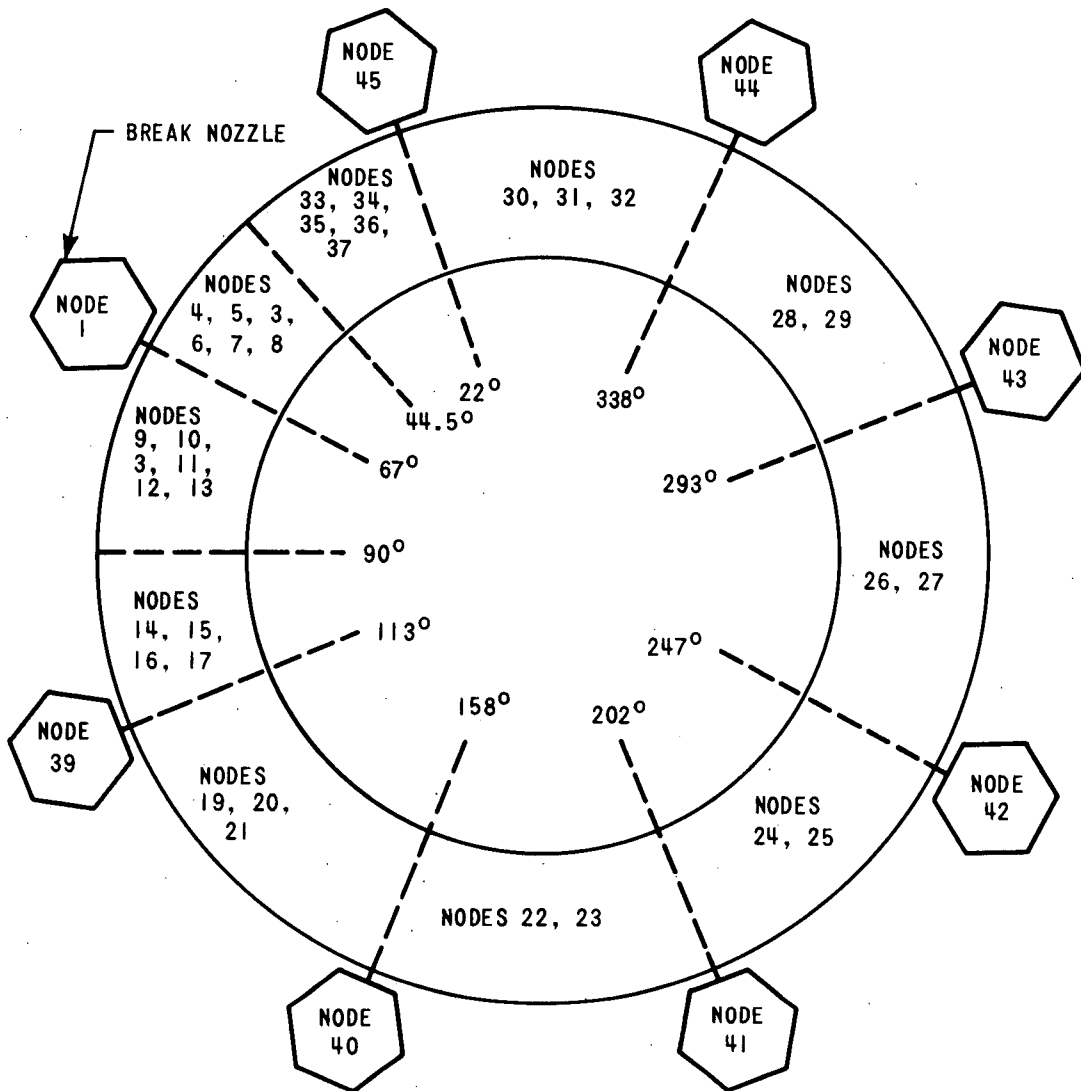
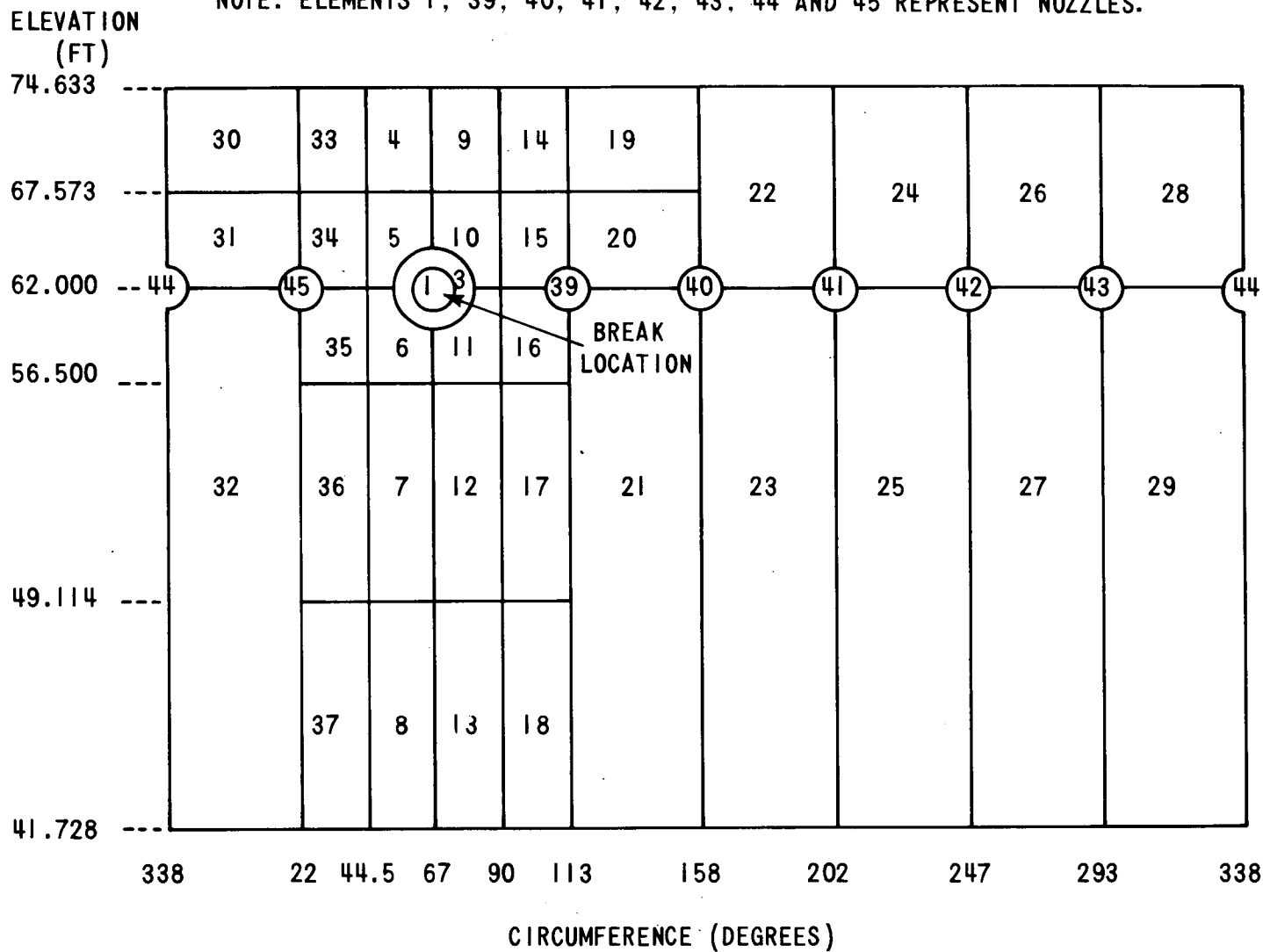


Figure 3-18. Reactor Vessel Annulus Elements (Top View)

NOTE: ELEMENTS 1, 39, 40, 41, 42, 43, 44 AND 45 REPRESENT NOZZLES.



3-50

Figure 3-19. Reactor Vessel Annulus Elements

3-51

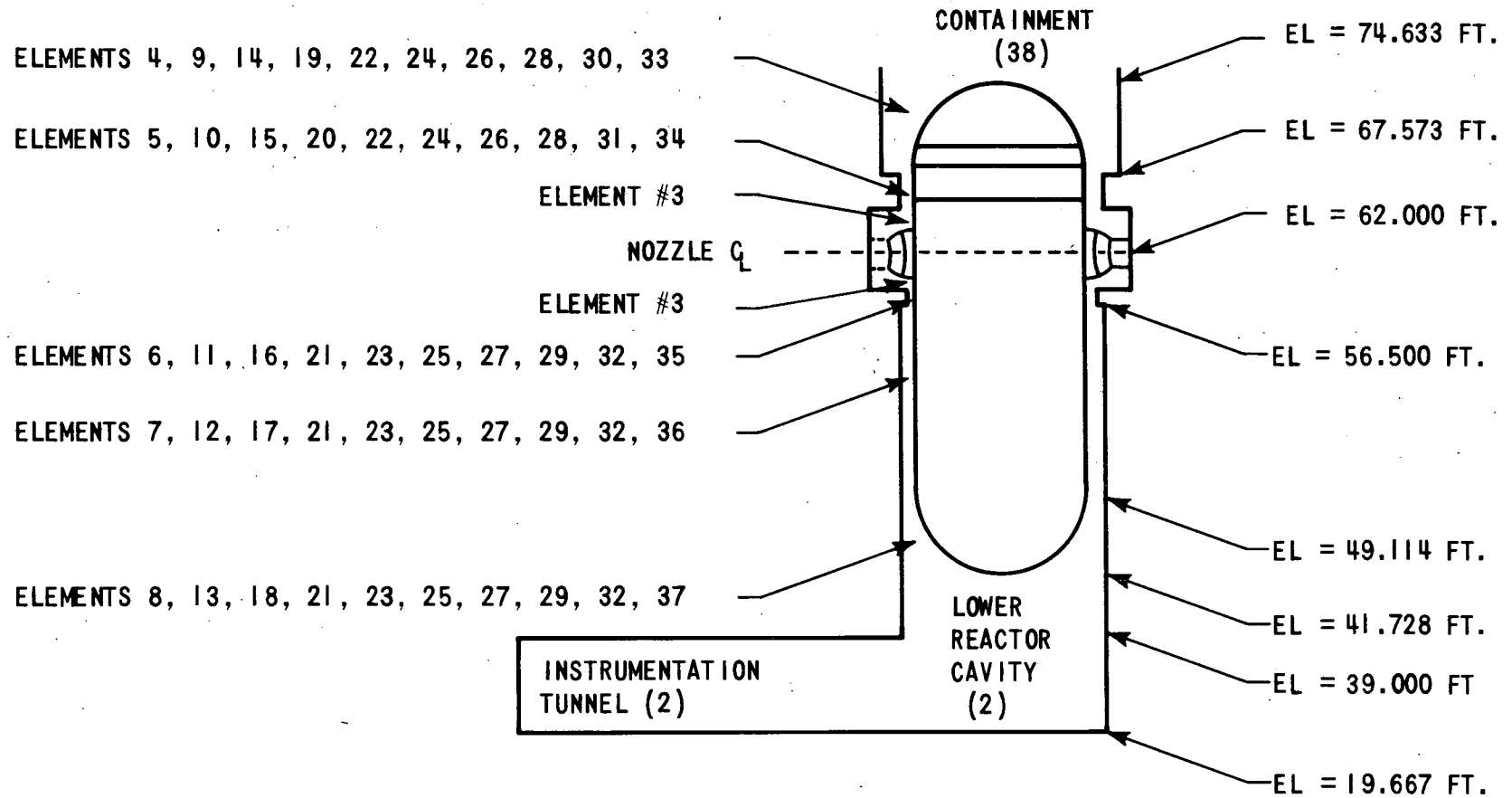


Figure 3-20 Reactor Vessel Annulus Elements (Side View)

Tables 3-8 and 3-9 show the peak pressures and time of peak pressures for all the elements. These tables also conservatively estimate the peak differential pressures acting across the primary shield wall. These tables demonstrate that the pressure gradient is steep near the break location and is very gradual farther away from the break. This indicates that the model must be very detailed close to the break location, but that less detail is required with increasing distance. Figures 3-22a, 3-22b, 3-23a, and 3-23b present for both the inlet and outlet breaks the pressure time histories for the break element (#1) and the reactor vessel annulus element (#3) that experiences the largest pressure following a break. [

b,c

]

TABLE 3-9
PEAK PRESSURES AND TIME OF PEAK PRESSURES
110 SQUARE INCH HOT LEG BREAK

Element	Pressure (Psig)	Time (Sec)	Element	Pressure (Psig)	Time (Sec)
1		b,c	31		b,c
2			32		
3			33		
4			34		
5			35		
6			36		
7			37		
8			38		
9			39		
10			40		
11			41		
12			42		
13			43		
14			44		
15			45		
16			46		
17			47		
18			48		
19			49		
20			50		
21			51		
22			52		
23			53		
24			54		
25			55		
26			56		
27			57		
28			58		
29			59		
30			60		
			61		

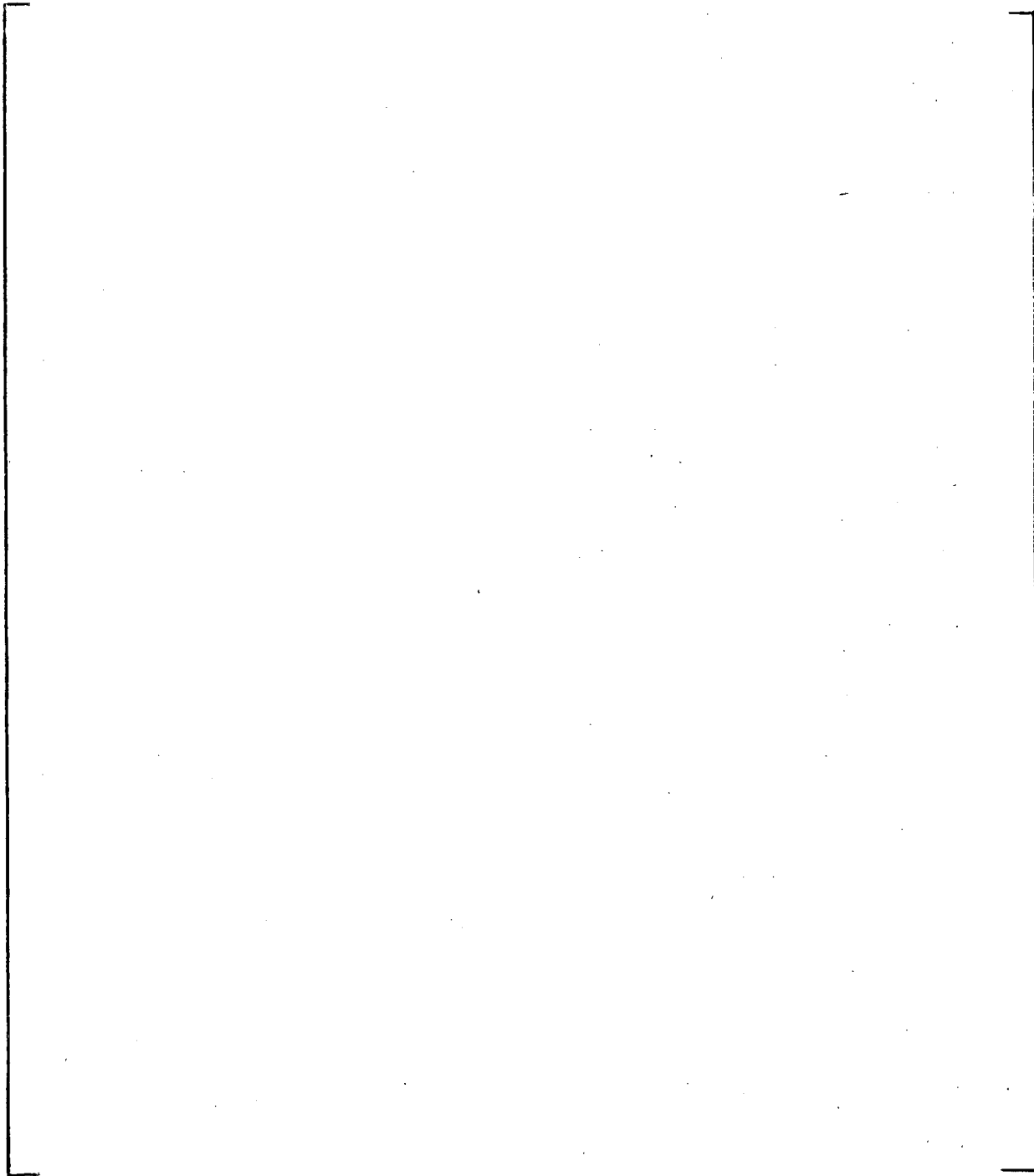


Figure 3-22a. Pressure Time History for the Break Element (#1) 110 in² Cold Leg Break

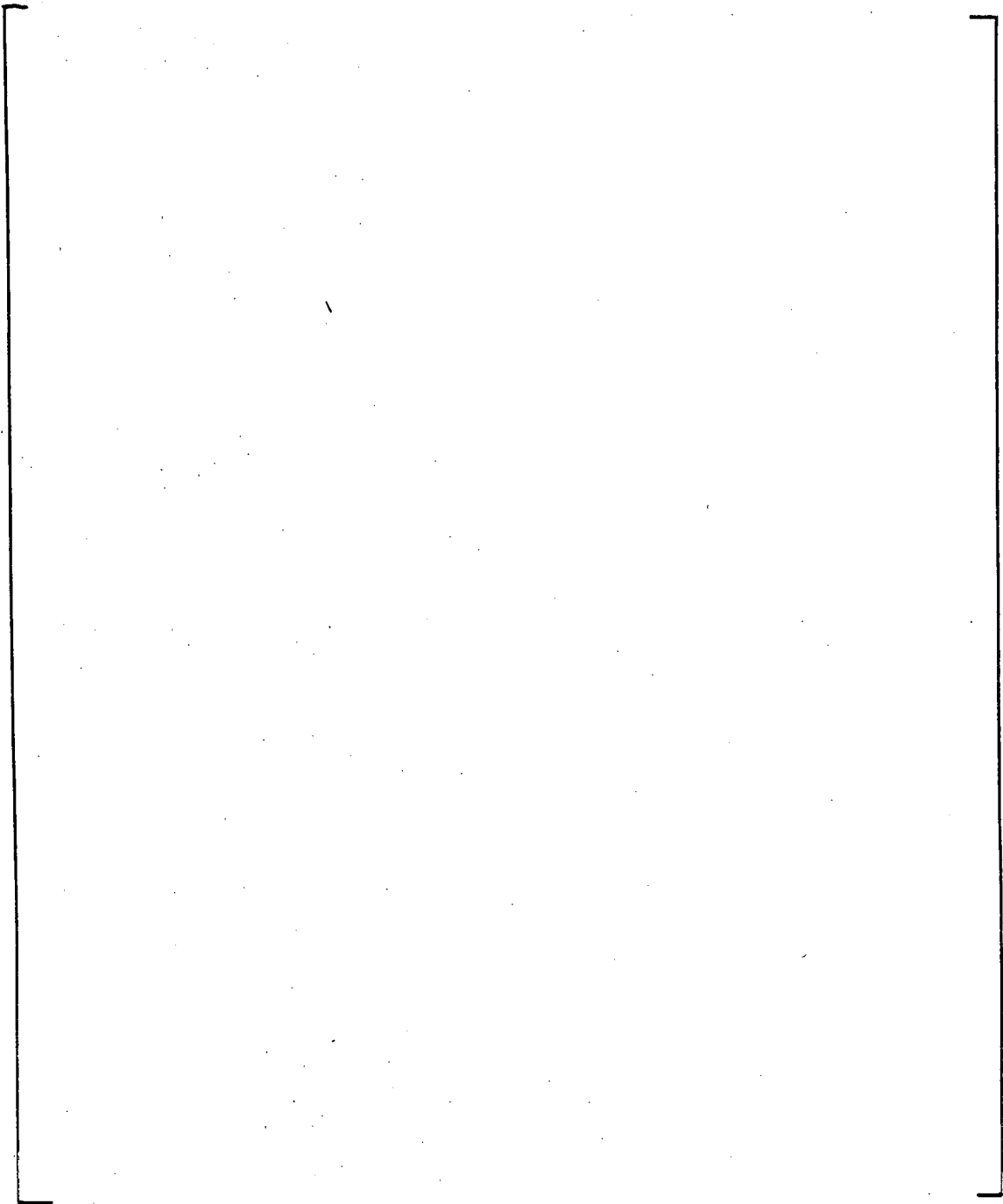


Figure 3-22b Pressure Time History for a Reactor Vessel Annulus Element (#3)
110 in² Cold Leg Break

b,c

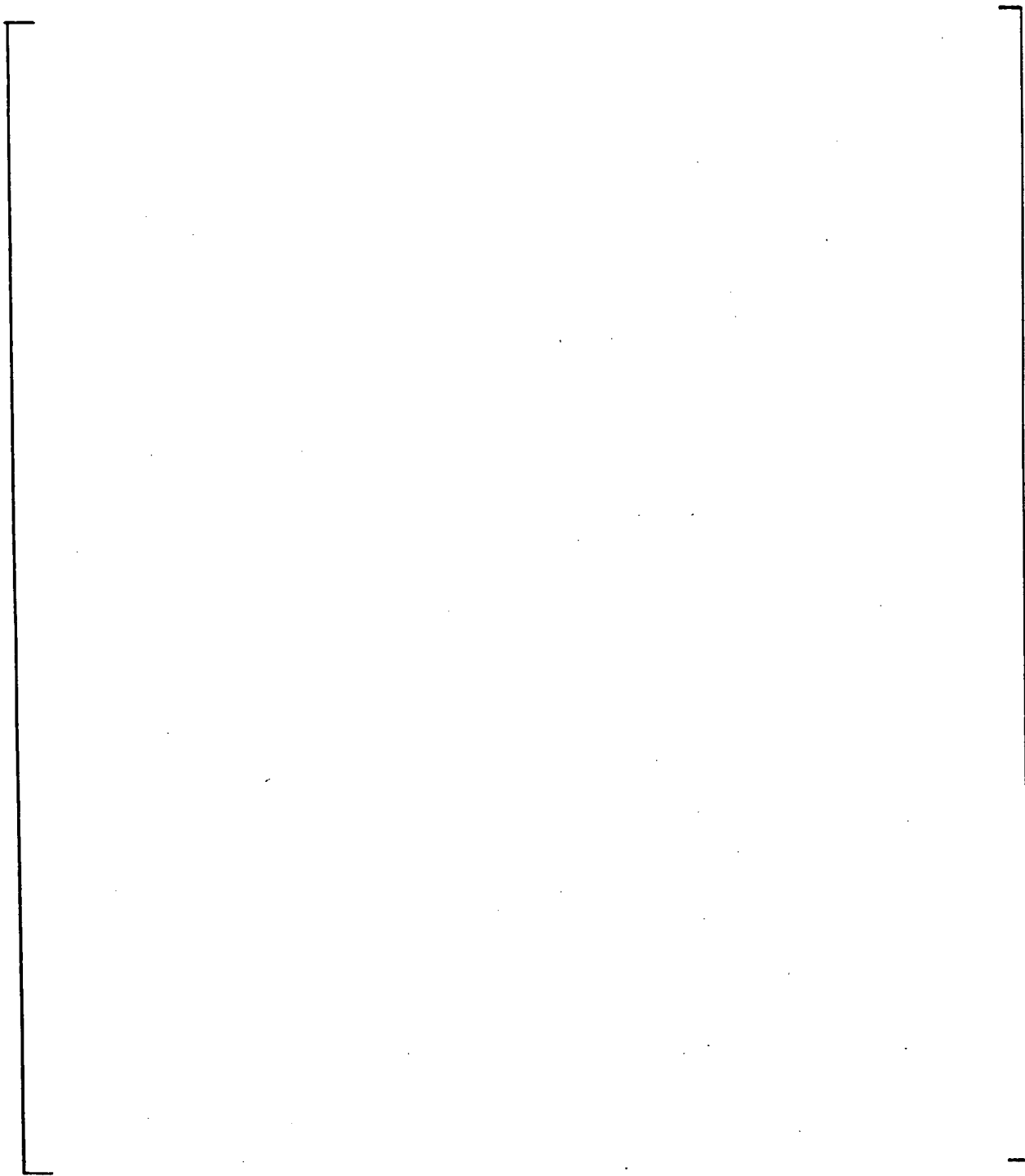
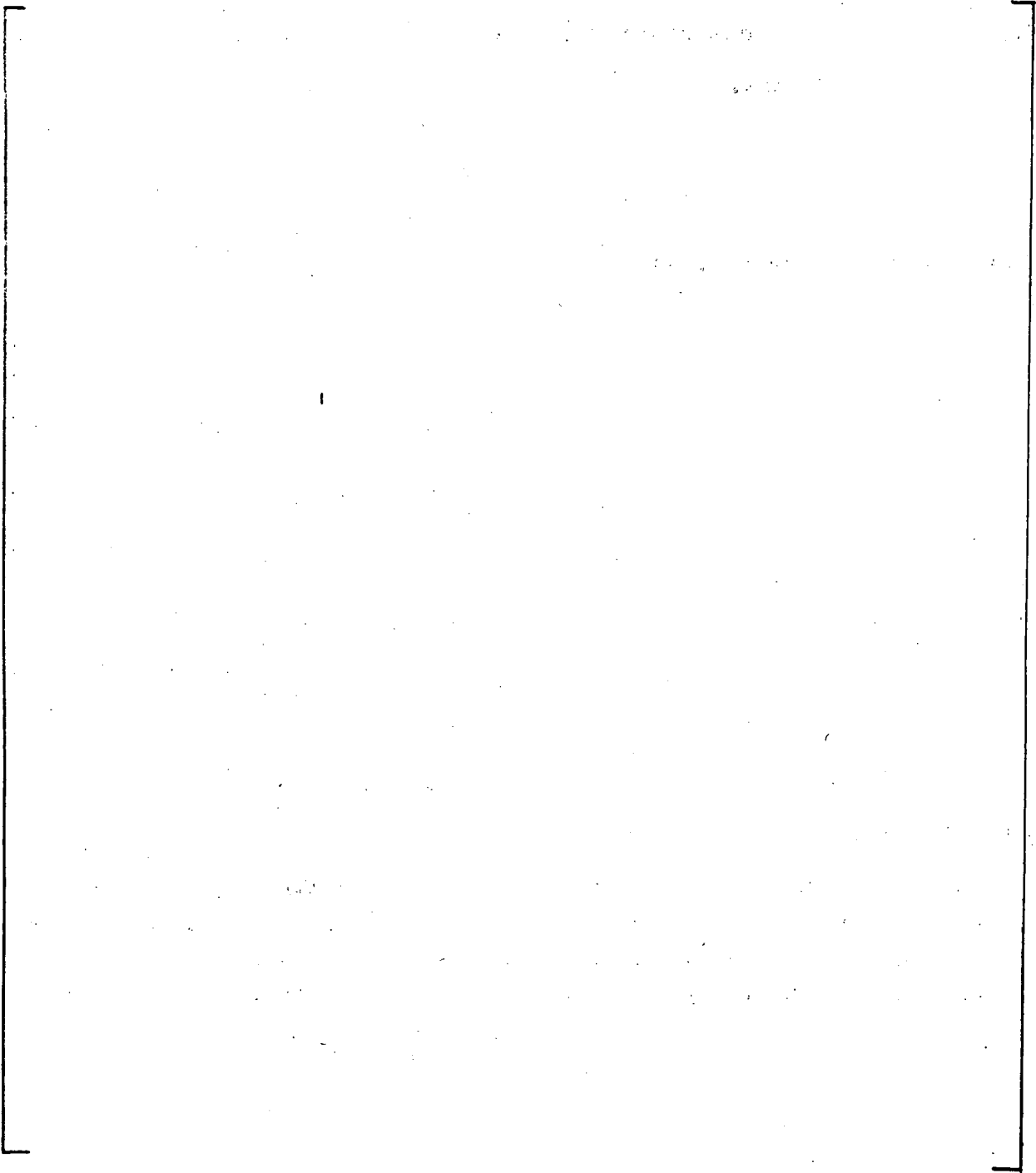


Figure 3-23a Pressure Time History For the Break Element (#1) 110 in² Hot Leg Break



b,c

Figure 3-23b Pressure Time History for a Reactor Vessel Annulus Element (#3)
110 in² Hot Leg Break

3-8. REACTOR COOLANT LOOP PIPING AND SUPPORTS STATIC ANALYSIS

The following paragraphs describe the RCL piping and supports static analysis.

3-9. Purpose of Analysis

[] a,c

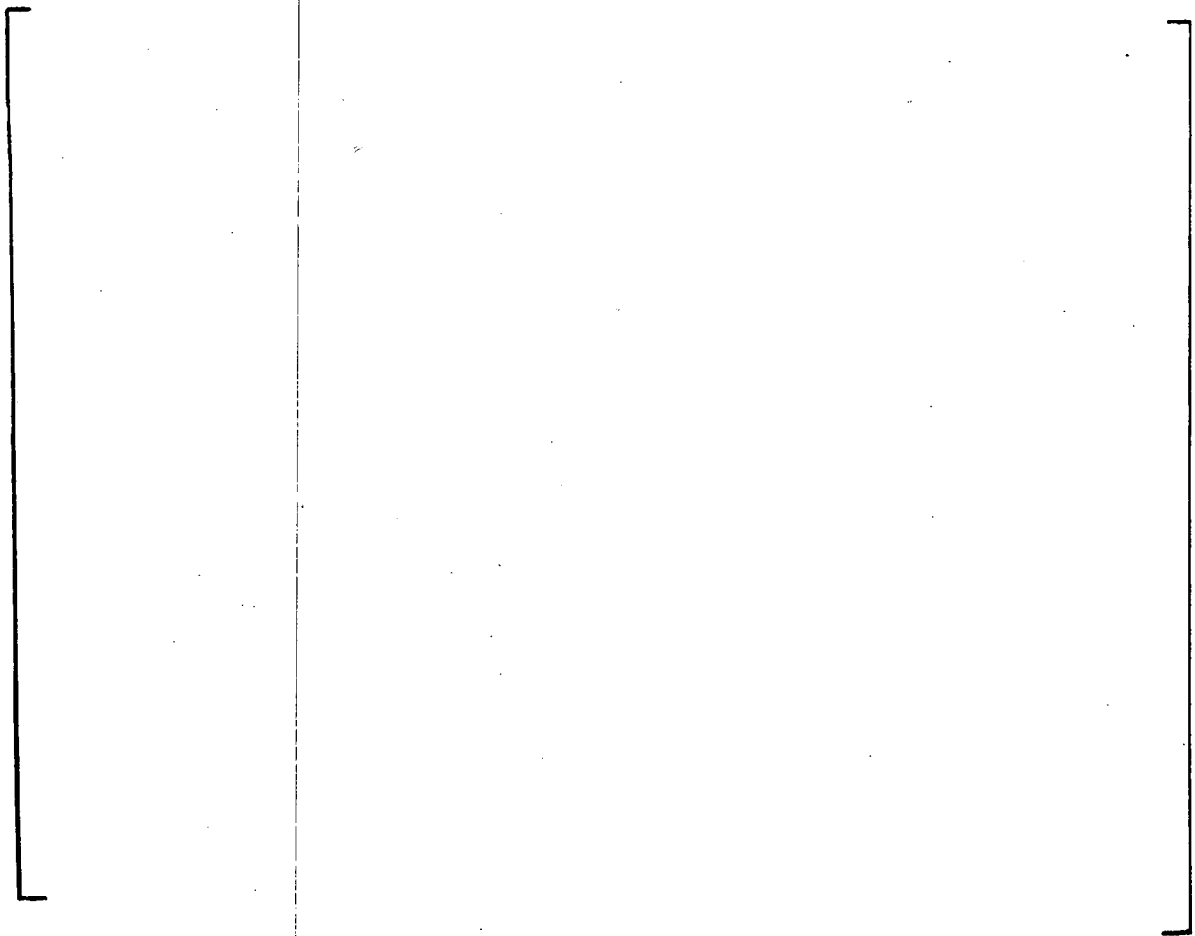
3-10. General Description of Method

[] a,c

3-11. Description of Model

The reactor coolant loop piping, equipment, and supports model was developed for the WECAN computer program⁵. WECAN is a general purpose finite element program developed by Westinghouse. It has a comprehensive element library and the ability to handle large-sized structural problems including gaps, single-acting members, coupled nodes, and plasticity.

[] a,c

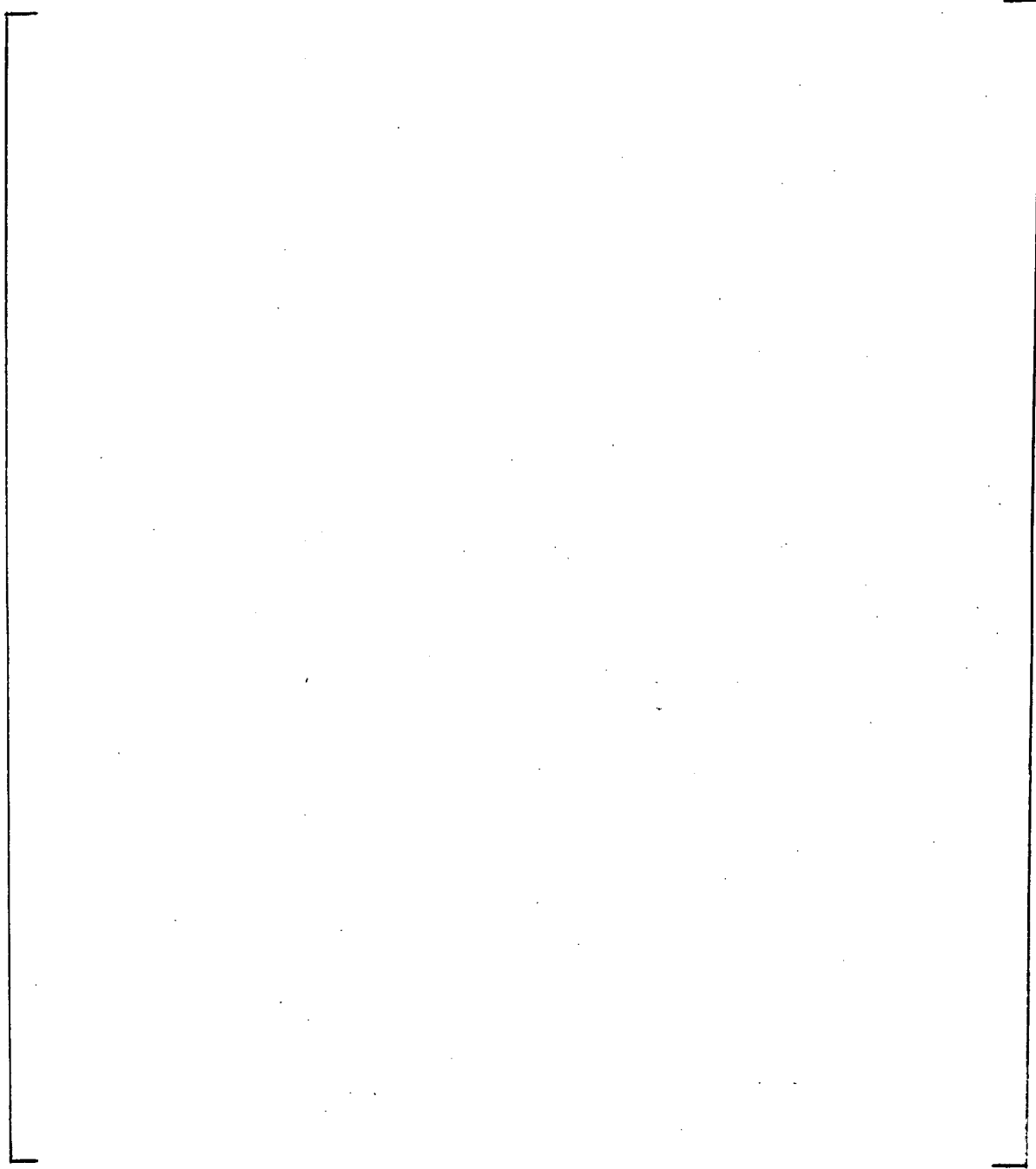


a,c

Figures 3-24 through 3-32 show the overall arrangement of the model including the steam generator and pump supports which are described below. Figure 3-24 shows the plan view of the model with the different loops numbered and node numbers shown. Figure 3-25 is the same view without node numbers showing the break location for the RPV inlet break in loop 31. Figures 3-26 through 3-28 are different views of the overall model. Figures 3-29 and 3-30 show the model for the RPV outlet nozzle break showing the break location and the overall model. Figures 3-31 and 3-32 are views of the RCP and steam generator support models.



a,c



a,c

Figure 3-24. Plan View of Steam Generator and Pump Support Model with Numbered Loops and Nodes

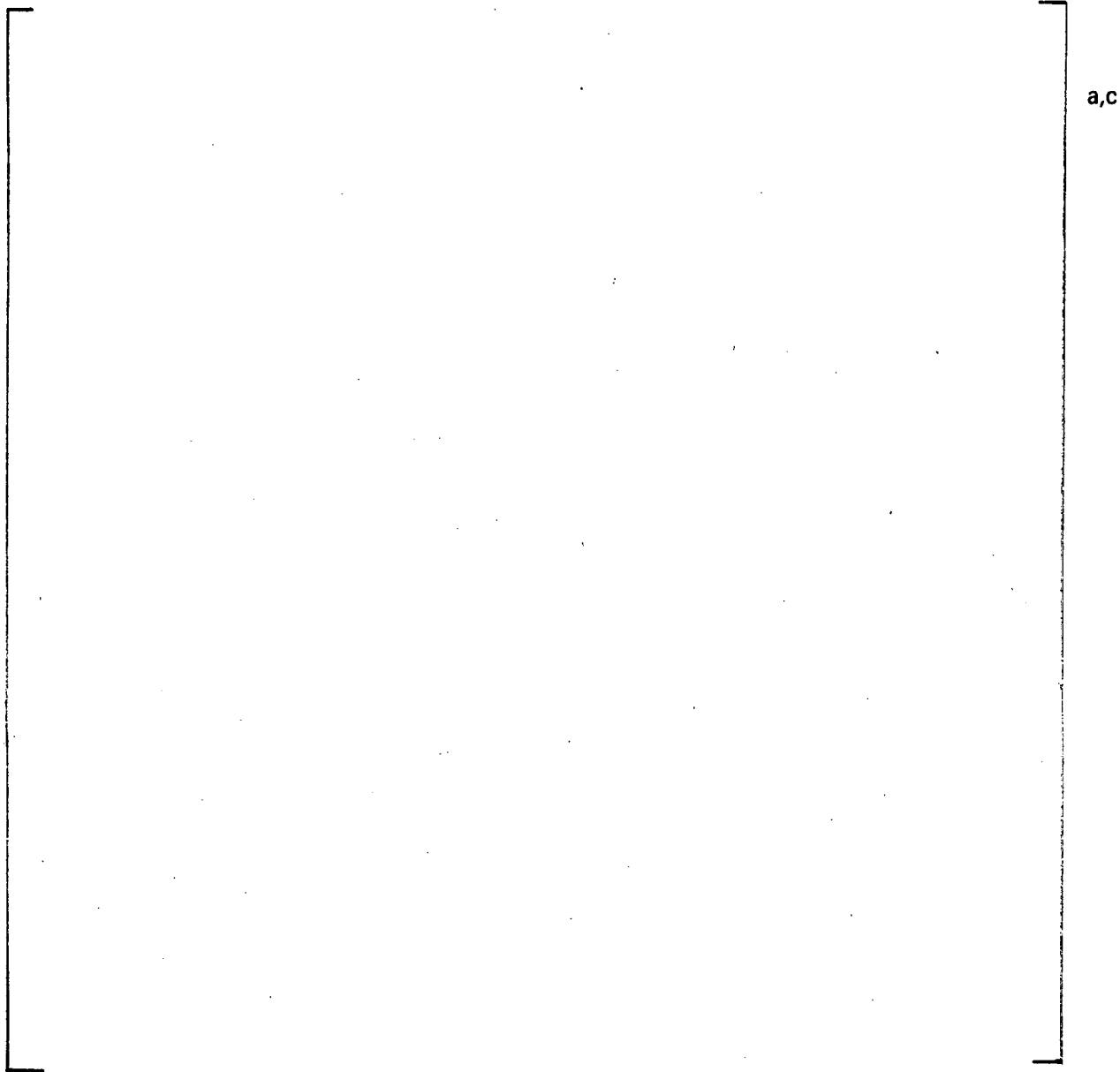
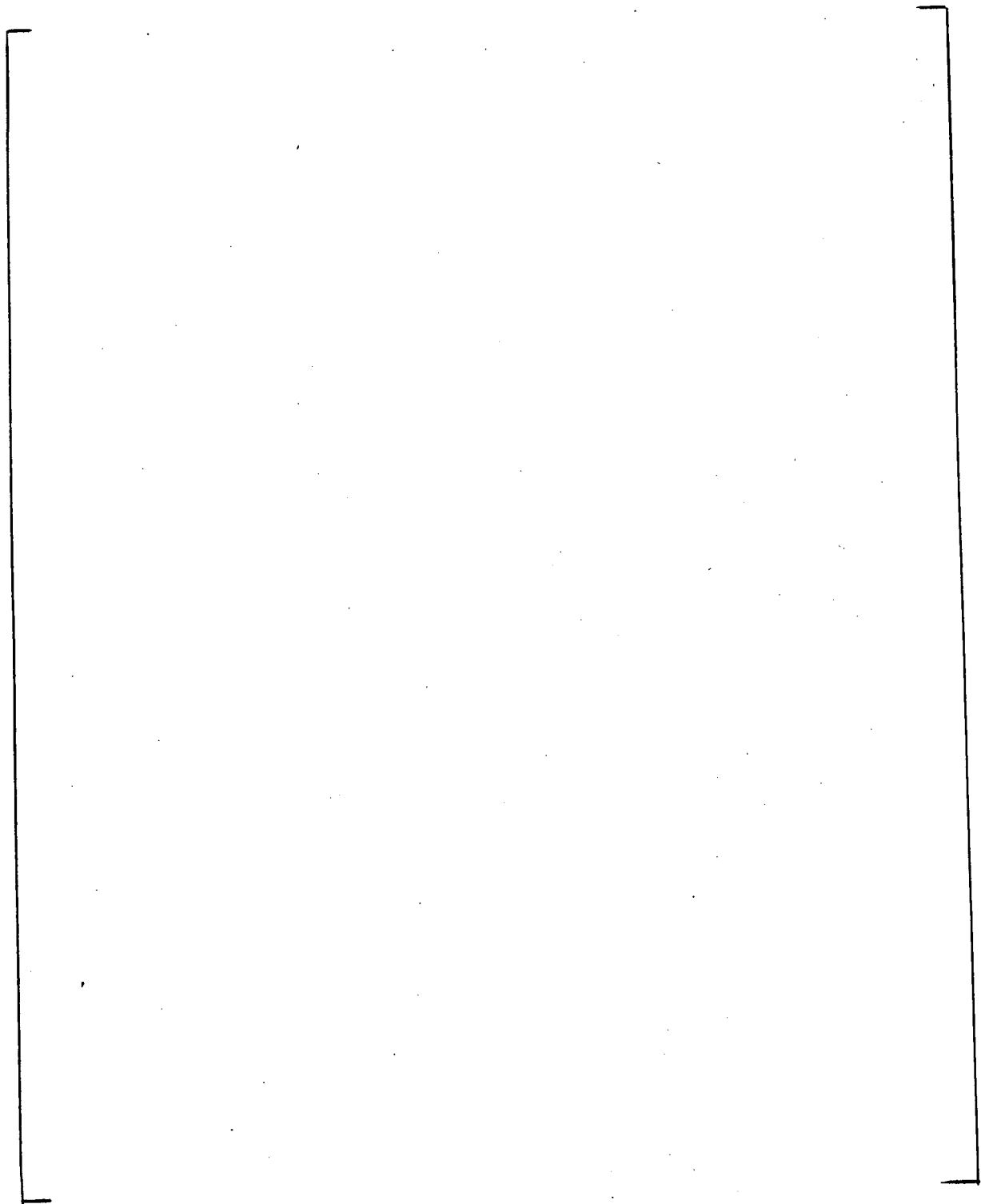


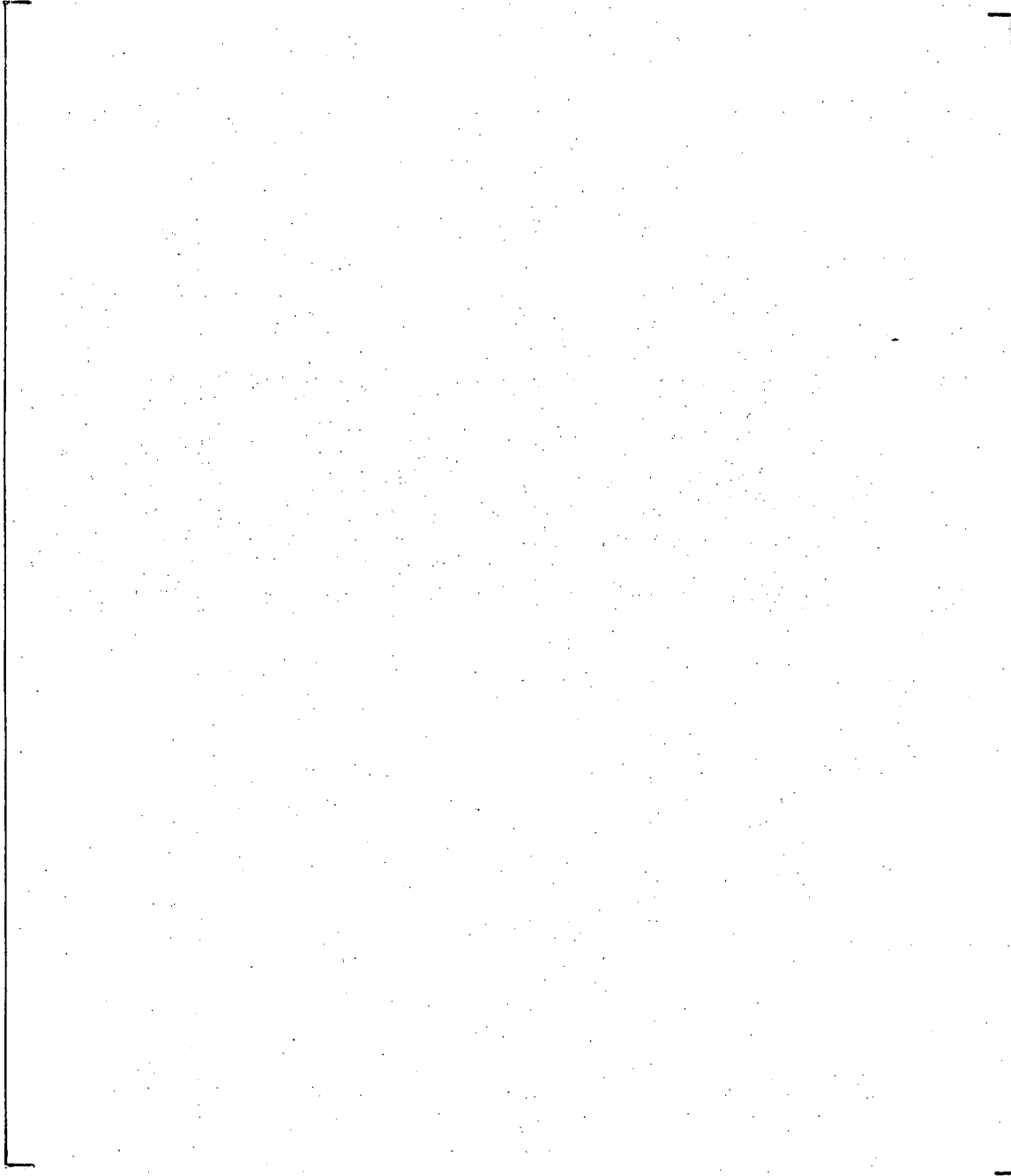
Figure 3-25. Plan View of Reactor Coolant Loop Model
Showing Break Location



a,c



Figure 3-26. Reactor Coolant Loop Support Model (View A)

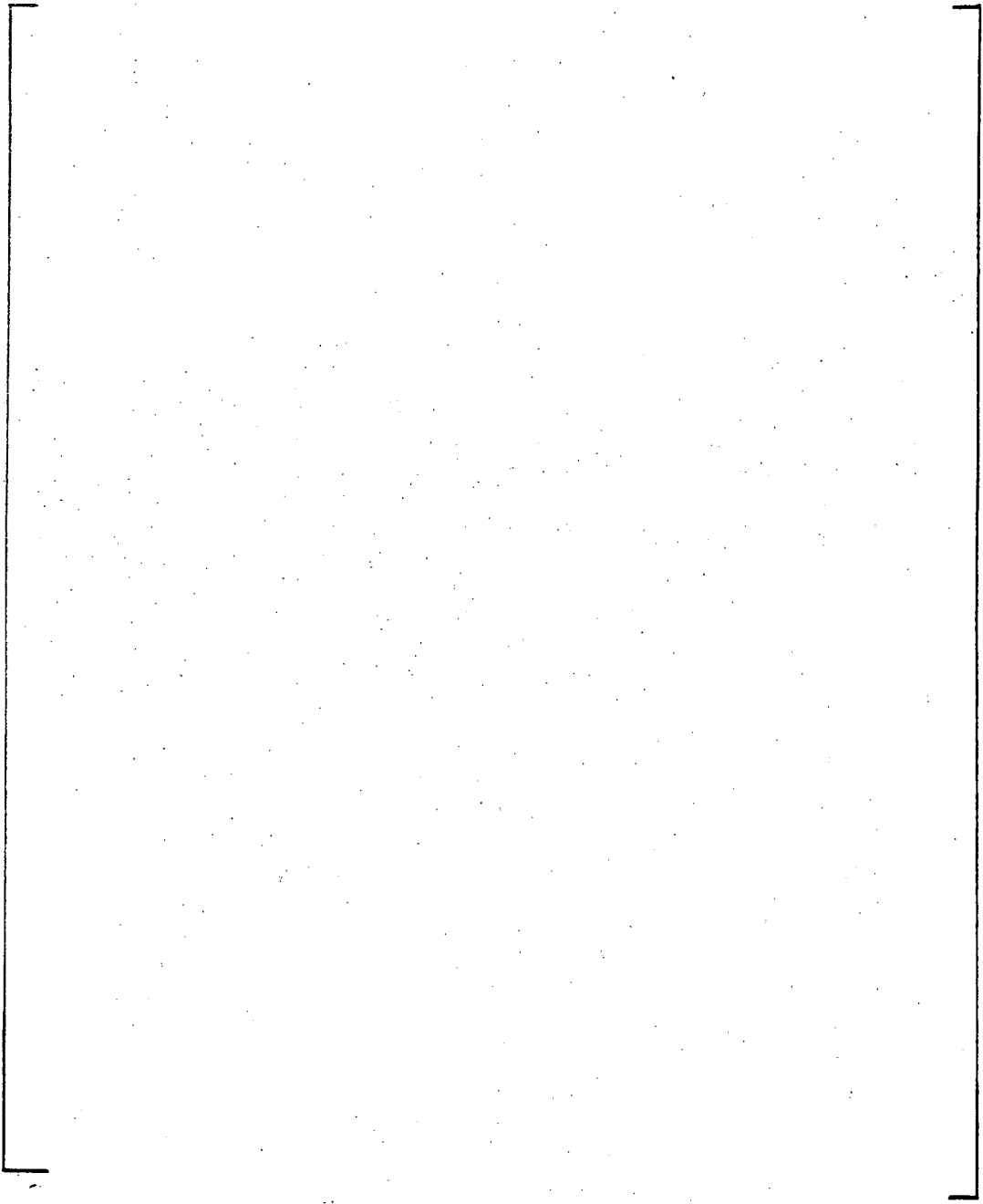


a,c

Figure 3-27. Reactor Coolant Loop Support Model (View B)

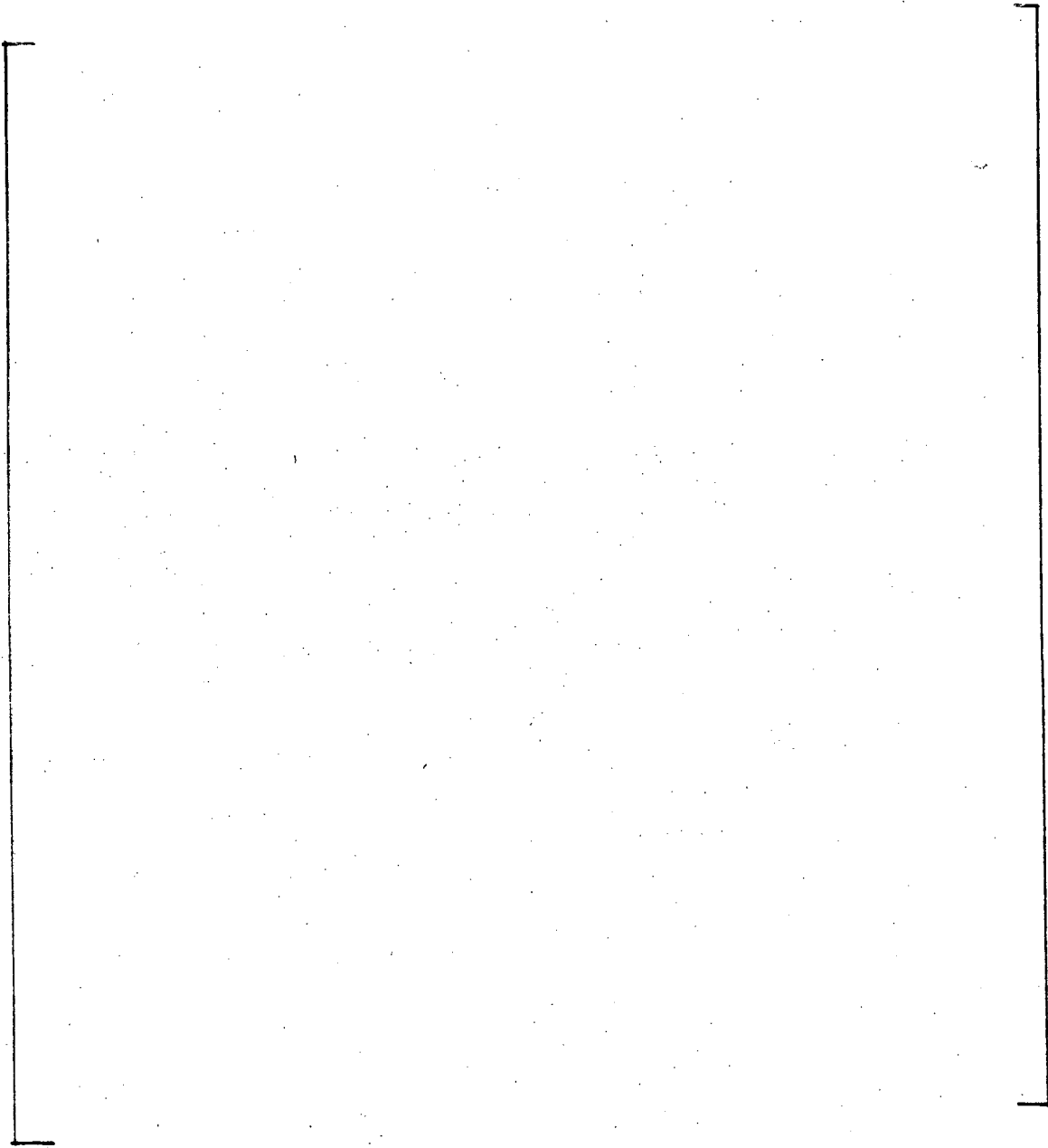
a,c

Figure 3-28. Reactor Coolant Loop Model (View C)



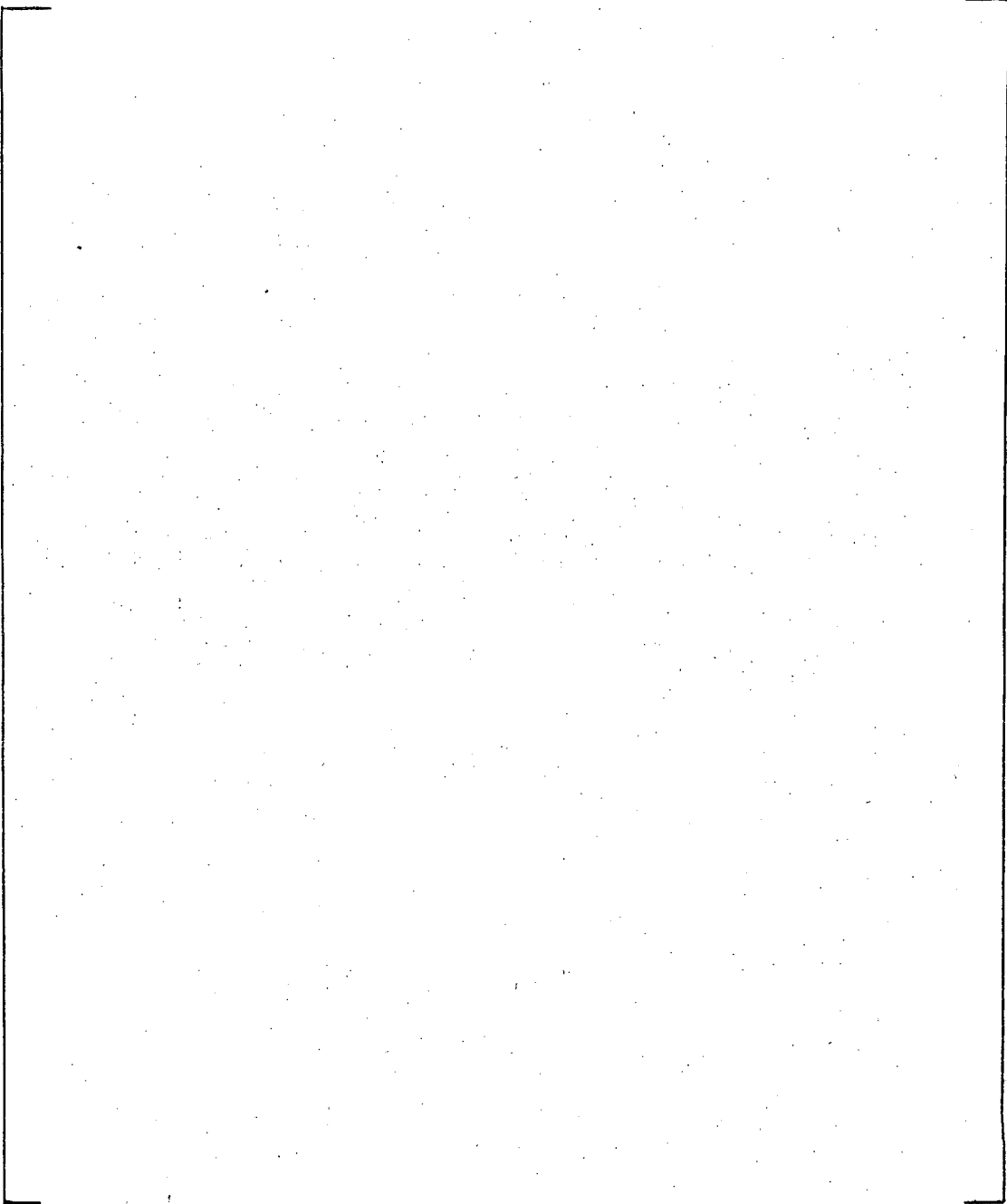
a,c

Figure 3-29. Model of RPV Outlet Nozzle Break Model Showing Break Location



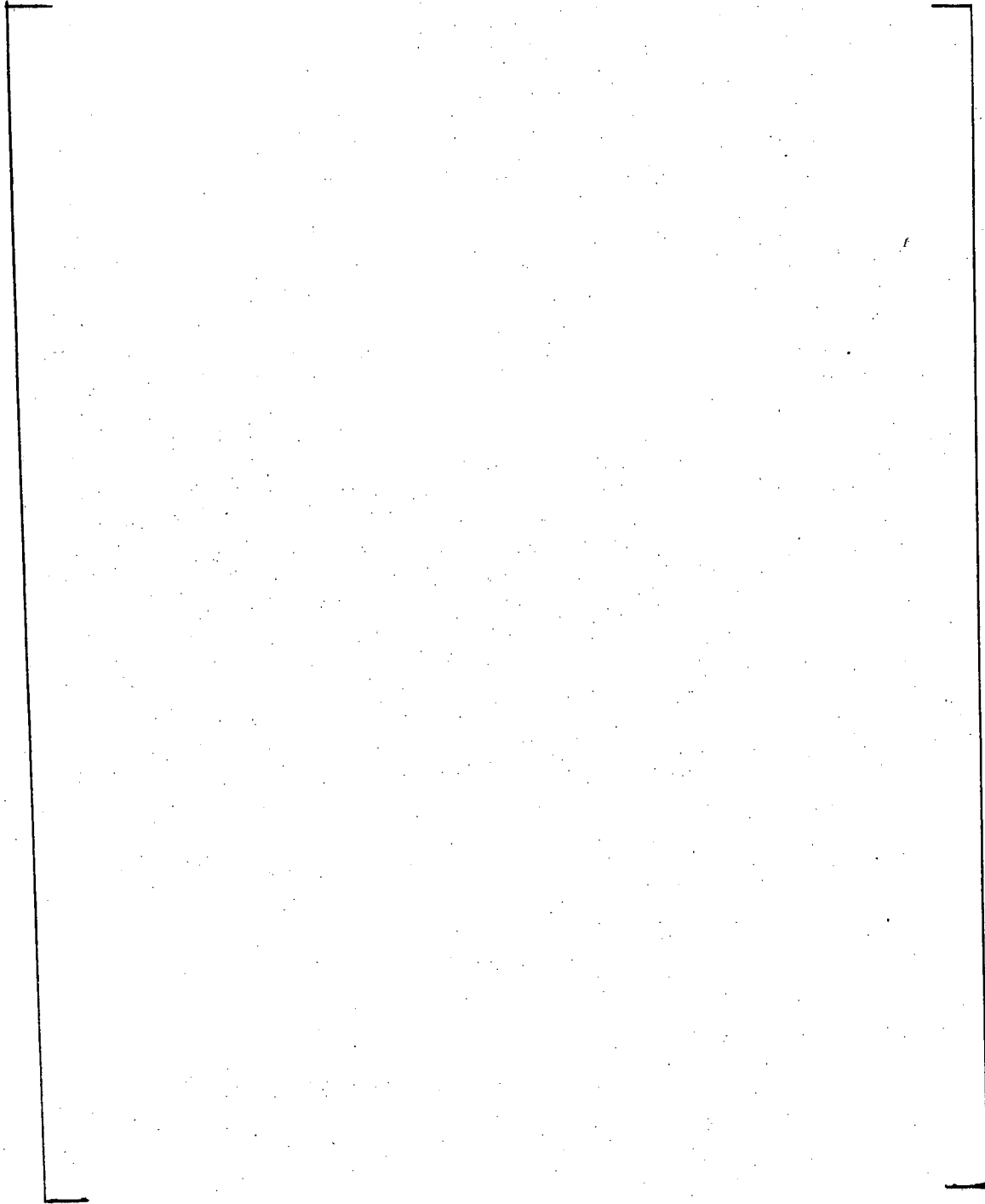
a,c

Figure 3-30. Overall View of RPV Outlet Nozzle Break Model



a,c

Figure 3-31. Steam Generator and Reactor Coolant Pump Support Model (View A)



a,c

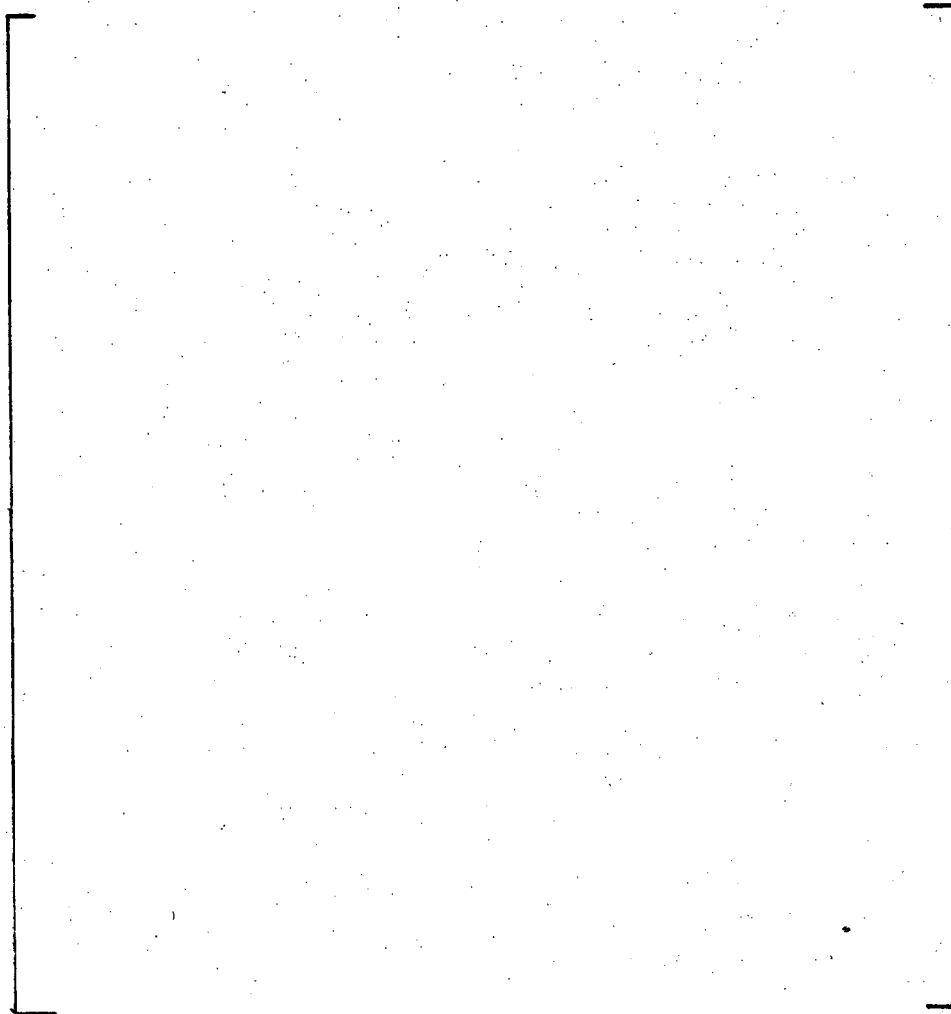
Figure 3-32. Steam Generator and Reactor Coolant Pump Support Model (View B)



The steam generator support is a rectangular, frame-type structure fastened at the bottom to the containment floor, and at the top to the operating floor. This structure gives both vertical and lateral support to the steam generator at the four support pads on the lower steam generator head, plus lateral support just below the transition cone on the steam generator shell. The lower and upper support frame connections to the containment floor and operating decks, respectively, are designed to slide to allow unrestrained thermal displacement of the steam generator during plant heatup. Bumper hard stops at the top and bottom of each of the four vertical columns of the support frame prevent movement of the frame perpendicular to the hot leg. A combination of bumper hard stops and hydraulic snubbers restrain the frame against sudden movements (for example, those caused by a postulated LOCA event) parallel to the hot leg.

The steam generator support structures are constructed mostly from wide flange members with some plate and pipe elements.

The reactor coolant pump receives vertical support from a triangular frame-type structure, and lateral support from tie rods that extend both to the steam generator support and the primary shield wall. The frame rests on a concrete pedestal on the containment floor. The frame base

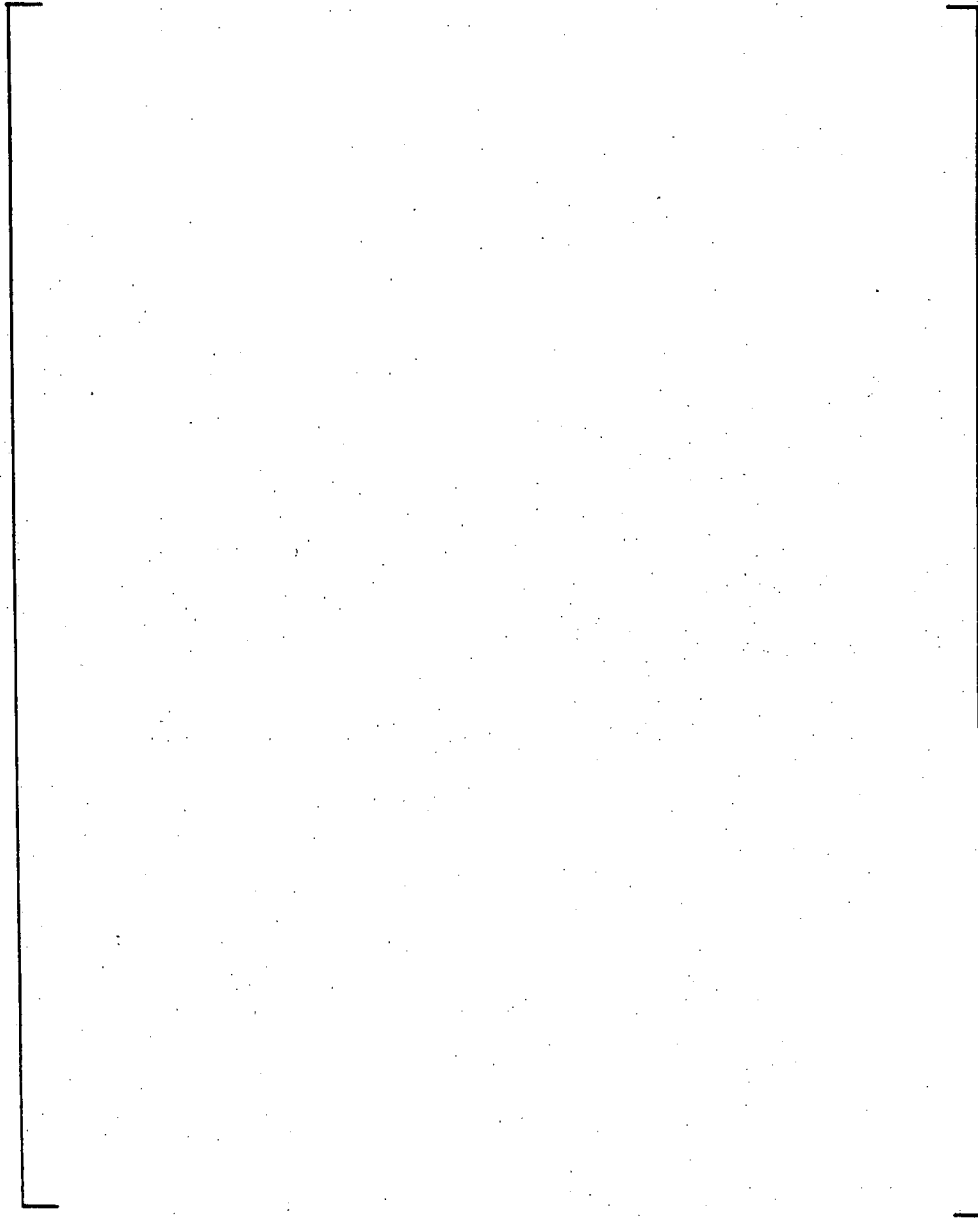


b,c

Figure 3-33a. RCL Load vs. Deflection - RCL Cold Leg Break Without Pipe Displacement Restraints

b,c

Figure 3-33b. RCL Load vs. Deflection - RCL Cold Leg Break
With Pipe Displacement Restraints



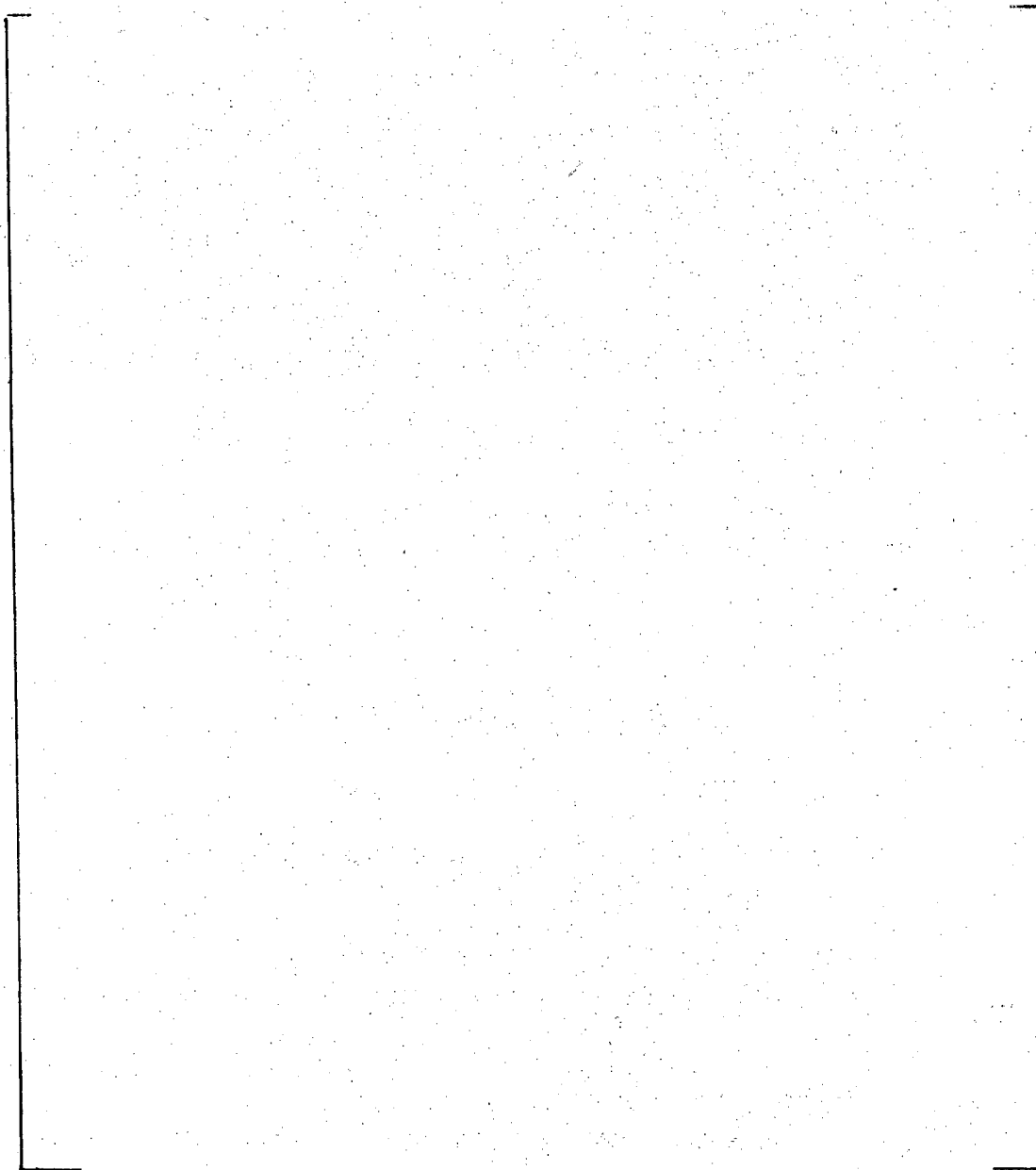
b,c

Figure 3-34 RCL Load vs Deflection
RCL Hot Leg Break
with Pipe Displacement Restraints

plates have oversized anchor bolt holes to allow thermal displacement of the pump during plant heatup.

The pump support frame has pipe columns, and utilizes wide flange shapes and plates for bracing. A large diameter bolt connects each pump foot to a support column.

The reactor vessel is supported by shoes under two inlet and two outlet nozzles. The shoes are mounted on a steel ring girder, which in turn is embedded in the primary shield wall concrete. The shoes permit radial expansion of the reactor vessel, but restrain vessel tangential motion.



a,c

a,c

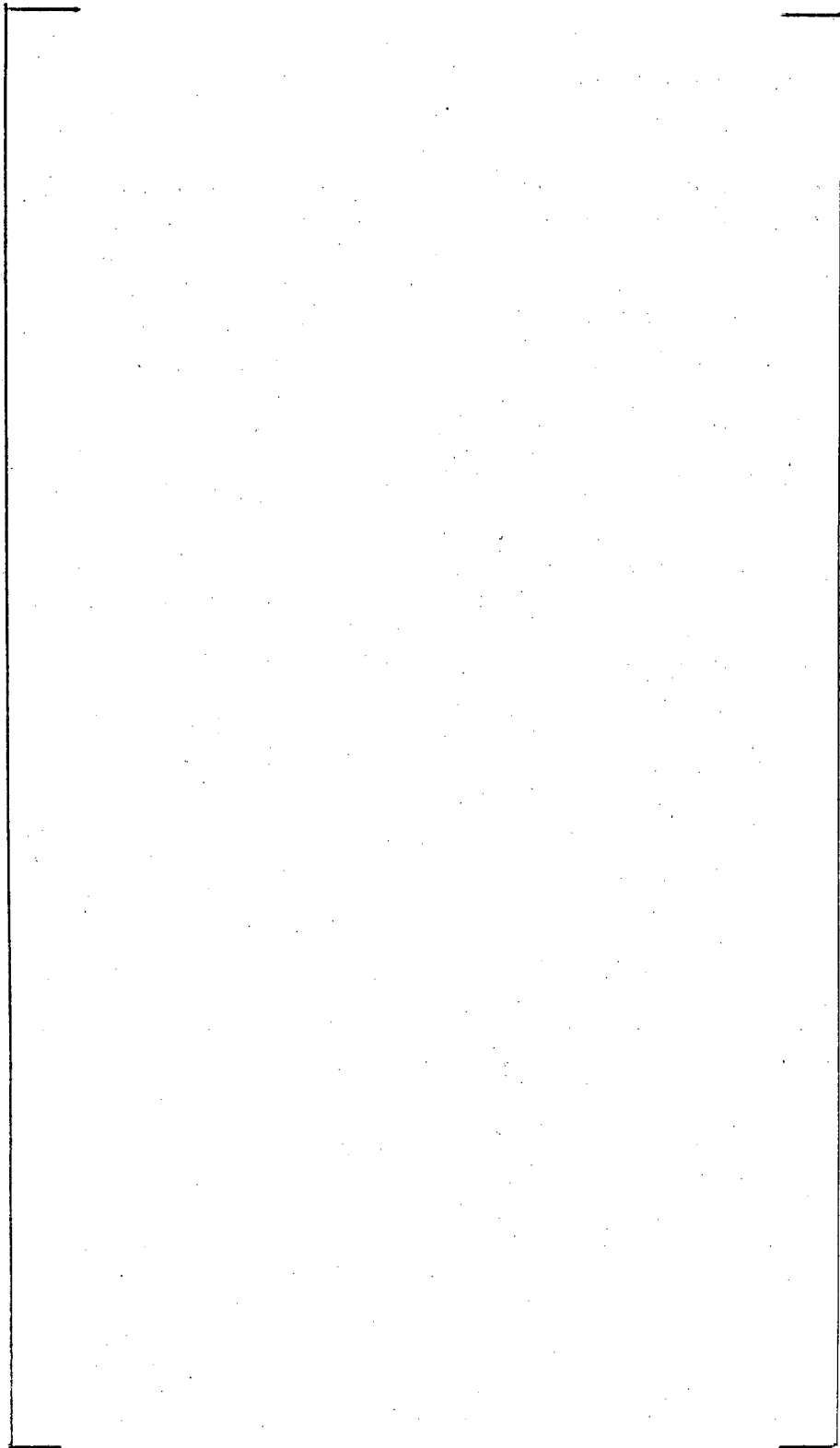
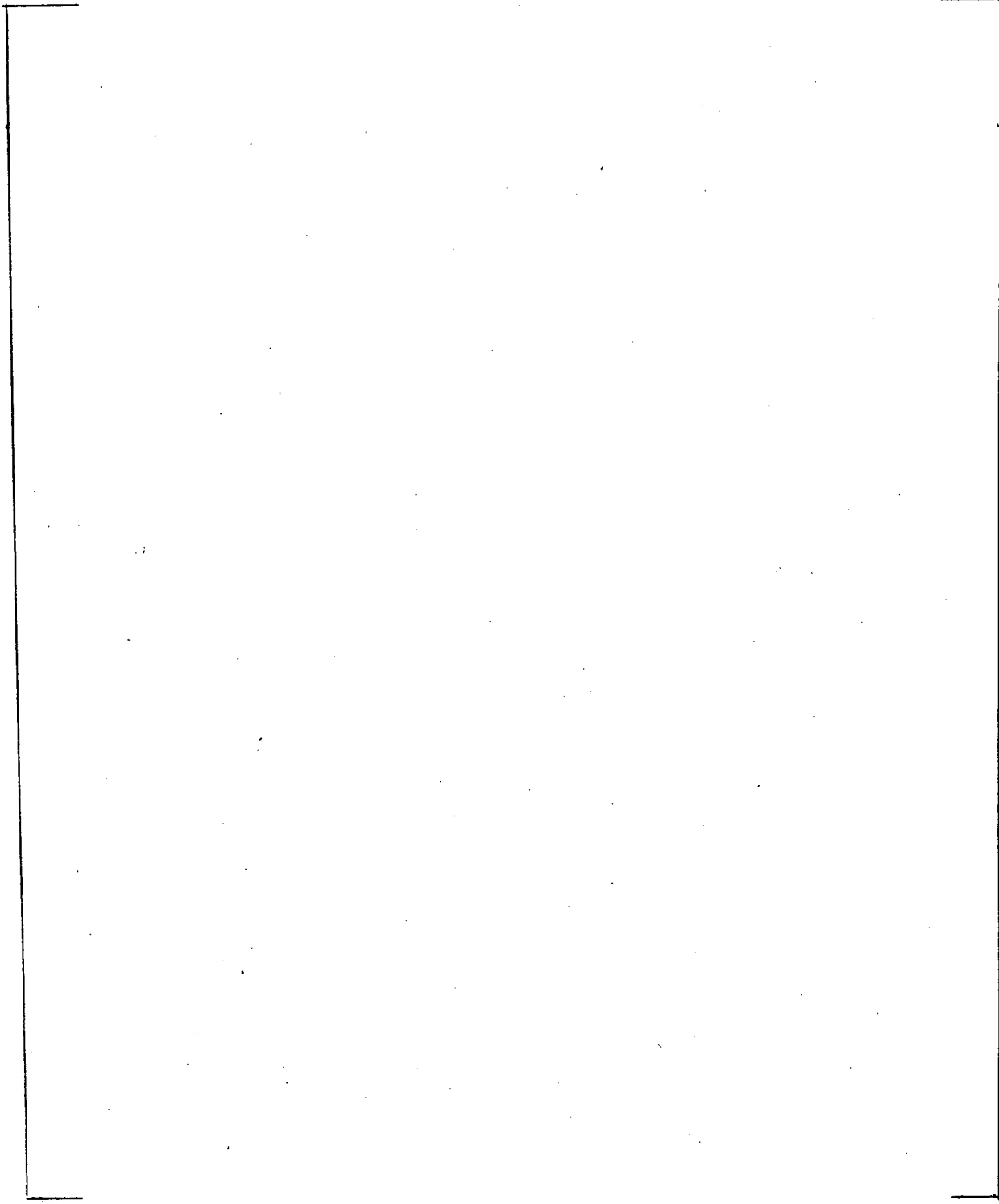


Figure 3-35 Steam Generator Support Model

a,c



a,c



Figure 3-36. Steam Generator Shell/Upper Support Model

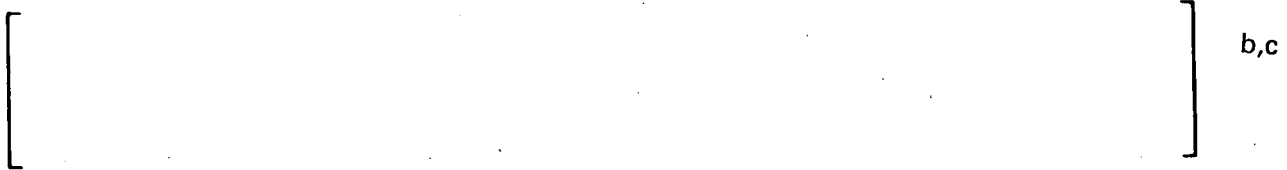
a,c

Figure 3-37. Reactor Coolant Pump Support Model

a,c

3-13. Test Results - Reactor Support Shoes

A test was performed on the reactor vessel support shoe in order to determine its load carrying capability and load-deflection curve. The details of the test are presented in appendix B. Included in the test were the vessel nozzle pad (weld buildup), support shoe, shims, bolts, cooling plate, and ring girder. The test specimens were scaled to 1/8 of the prototype.



A typical resulting load vs. displacement curve which was used in the RPV blowdown analysis is shown in figure 3-38.

3-14. REACTOR PRESSURE VESSEL DYNAMIC ANALYSIS



Three postulated pipe ruptures are considered in this report. They are specifically the pipe breaks at the vessel inlet nozzle, the vessel outlet nozzle and the reactor coolant pump discharge nozzle. The RPV mathematical model is discussed in subsequent sections.

3-15. Mathematical Model and Method

The general assembly of the reactor pressure vessel is shown in figure 1-2. The mathematical model which represents the RPV may be discussed as two, non-linear models connected at a

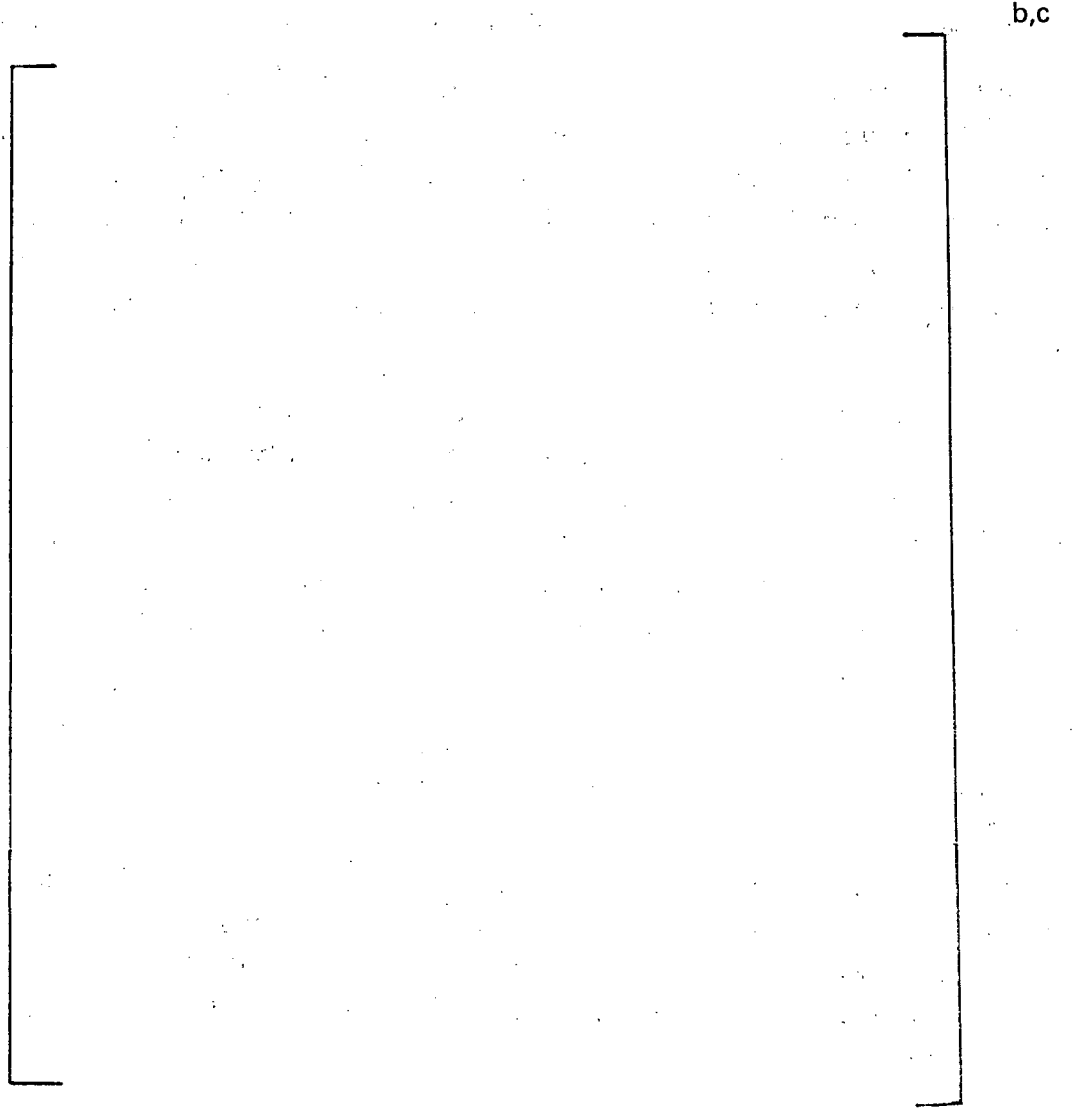


Figure 3-38 Vessel Support Test Load vs Deflection

common node. The one model (WOSTAS) represents the dynamic vertical characteristics of the vessel and its internals, and the other model (DARI) represents the horizontal and rotational characteristics of the vessel in one plane. These two models are combined in the DARI-WOSTAS⁴ code to represent planar motion of the reactor vessel and its internals. The plane of response for postulated breaks is the plane containing the x and y axes of figure 3-2.

The model for horizontal motion (DARI) is shown in figure 3-39. Each node has one translational and one rotational degree of freedom in the vertical plane which contains the broken nozzle centerline. A combination of beam elements and concentrated masses is used to represent the components (including the vessel, core barrel, fuel assemblies, water mass, and upper support columns). All the elements are assumed to lie along the vessel centerline. These components are connected by rigid links, translational impact springs with dashpots, or rotational springs.

The model for vertical motion (WOSTAS) is shown in figure 3-40. Each mass node has one translational degree of freedom. All elements are assumed to lie along a single vertical axis which coincides with the vessel centerline. The structure is represented by concentrated masses, springs, dashpots, gaps, and frictional elements. The model includes: the core barrel, lower support columns, bottom nozzles, skeletons, fuel rods, top nozzles, upper support columns, upper support structure, water mass, and reactor vessel. The core barrel and thermal shields are represented by masses 4, 5, 6, 7 and 8.

Node 1 of the horizontal model (DARI) is coupled to node 2 of the vertical model (WOSTAS). This point represents the intersection of the vessel vertical centerline and the nozzle centerline.

The reactor pressure vessel is restrained by four (4) reactor vessel supports (situated beneath alternate nozzles) and by the attached piping. A schematic of the reactor vessel support mechanism is shown in figure 1-3. These supports are represented as horizontal stiffnesses and vertical stiffnesses. Since the vessel support design does not provide for holddown restraint, the vertical spring acts only in the vertical downward direction.

[] a,c

The DARI-WOSTAS computer code first formulates a set of equilibrium equations for the structural model and then integrates the equations directly. Time-history nodal information obtained from the computer run includes the reactor vessel displacements.

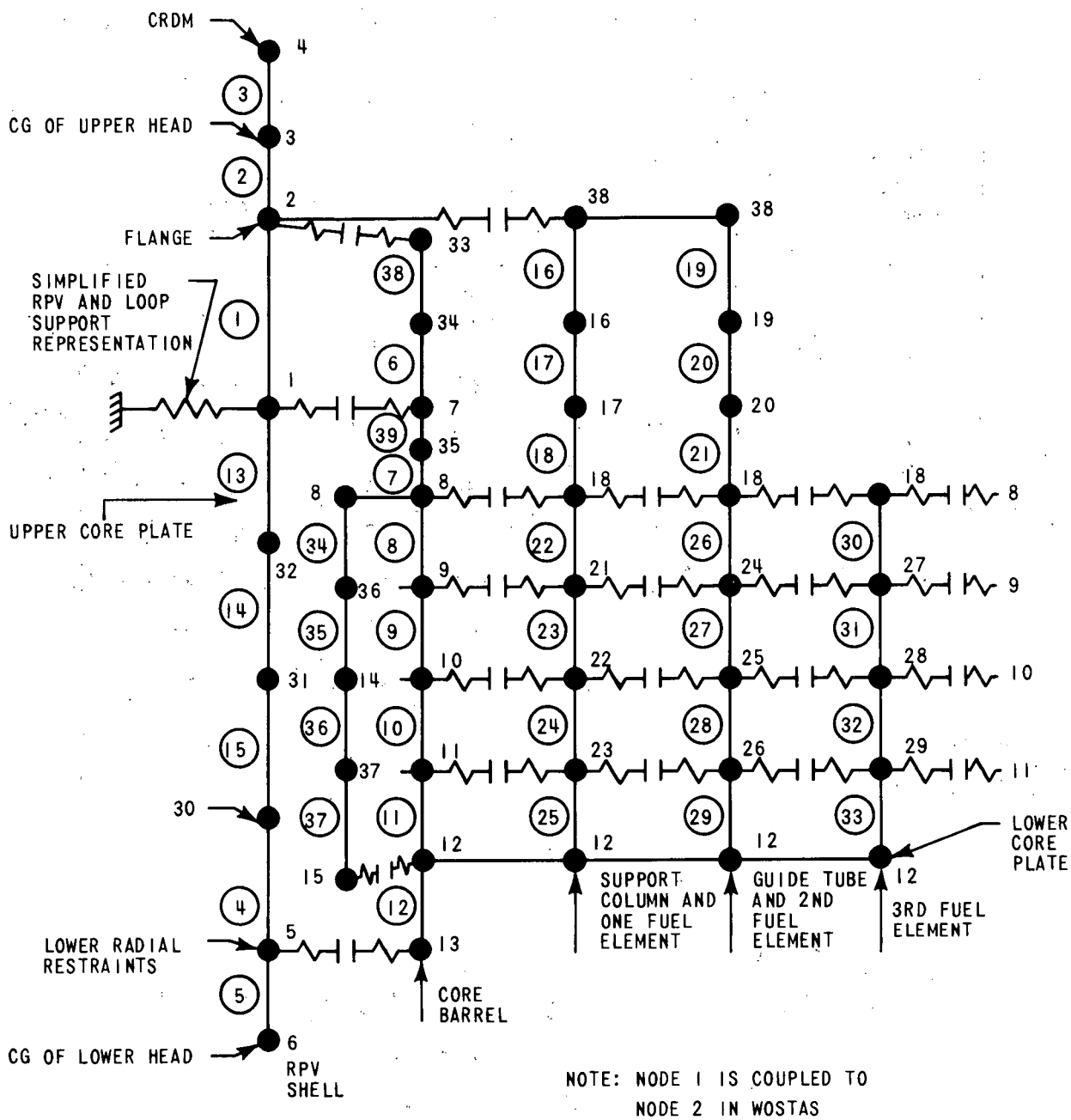


Figure 3-39 DARI Reactor Internals Model

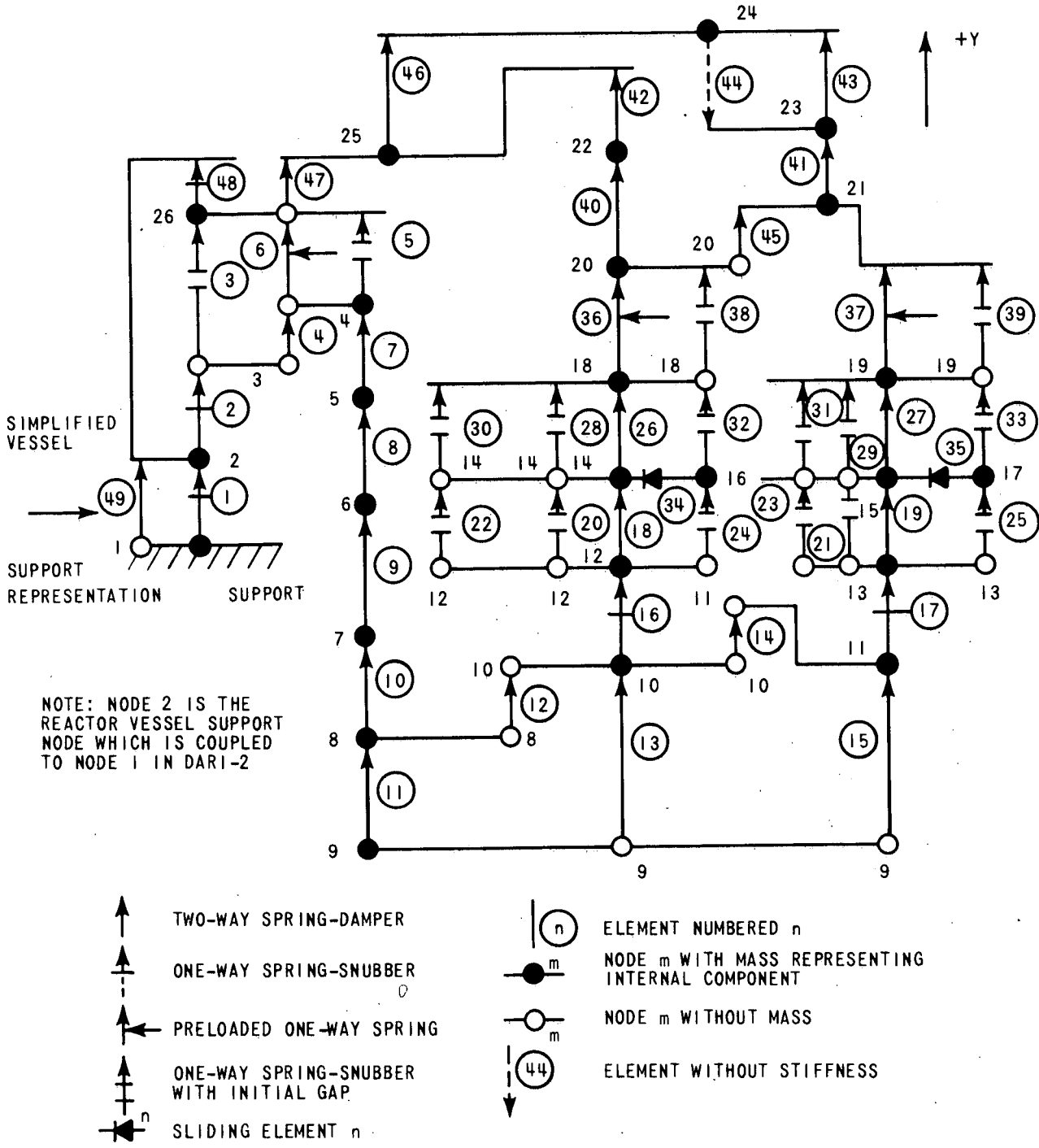


Figure 3-40. Reactor Internals Mathematical Model for WOSTAS Variables

The governing differential equations of motion for nodal freedom are divided into two categories:

- Differential equations describing the transverse vibration of the reactor internals with one translational (u) and one in-plane rotational (θ) freedom per node
- Differential equations describing the vertical vibration of the reactor internals with one vertical displacement freedom per node (y)

The differential equations of both models are:

$$[M] \{\ddot{U}\} + [D] \{\dot{U}\} + [K] \{U\} = \{F\} \quad (3-3)$$

where

$[M]$ = Global inertia matrix

$[D]$ = Global damping matrix

$[K]$ = Global stiffness matrix

$\{\ddot{U}\}$ = Acceleration array

$\{\dot{U}\}$ = Velocity array

$\{U\}$ = Displacement array

$\{F\}$ = Force array, including impact, thrust forces, hydraulic forces, constraints, weight, etc.

Defining a velocity vector, W , the system of second order differential equation (3-1) is reduced to a system of first order equations:

$$\{\dot{U}\} = \{W\} \quad (3-4)$$

$$\{W\} = [M]^{-1} \left[\{F\} - [D] \{W\} - [K] \{U\} \right] \quad (3-5)$$

For the reactor internal structure consisting of n nodes, equations (3-4) and (3-5) define a system of $6n$ simultaneous equations in $6n$ unknowns. The HPCG integration routine developed by IBM is used for the numerical solution of the governing differential equations. This integration routine uses Hamming's modified predictor-corrector method; it is equipped with facilities for automatic starting, numerical stability, and automatic adjustment of integration step size. The HPCG scheme is capable of adjusting the integration time increment to obtain a stable and convergent solution with prescribed accuracy.

Initially, the reactor structure is assumed to be at rest. Prior to the dynamic solution, a static analysis is performed to determine the actual values of the initial vertical displacements which exist due to the preloads, the weight, and the operating initial hydraulic forces in the vertical model. The governing equation for the static solution is obtained from equation (3-5) by neglecting terms involving velocity, acceleration, and impact force with open initial gaps. The

differential equations involving u and θ freedoms are removed. The resulting linear algebraic equations are rearranged in matrix form:

$$[A] \{y\} = \{B\} \quad (3-6)$$

where

$[A]$ = Coefficient matrix

$\{y\}$ = Initial vertical displacement array

$\{B\}$ = Weight plus initial value of hydraulic and constraining forces

The initial values of the vertical displacements are obtained by solving equation (3-6).

In the finite element approach, the structure is divided into a finite number of members or elements. The inertia and stiffness matrices, as well as the force array, are first calculated for each element in the local coordinates. Employing appropriate transformation, the element global matrices and arrays are then computed. Finally, the global element matrices and arrays are assembled into the global structural matrices and arrays, and used for dynamic solution of equation (3-3).

The DARIWOSTAS program employs the following finite element library:

- Two dimensional beam element for the transverse model, connecting two nodes, each with two degrees of freedom (U and θ)
- Pin joint element for the transverse model, connecting two nodes having an equal transverse displacement (u) but different rotations
- Impact elements, with a spring, a damper, and a gap for both vertical and transverse models
- Spring-damper element, with a spring and a damper for both vertical and transverse models
- Double impact element for the transverse model, with springs, dampers, and gaps on both the right and left sides of the node
- Slider element, simulating the friction between the fuel rods in the fuel assembly and the grids
- Rotational spring element

3-16. REACTOR PRESSURE VESSEL LOCA ANALYSIS

The following sections discuss the LOCA analysis on the reactor pressure vessel.

3-17. Vessel Displacements

The severity of a postulated break in a reactor coolant system is related to two factors: the distance from the reactor vessel to the break location, and the break opening area. Pipe breaks further away from the reactor vessel are less severe because the pressure wave attenuates as it propagates toward the reactor vessel. The nature of the reactor vessel decompression following a LOCA, as controlled by the internal structural configuration previously discussed, results in larger reactor internal hydraulic forces for pipe breaks in the cold leg than in the hot leg (for breaks of similar area and distance from the RPV). Therefore pipe breaks at the reactor vessel inlet nozzle are more severe, due to the absence of pressure wave attenuation and due to the structural configuration of the core. Since reactor cavity pressurization effects occur only for postulated pipe breaks at the vessel nozzles, the vessel LOCA response for breaks outside the primary shield wall are controlled by internal reaction forces. Of the breaks outside the shield wall, the pump discharge break is the most severe because it has the highest internal loads. Three pipe rupture locations were analyzed: 1) RPV inlet nozzle safe end, 2) RPV outlet nozzle safe end and 3) reactor coolant pump outlet nozzle terminal end.

All the loads that would result from the break described in section 3-1 were applied to a DARIWOSTAS model of the reactor pressure vessel. All input to the analysis was specifically applicable to the Indian Point 3 Plant.

[] a,c

The results of the analyses are summarized in tables 3-10 and 3-11. The tables present the maximum reactor vessel displacements and maximum reactor vessel pad support loads.

Figure 3-41 is included to identify both the coordinate system for displacements and the support pad numbering scheme.

The reactor vessel support loads are used to verify the adequacy of the reactor vessel support mechanism, as discussed in section 4-9. Core plate motions are employed in the evaluation of the reactor core, as discussed in section 4-13. The reactor vessel displacements are applied to the reactor coolant loop model; this analysis is discussed in section 4-8.

3-18. Postulated RPV Inlet Nozzle Break

An analysis was performed for a 110-square-inch guillotine reactor vessel inlet nozzle break. The peak RPV horizontal displacement, vertical displacement, and rotation are [] inch, [] inch, and [] radian, respectively. Time-history displacements of the RPV are shown in figures 3-42 through 3-44. The upper and lower core plate horizontal displacements are shown in figures 3-45 and 3-46 respectively. b,c b,c

**TABLE 3-10
MAXIMUM RPV DISPLACEMENTS**

	Horizontal (in.)	Vertical (in.)	Rotation (rad)
RPV Inlet Break	[]]
RPV Outlet Break			
RCP Outlet Break			

b,c

**TABLE 3-11
MAXIMUM RPV SUPPORT LOADS**

	Horizontal (kip)	Vertical (kip)
RPV Inlet Break	[]
RPV Outlet Break		
RCP Outlet Break		

b,c

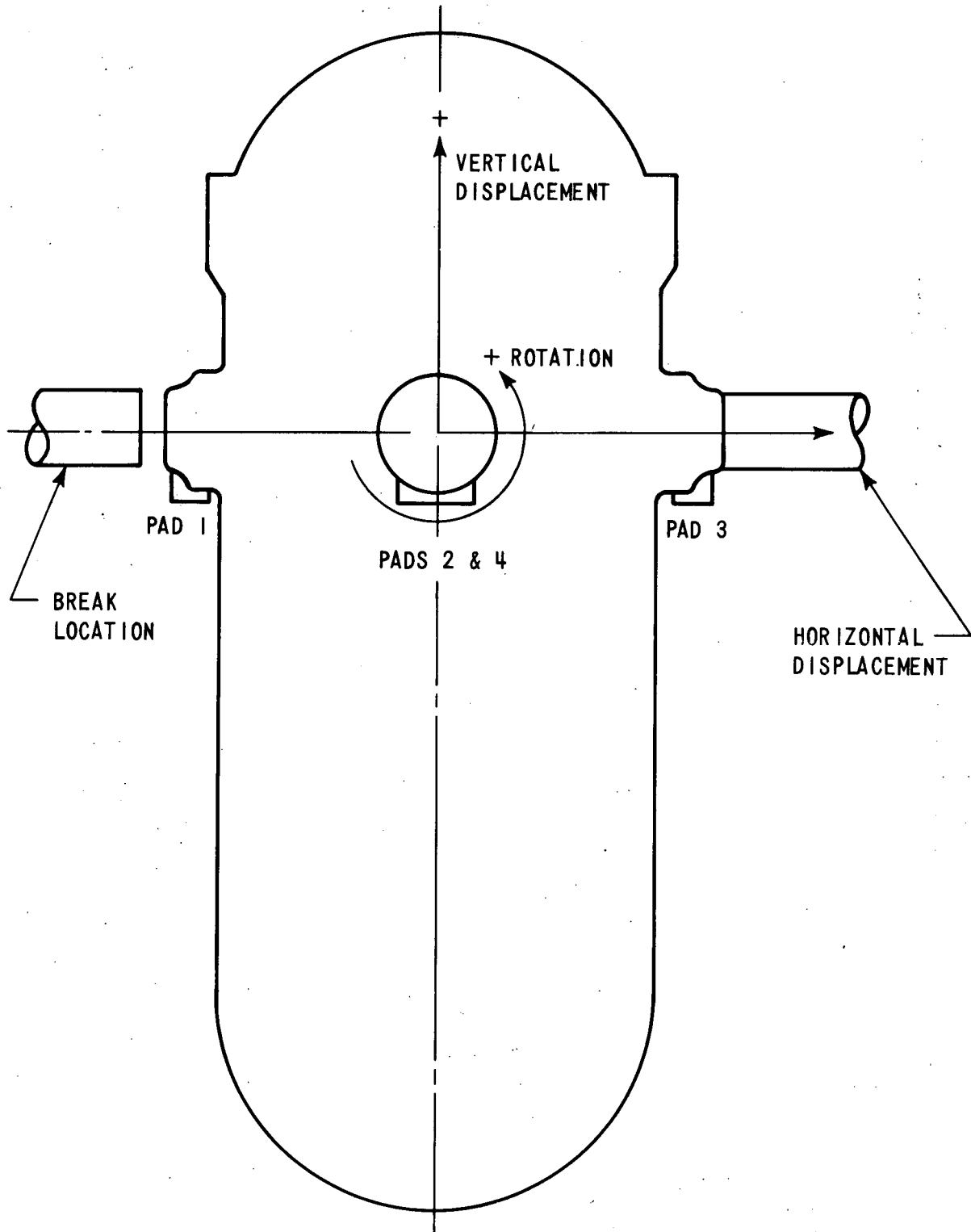


Figure 3-41. Displacement Coordinates and Support Pad Numbering Scheme

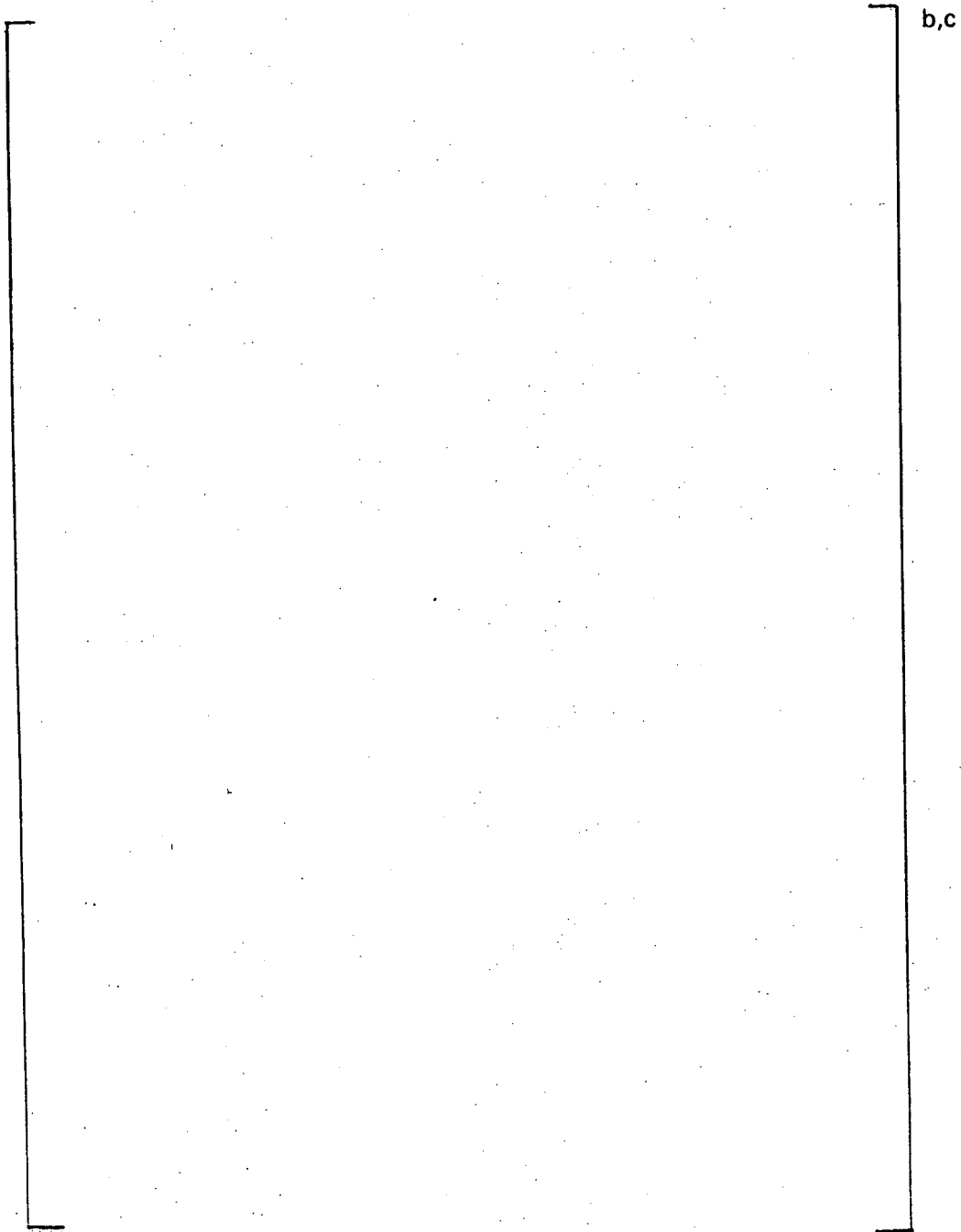
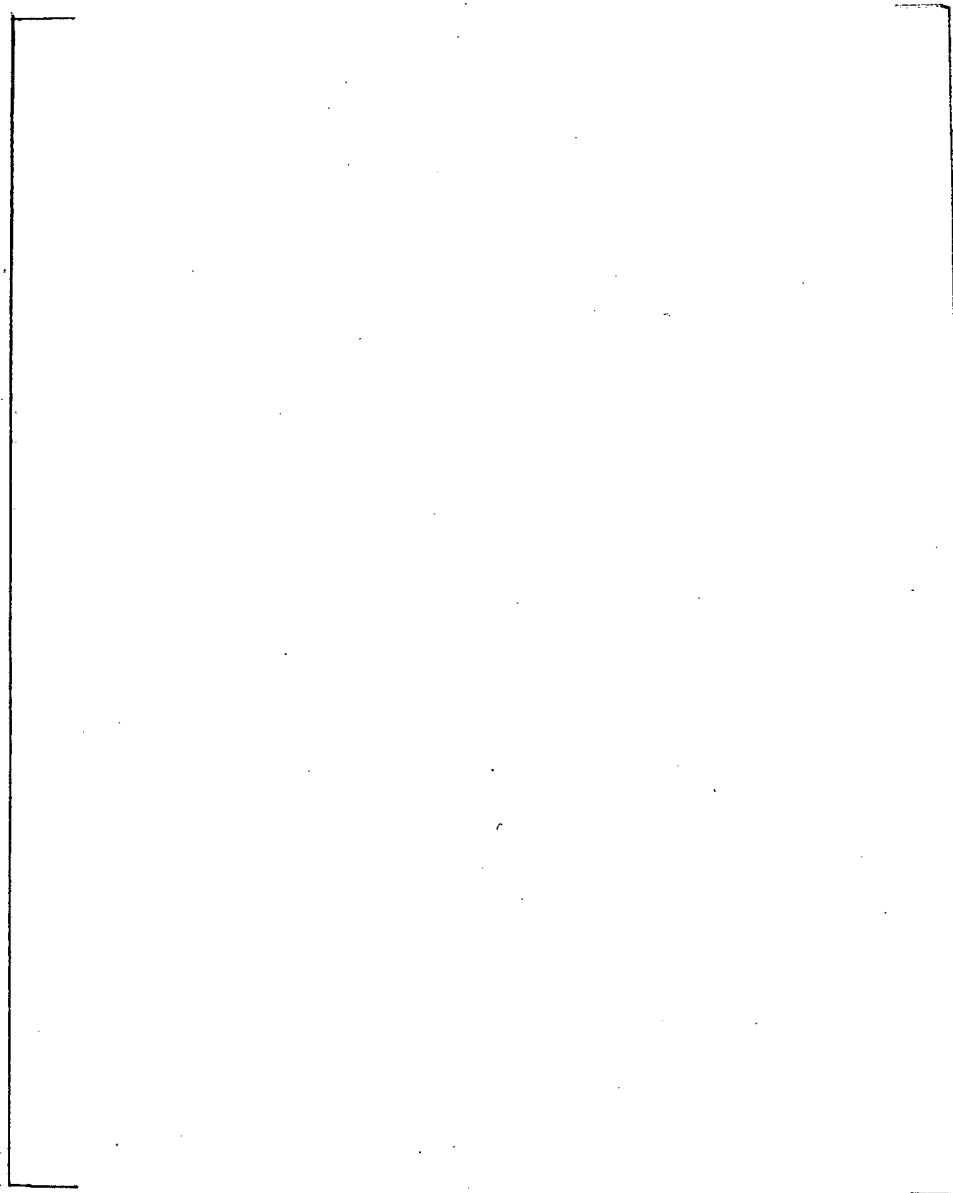


Figure 3-42. Nozzle/Vessel Centerline Horizontal Displacement:
RPV Inlet Nozzle Break

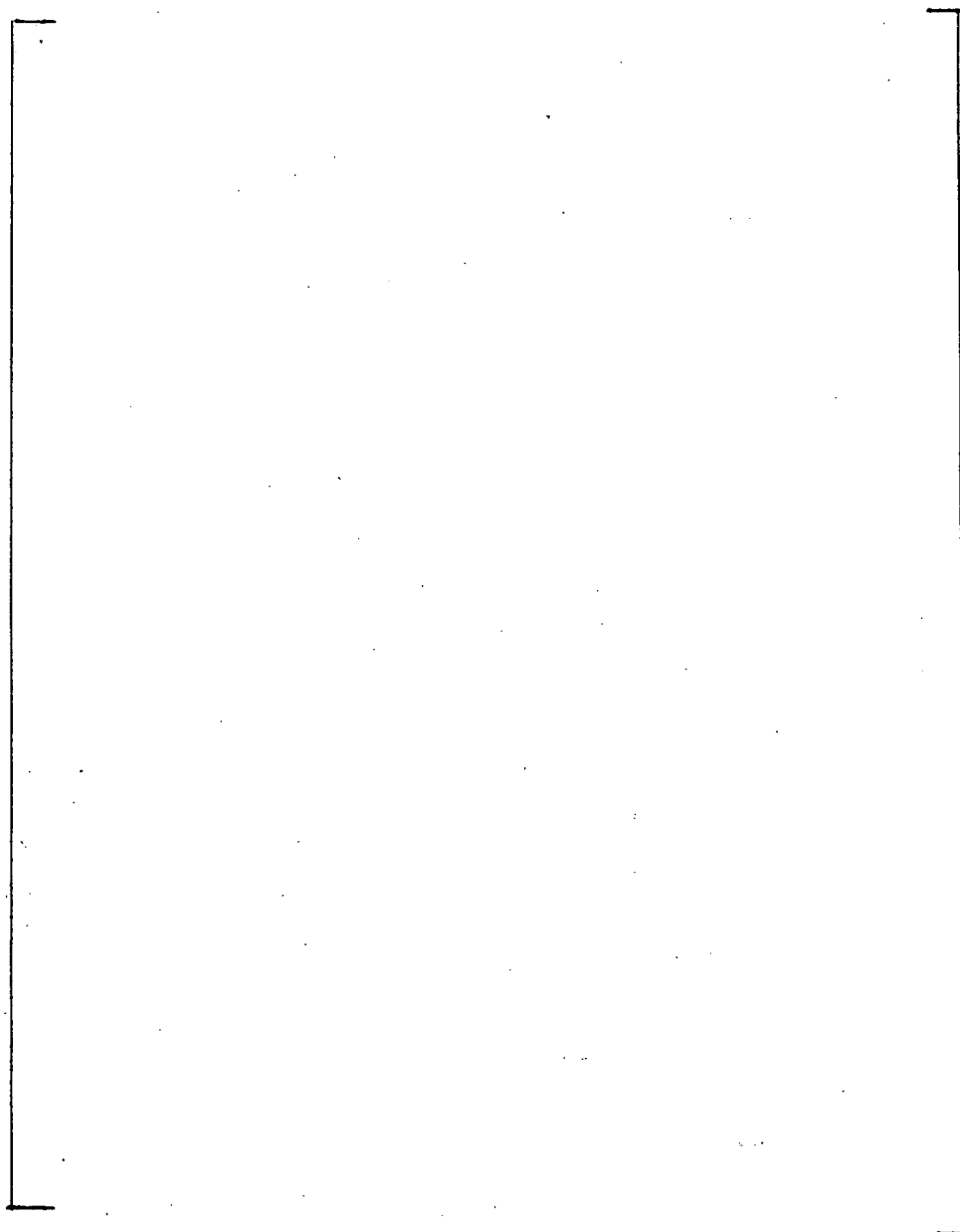


b,c

Figure 3-43. Nozzle/Vessel Centerline Vertical Displacement:
RPV Inlet Nozzle Break

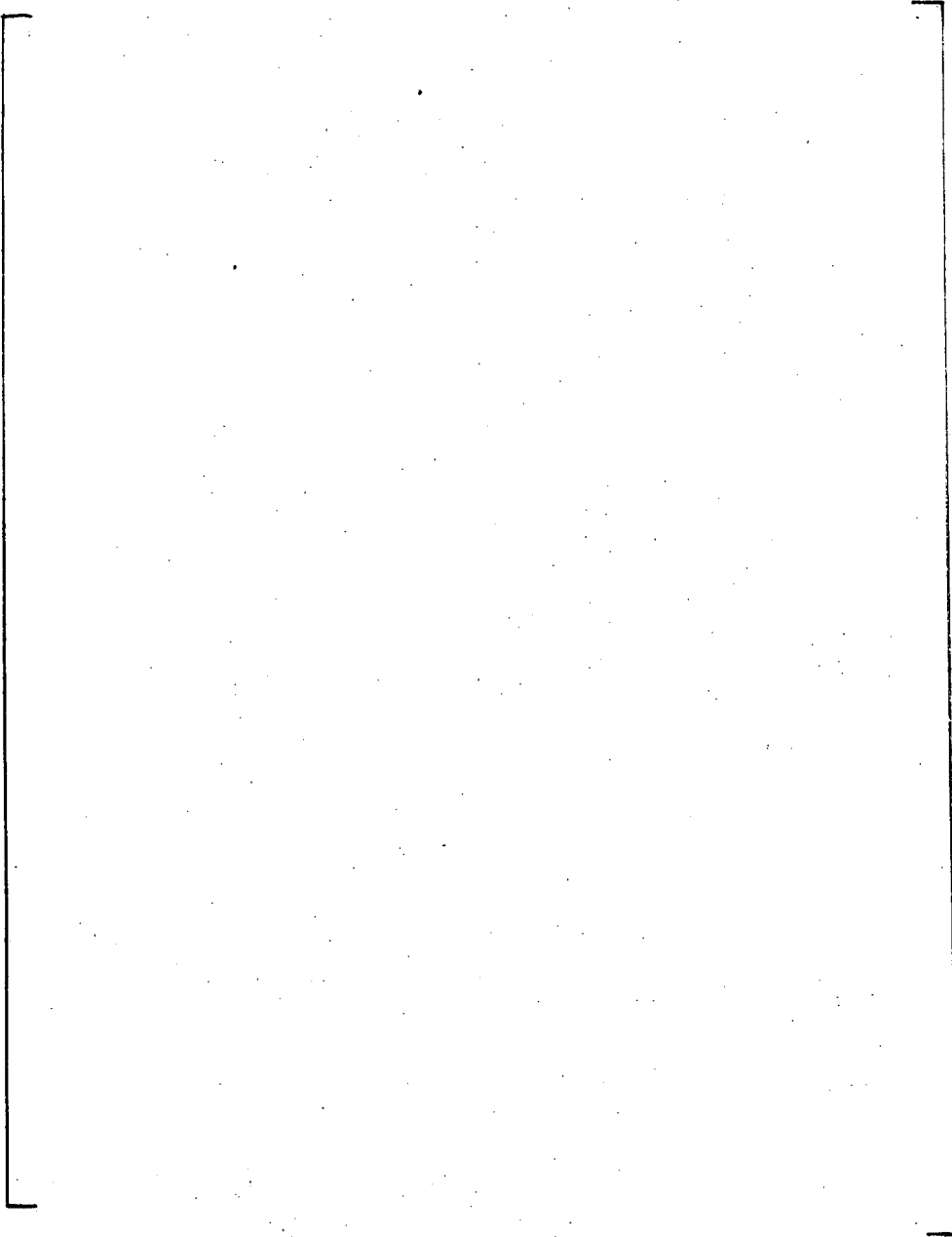
b,c

Figure 3-44. Nozzle/Vessel Centerline Rotation:
RPV Inlet Nozzle Break



b,c

Figure 3.45. Upper Core Plate Horizontal Motion:
RPV Inlet Nozzle Break



b,c

Figure 3-46. Lower Core Plate Horizontal Motion:
RPV Inlet Nozzle Break

3-19. Postulated RPV Outlet Nozzle Break

An analysis was performed for a 110 square-inch guillotine reactor vessel outlet nozzle break. The peak RPV horizontal displacement, vertical displacement, and rotation are [] inch, [] inch, and [] radian, respectively. Time-history displacements of the RPV are shown in figures 3-47 through 3-49. The upper and lower core plate horizontal displacements are shown in figures 3-50 and 3-51, respectively. b,c

3-20. Postulated RCP Outlet Nozzle Break

An analysis was performed for a guillotine reactor coolant pump outlet nozzle break with a break opening area to twice the pipe cross-sectional flow area. The peak RPV horizontal displacement, vertical displacement, and rotation are [] inch, [] inch, and [] radian, respectively. Time-history displacements of the RPV are shown in figures 3-52 through 3-54. The upper and lower core plate horizontal displacements are shown in figures 3-55 and 3-56 respectively. b,c

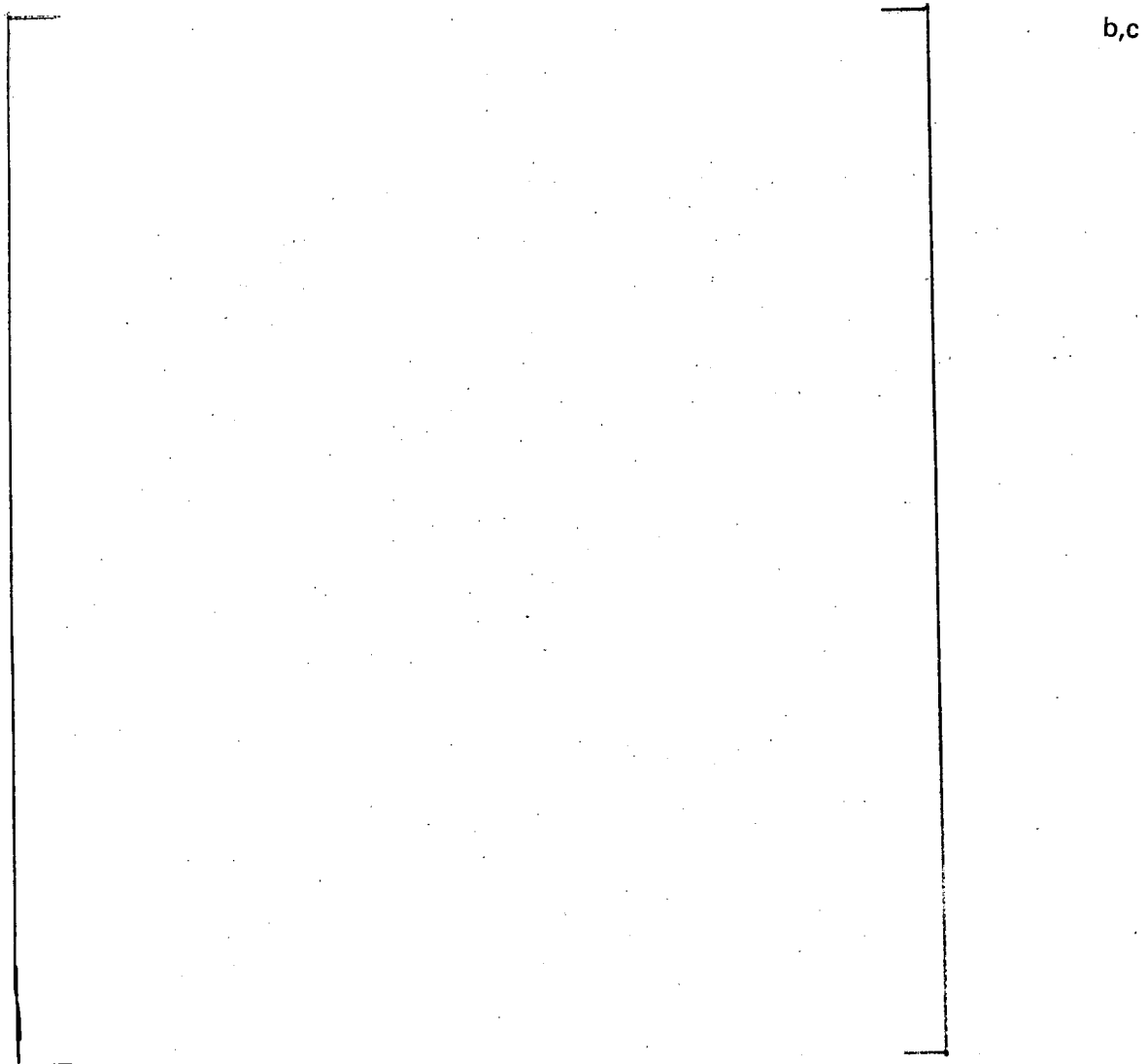


Figure 3-47. Nozzle/Vessel Centerline Horizontal Displacement:
RPV Outlet Nozzle Break

b,c

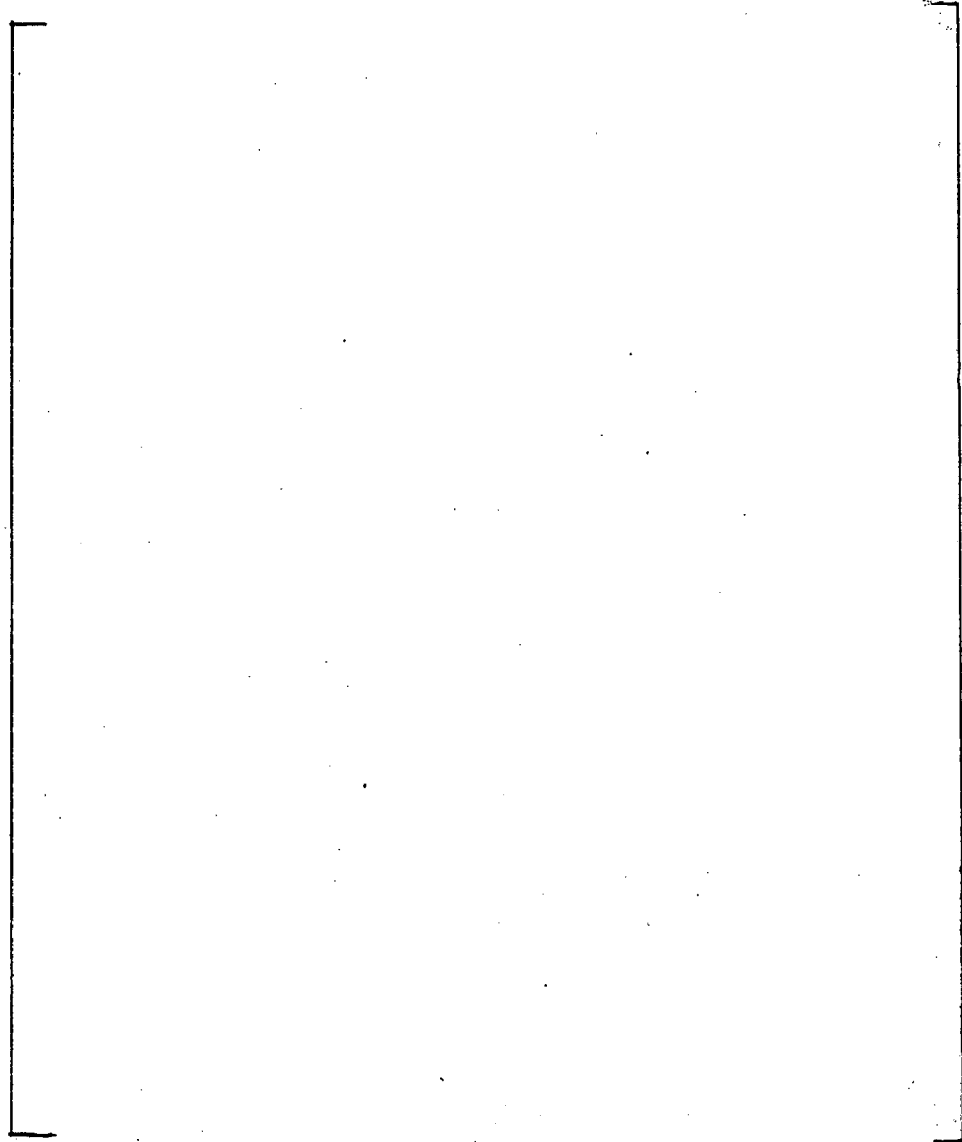
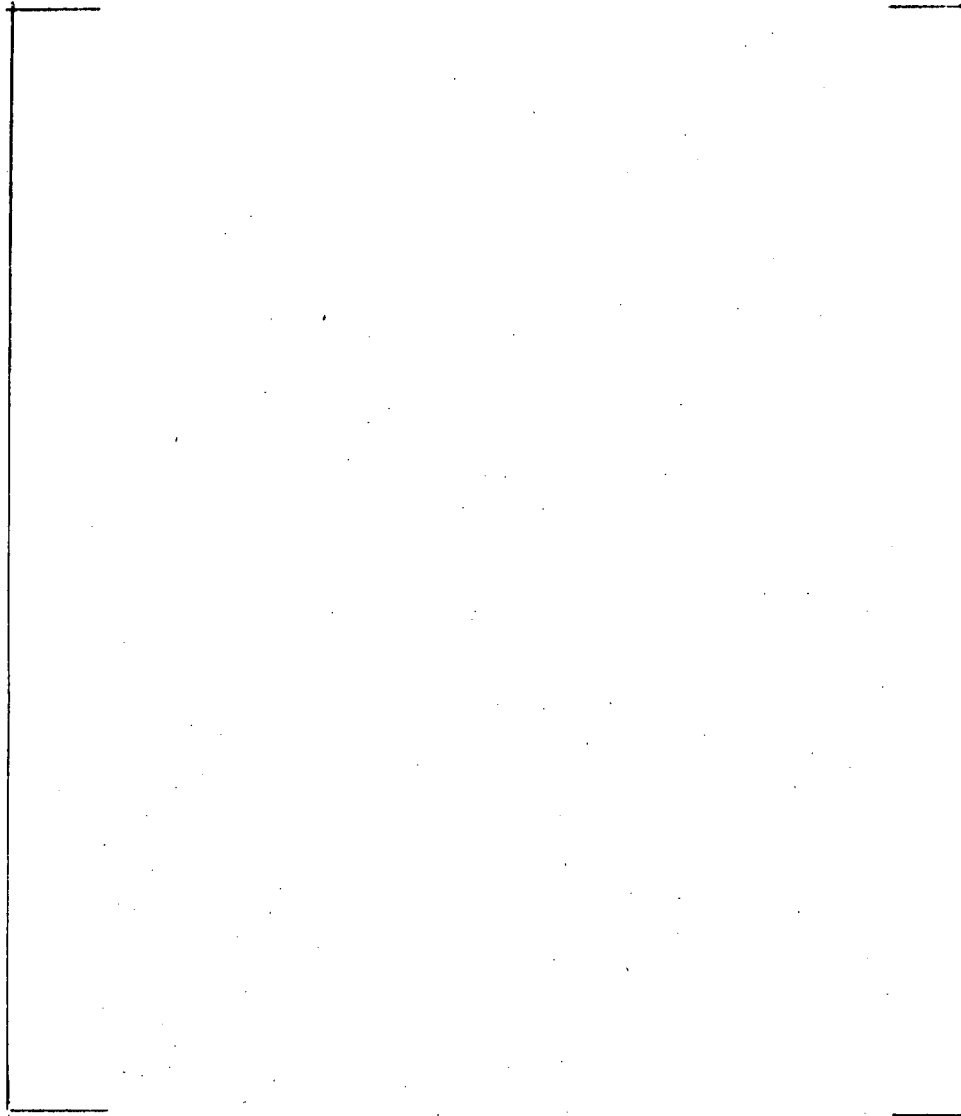


Figure 3-48. Nozzle/Vessel Centerline Vertical Displacement:
RPV Outlet Nozzle Break



b,c

Figure 3-49. Nozzle/Vessel Centerline Rotation:
RPV Outlet Nozzle Break

b,c

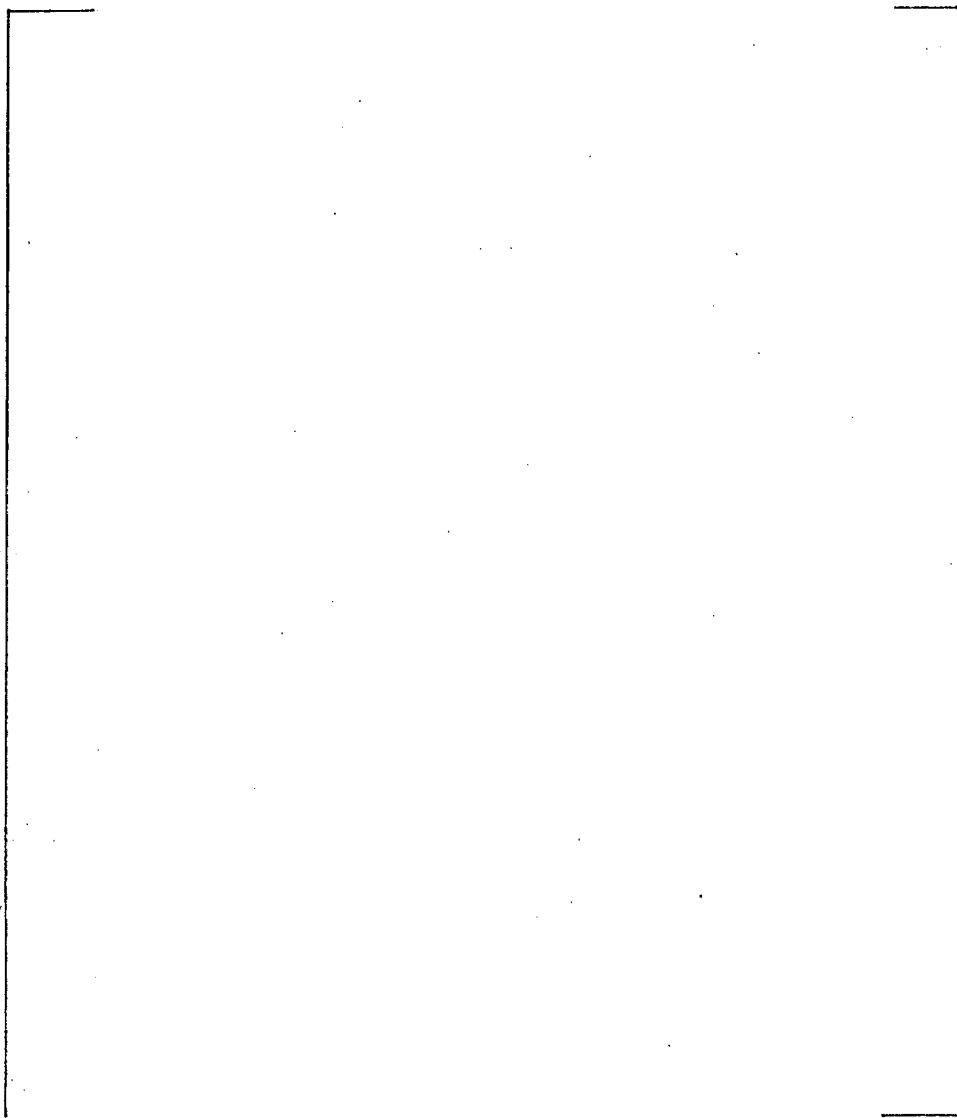
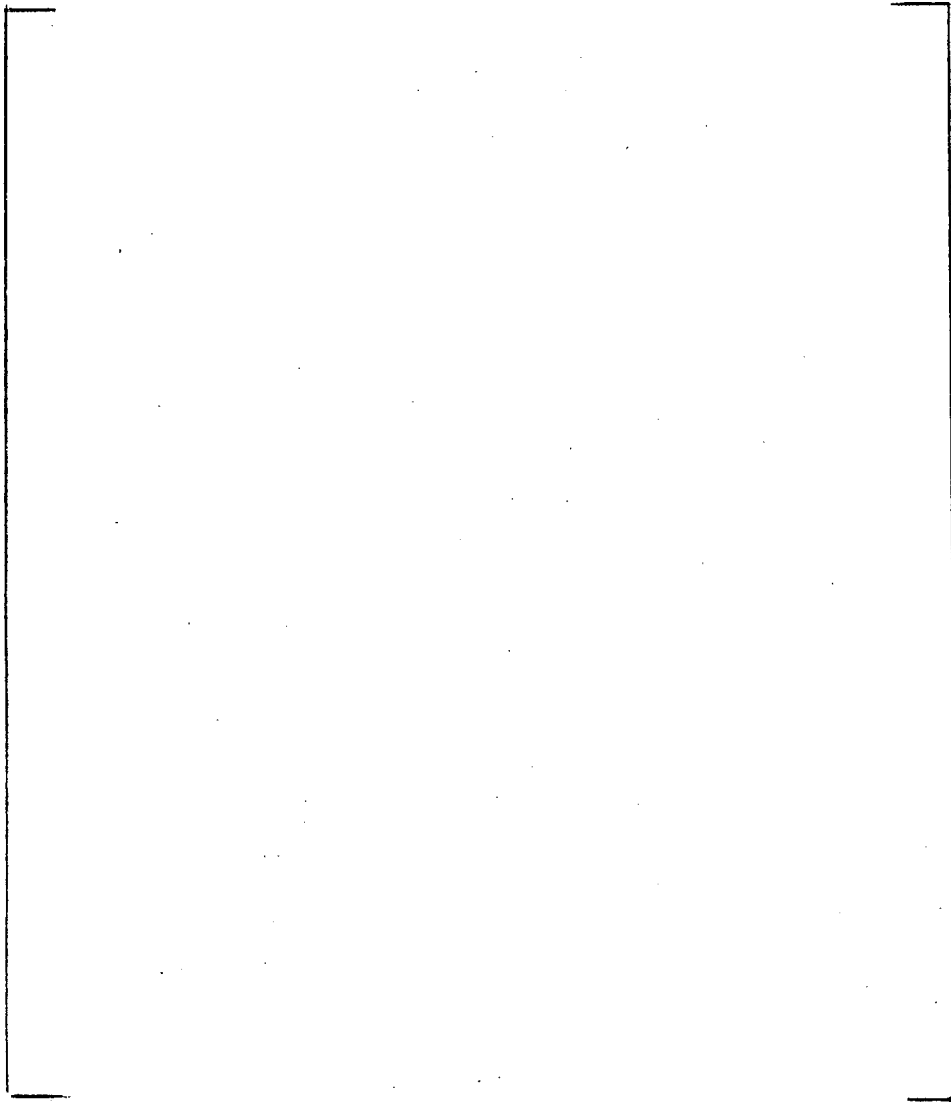


Figure 3-50 Upper Core Plate Horizontal Motion:
RPV Outlet Nozzle Break



b,c

Figure 3-51. Lower Core Plate Horizontal Motion:
RPV Outlet Nozzle Break

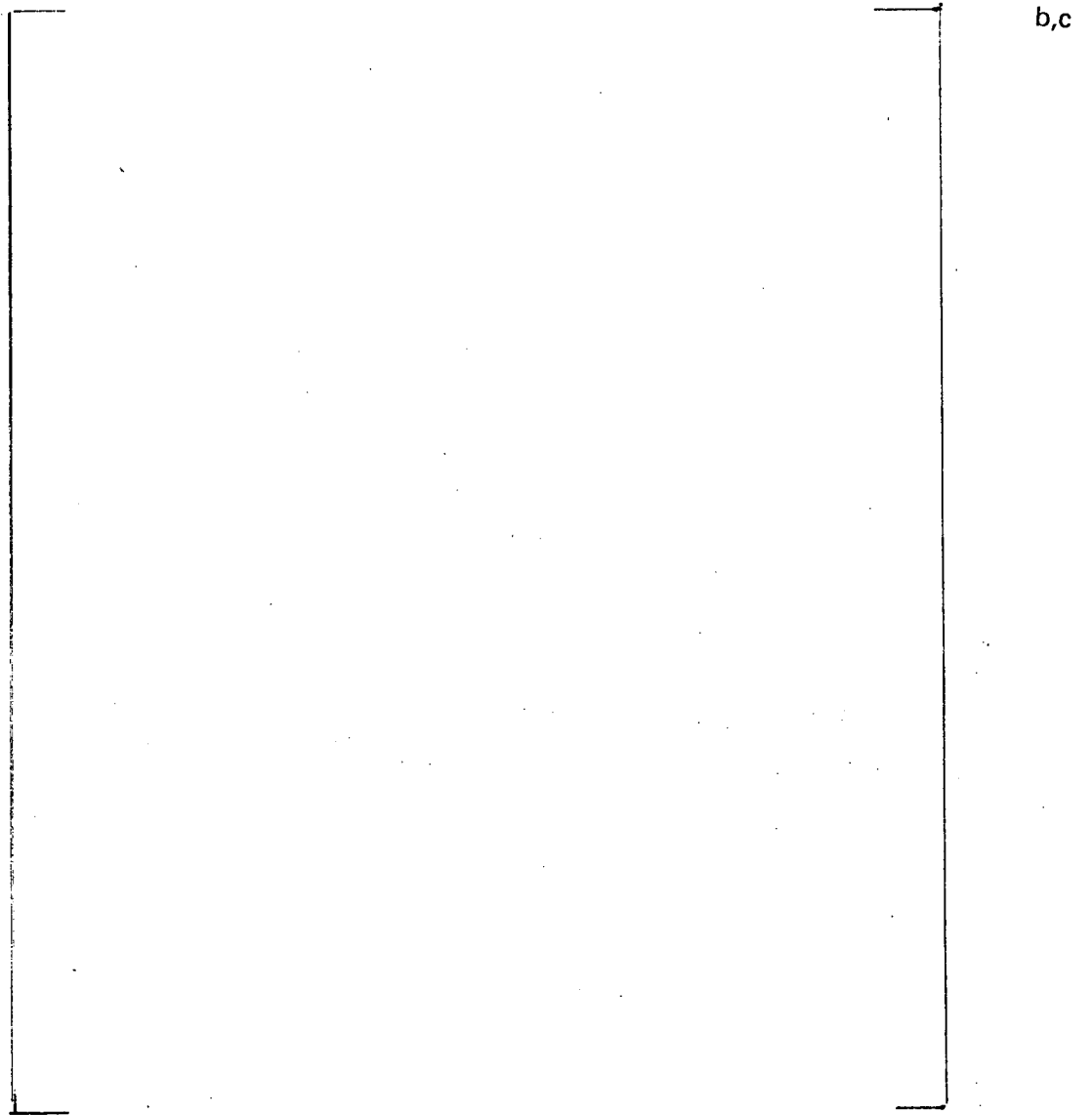


Figure 3-52. Nozzle/Vessel Centerline Horizontal Displacement:
RCP Outlet Nozzle Break

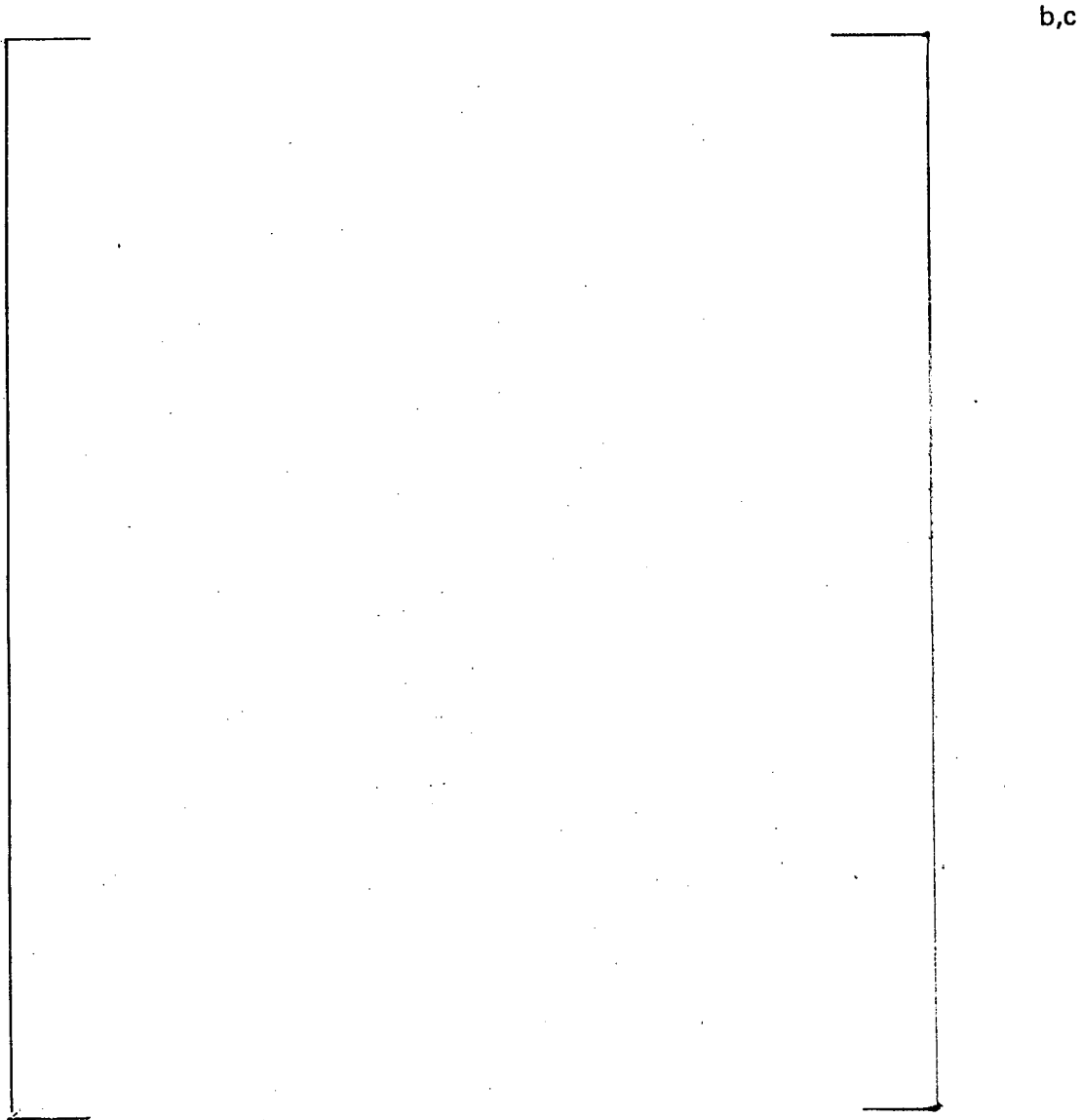


Figure 3-53. Nozzle/Vessel Centerline Vertical Displacement:
RCP Outlet Nozzle Break

b,c

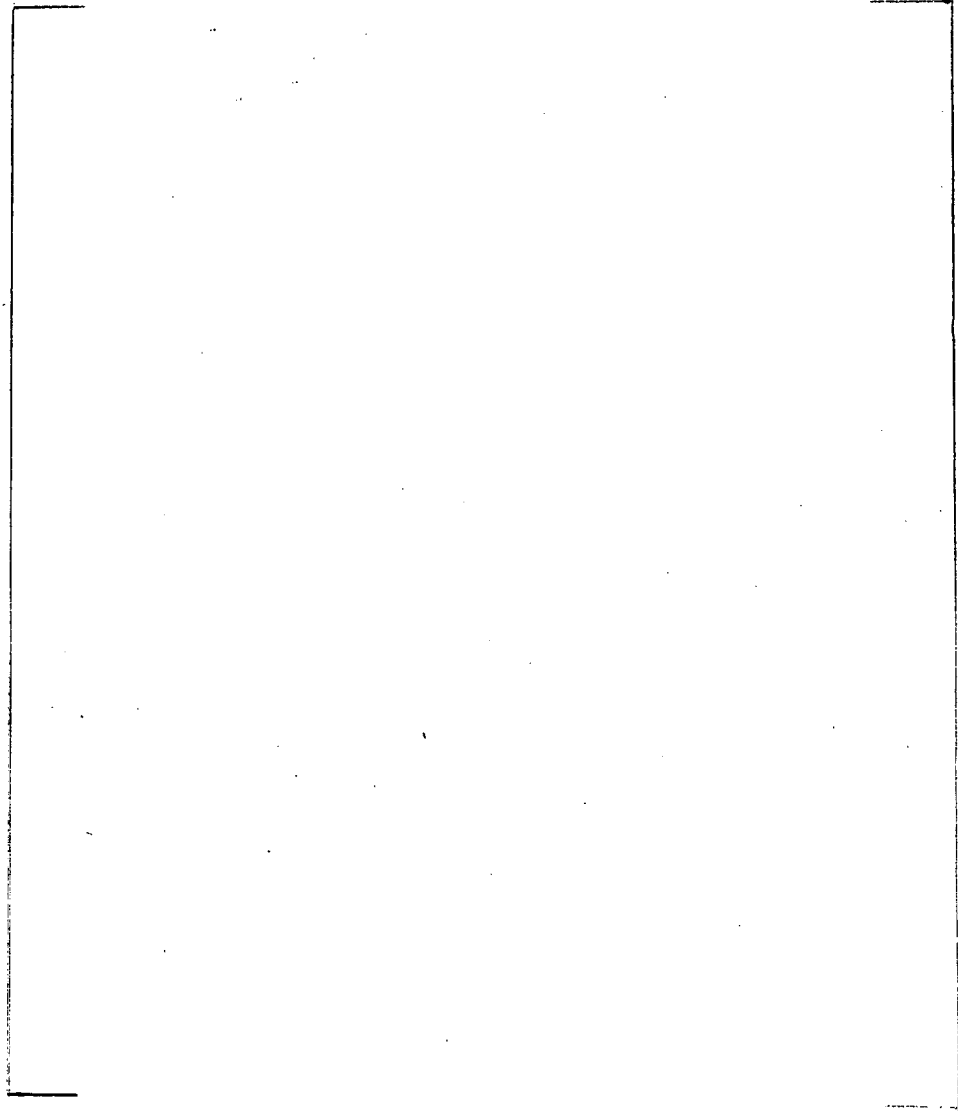


Figure 3-54. Nozzle/Vessel Centerline Rotation:
RCP Outlet Nozzle Break

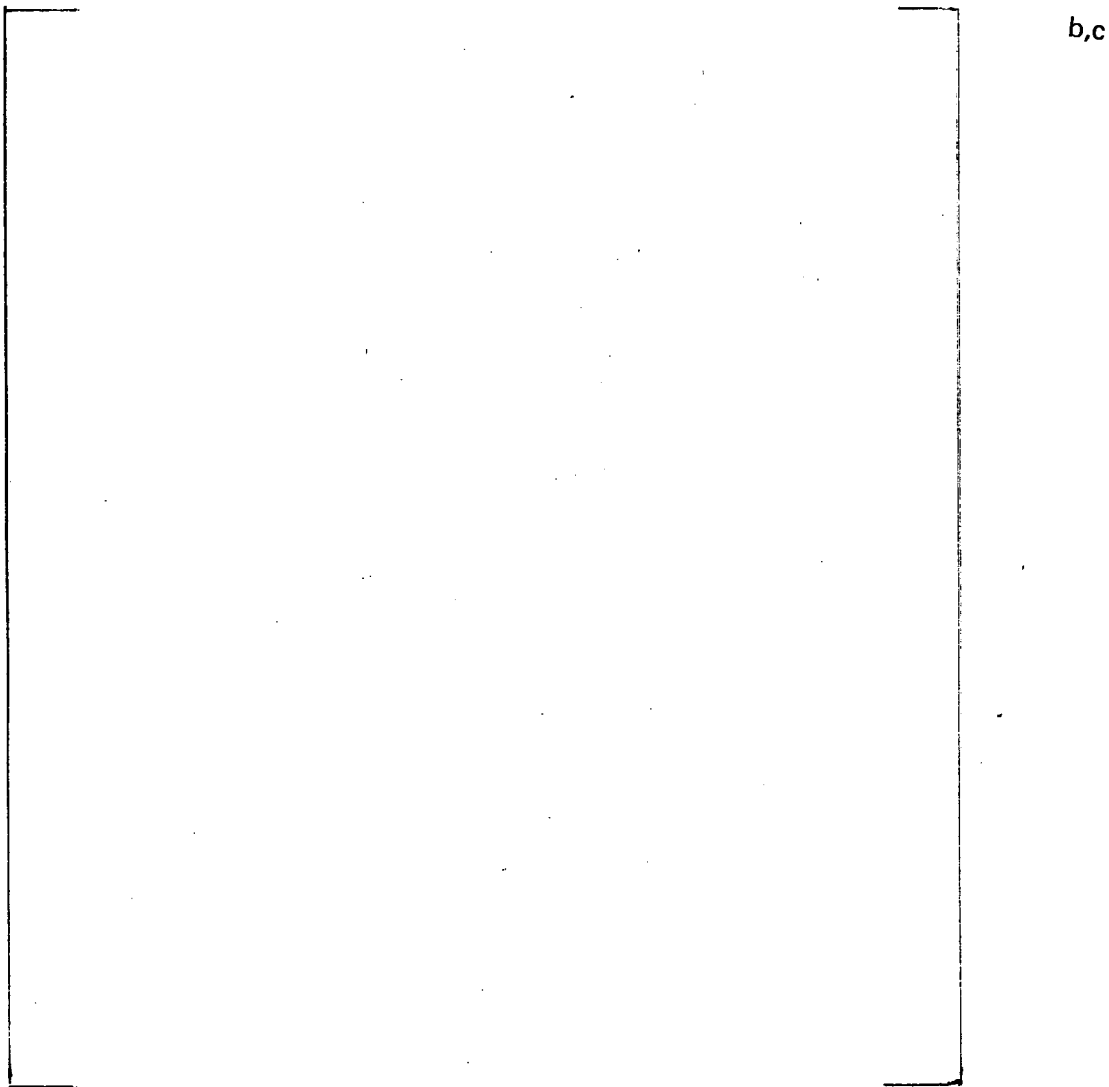


Figure 3-55. Upper Core Plate Horizontal Motion:
RCP Outlet Nozzle Break

b,c

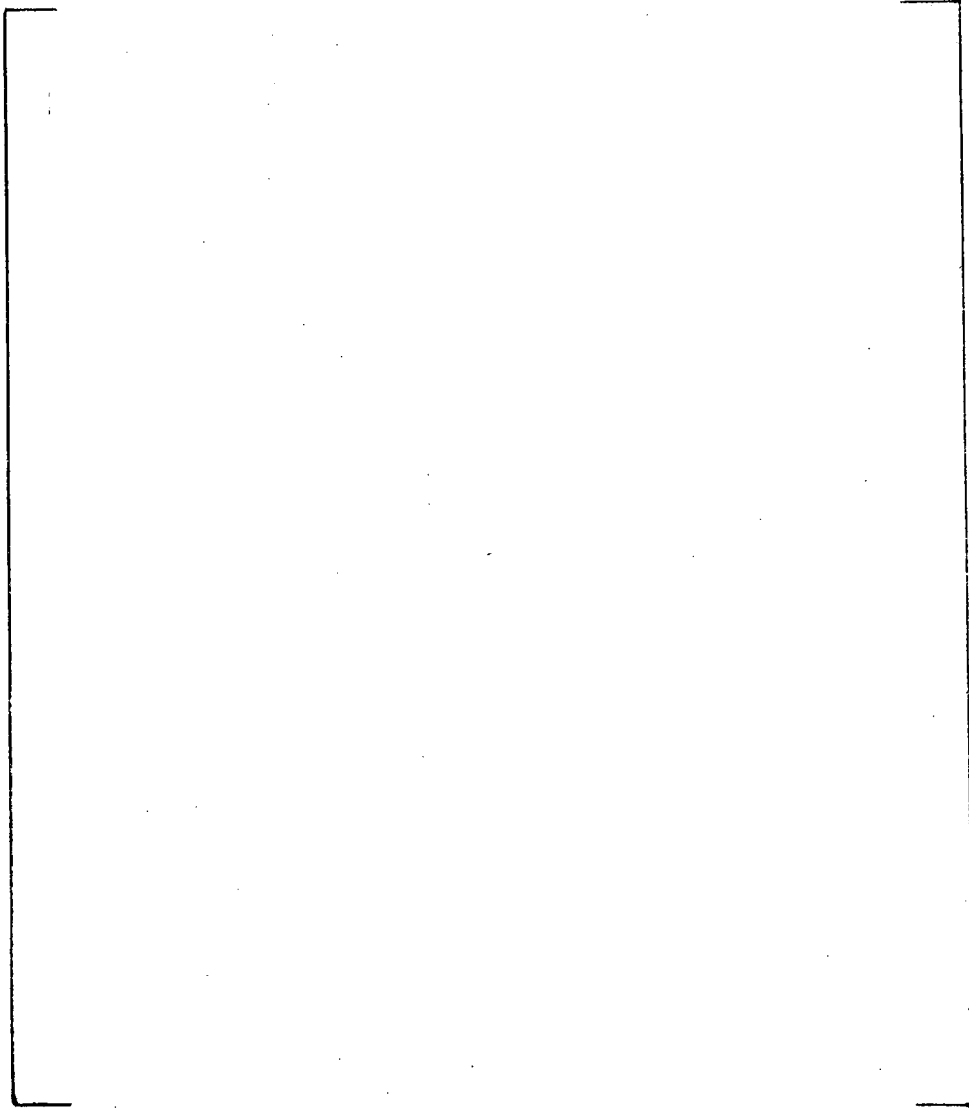


Figure 3-56. Lower Core Plate Horizontal Motion:
RCP Outlet Nozzle Break

SECTION 4 EVALUATION OF SYSTEM

The basic criteria of acceptability of the plant for the postulated pipe rupture are that the reactor can be safely shutdown and the fuel adequately cooled. Verification of this ability is the objective of the analysis. The criteria for acceptance and the results of the system analyses will be outlined in the subsequent sections.

The results of the elastic analysis, stresses in supports, components, piping, and the like, initially will be compared to the guidelines outlined in the current ASME Boiler and Pressure Vessel Code, Section III, Appendix F. Exceeding these stress limits will indicate the need for an inelastic evaluation. High stresses in isolated components may be acceptable depending on the location of the component and its effect on the system response.

4-1. EVALUATION CRITERIA

The basic overall criteria to be used for each of the individual components will be outlined in the following sections.

4-2. Reactor Core

The reactor core must be maintained in a coolable geometry. The fuel grids maintain the spacing of individual rods and the spacing of the fuel assemblies. The magnitude of the impact forces in these grids, therefore, is important in assuring the ability of the fuel to be cooled. The highest impact forces generally occur in the outer fuel assemblies due to impact into the core barrel baffle plates. The grid impact loads and the behavior of the fuel during the LOCA will be determined, and it will be demonstrated that the fuel can be adequately cooled. The stresses on the thimbles and fuel rods are limited to assure their integrity. Limits consistent with the guidelines set up in ASME Section III, Appendix F will be used.

4-3. Internals

The deformation of the core barrel and other core support structures are included in the evaluation in order to obtain accurate fuel core plate motions. Local plastic deformation in these components is acceptable. The criteria of Appendix F of the ASME Code will be used for the evaluation.

4-4. Piping

The Emergency Core Cooling System (ECCS) piping attached to the unbroken loops and the reactor coolant piping in the unbroken loops must retain their integrity to assure delivery of coolant to the core. [

a,c

] The stress and strain calculated in the piping must be sufficiently low to assure that the integrity of the piping is not jeopardized. The strain must be less than 50 percent of the uniform ultimate strain.

4-5. Components

The pressure boundaries of the steam generator, reactor coolant pump, reactor vessel, and CRDM's must retain their integrity. It must be demonstrated that the stresses in these components are sufficiently low to assure structural integrity. Appendix F criteria of the ASME Code will be used for these evaluations.

4-6. Component Supports

The supports of the reactor vessel, reactor coolant pump, and steam generator may sustain plastic deformations. Inelastic behavior of the supports will be included in the analysis to allow for an accurate determination of the motion of the reactor vessel and components.

4-7. Concrete

The concrete must retain its integrity in areas where its integrity is required to assure the safety of the plant. For instance, the concrete of the reactor cavity must be able to withstand the combination of pressure and applied load through the ring girder to assure adequate support of the vessel. Analyses may be performed which would allow cracking of concrete and redistribution. Deformation of concrete at embedments of the component supports may be acceptable if the effect is included in the structural analysis.

4-8. REACTOR COOLANT LOOP PIPING EVALUATION

[] a,c

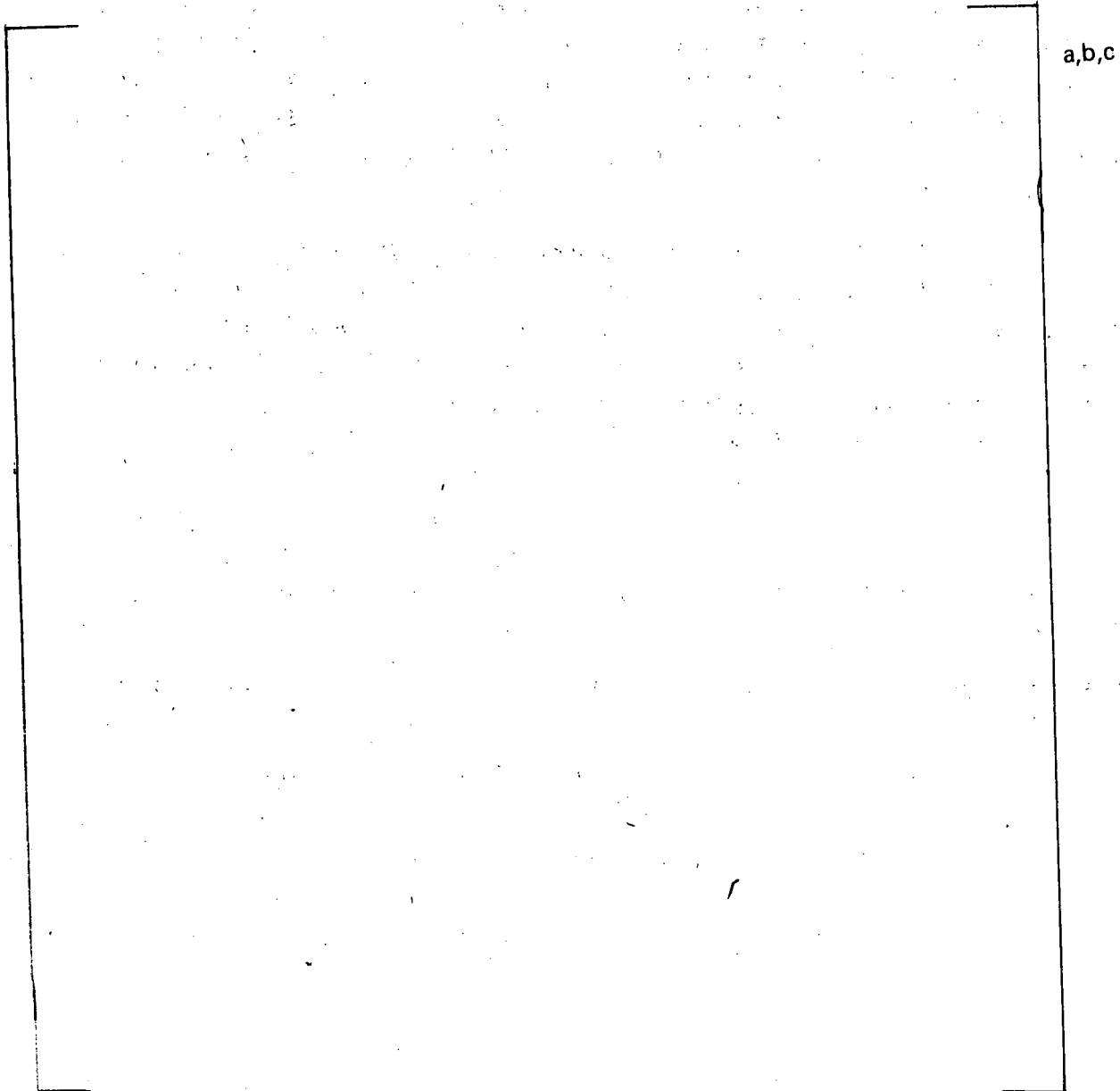
□

The model of the reactor coolant loop piping consists of elastic-plastic pipe and elbow elements. Stress and strain in these elements are calculated at eight locations around the

circumference at both ends of the element. The stresses and strains evaluated are total effective values which include both elastic and plastic components.

In the reactor coolant loop piping at locations away from the reactor vessel, the stresses in the pipe did not exceed yield. This is true of all crossover legs and those portions of the hot and cold legs nearer the steam generators and reactor coolant pumps.

Localized yielding did occur in the hot and cold legs near the reactor vessel. This is due to the loads induced on the pipe by the primary shield wall pipe restraints. These restraints load the pipe close to the vessel nozzles.



The maximum strain induced at any location in the piping is [] percent. This strain is approximately [] percent of the uniform ultimate strain of the material. This strain is sufficiently low to assure the integrity of the piping.

b,c

Additionally, the corresponding maximum stress of [] psi is less than $0.7S_u$ (46,700 psi) which is the limit given in Appendix F of the ASME Code for inelastic system analysis and inelastic component analysis.

b,c

4.9. SUPPORT STRUCTURE EVALUATION

The reactor vessel support integrity was verified using the results of the RPV blowdown analysis. The results of the analysis reveal a peak horizontal displacement of [] inches. This displacement is less than the approximately [] inch displacement required to produce support failure as determined by the reactor support tests. The maximum vertical support load is [] kips which is less than the support vertical load carrying capability. Thus, the reactor vessel support integrity is verified.

b,c

The steam generator and reactor coolant pump supports were evaluated using the criteria specified in Appendix XVII of the ASME Code, Section III. The member forces and moments taken from the WECAN computer code output were used in conjunction with the member properties to solve the yield and buckling interaction equations in Appendix XVII (equations 19, 20, and 21). The allowable stresses in Appendix XVII were increased by the appropriate stress increase factors specified in Appendix F of the Code. []

b,c

In addition, loads on concrete embedments have been compared with the embedment capabilities. []

a,c

A summary of the stresses in the most highly loaded members of the steam generator supports is given in table 4-1.

[]

b,c

A summary of the stresses in the most highly loaded members of the reactor coolant pump supports is given in table 4-2.

[] b,c

TABLE 4-1 SUMMARY OF MAXIMUM STEAM GENERATOR SUPPORT STRESSES		
Support Member Description	Max. Percent Allow. Stress	Comment
Upper Snubbers - Elev. 92' Lower Snubbers - Elev. 48' 12" pipe Stub columns between Elevs. 60' and 63'-6" 12W65 Stub column bracing members at Elev. 63'-6". Double 12" channel sections at Elev. 63'-6". 14W158 Outside Vert. Columns Elev. 60' to 68' 12W120 Diagonal bracing members between 14W158 columns - Elev. 60' to 68'	<div style="border: 1px solid black; width: 100%; height: 100%;"></div>	<div style="border: 1px solid black; width: 100%; height: 100%;"></div>

b,c

TABLE 4-2
SUMMARY OF MAXIMUM RCP SUPPORT STRESSES

Support Member Description	Max. Percent Allow. Stress	Comment
Tie Rods: Loop 31 Loop 32 Loop 33 Loop 34 Pipe Column Tops – Loop 34	[]

a,b,c

The highest stressed portions of the loop 34 reactor coolant pump support frame are the tops of the three pipe columns and the two tie rods along the cold leg. One tie rod yields and the tops of the columns yield under high bending loads. The maximum total equivalent strain in the pump supports was 0.44 percent.

These evaluations demonstrate that the stresses and strains in the component supports are acceptable and that the function of supporting the components will be maintained.

4-10. AUXILIARY BRANCH LINES

In order to verify the adequacy of the reactor coolant system of Indian Point 3, it must be demonstrated that lines attached to the primary coolant piping in the unbroken loops remain intact. The analysis by Westinghouse considered the most highly-stressed auxiliary lines, which are the [

] a,b,c

The analysis was performed using the WECAN program, which is a large-scale finite element analysis program developed by Westinghouse. The program is capable of performing dynamic analyses of large structural models, with time-history displacements, concentrated forces, or distributed loads applied.

a,c

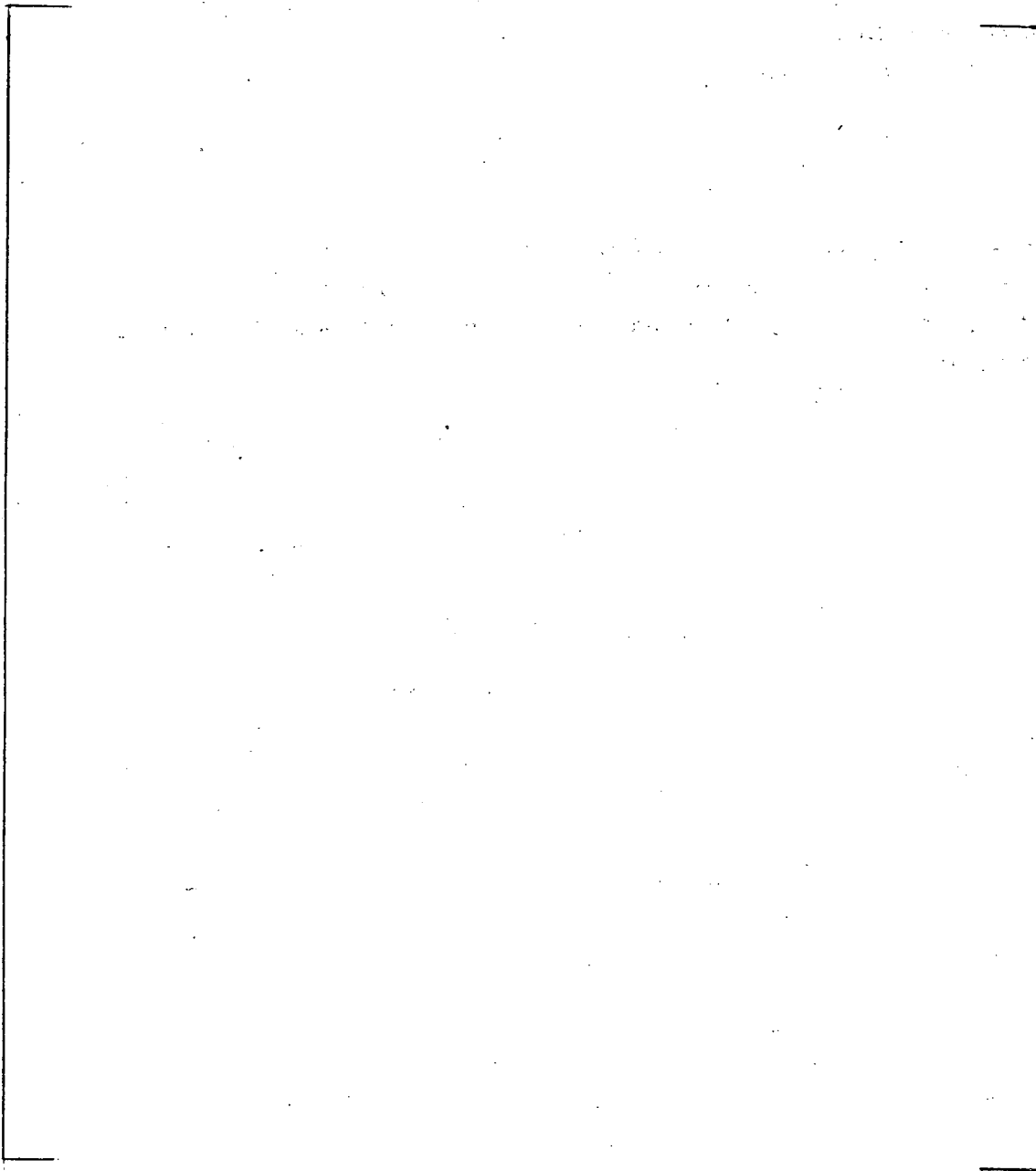
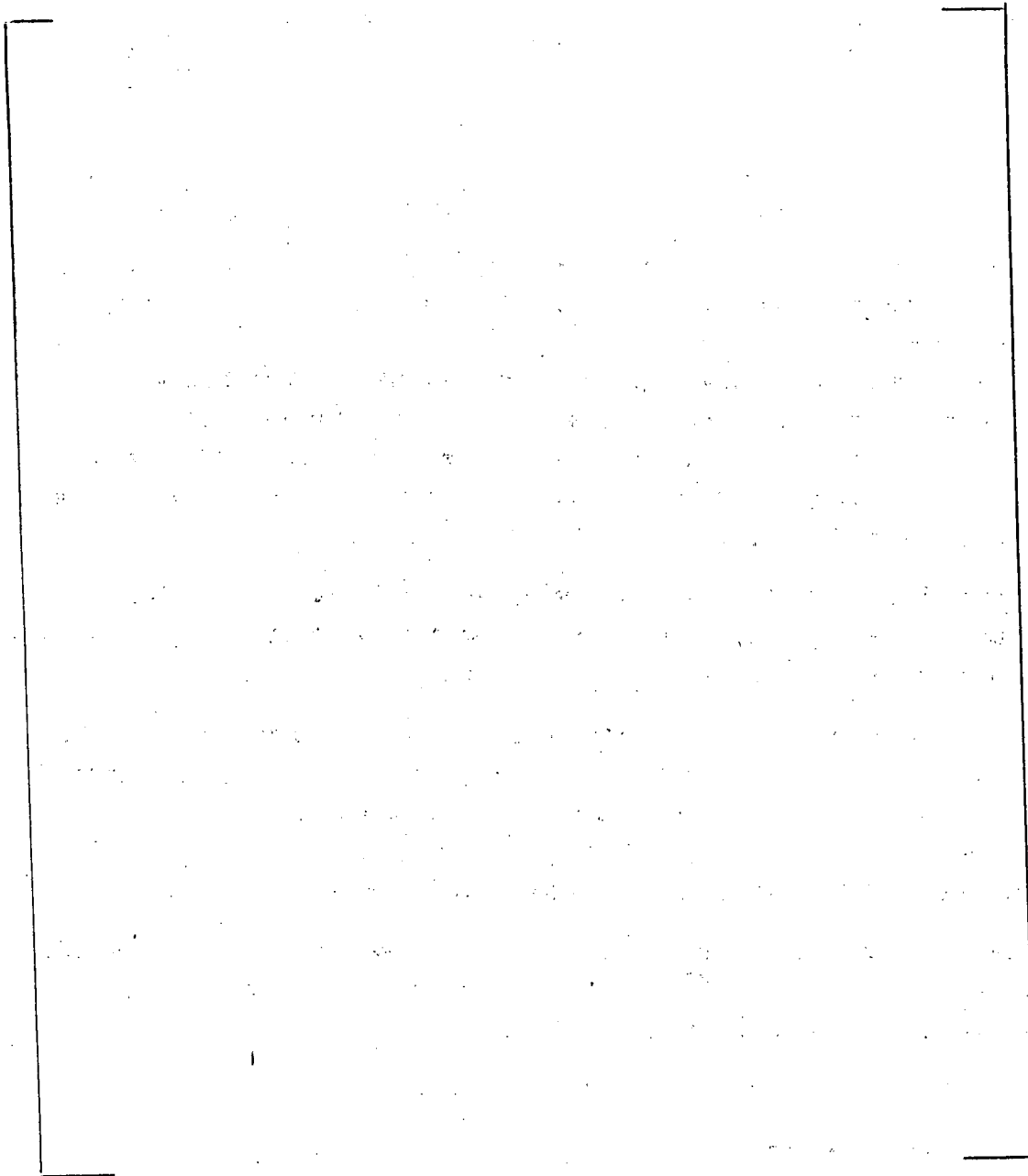


Figure 4-1. Accumulator Line Model X-Z Plane



a,c

Figure 4-2. Accumulator Line Model X-Y Plane

The model of the RHR line, [] is shown in figures 4-3 and 4-4. []

] is shown in figures a,c

[] a,c

The results of the analysis include stress intensities in the pipe and elbow elements and forces in the restraints. The maximum stress in the accumulator line is [] ksi. The yield stress in the material is [] ksi. [] The branch nozzle was evaluated using elastic component analysis methods with appropriate stress intensification factors. The elastically calculated stress in the branch connection is [] ksi. According to Appendix F of the ASME Code, for an inelastic system analysis and elastic component analysis, 0.7 Su is an appropriate stress limit. The limit is [] ksi which demonstrates the adequacy of the branch line nozzle.

b,c

The maximum stress in the RHR line is [] ksi. The yield stress is also [] ksi. The branch nozzle saw an elastically calculated stress of [] ksi. The limit based on Appendix F is [] ksi which confirms the adequacy of the branch nozzle.

b,c

The stresses in the branch piping are low and the stresses in the nozzles are satisfactory. These analyses performed [] demonstrate the adequacy and margin inherent in the design of the branch lines attached to the reactor coolant loop piping.

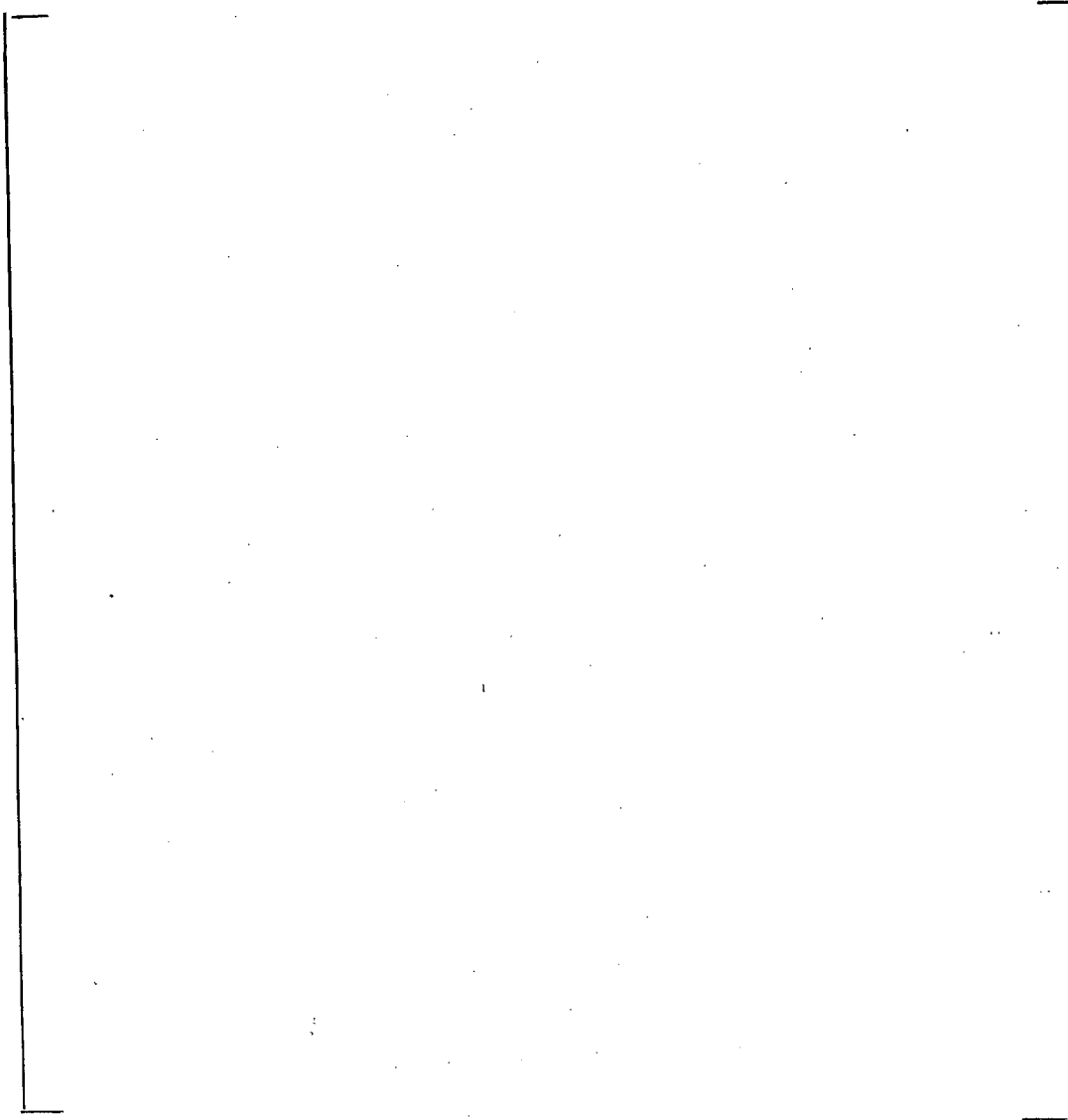
a,c

4-11. LOADS ON REACTOR COOLANT SYSTEM COMPONENTS

The external loads imposed on the reactor coolant system components were evaluated. All of the nozzles and support feet for the RCS components are capable of withstanding all of the accident loads. The review included the following locations:

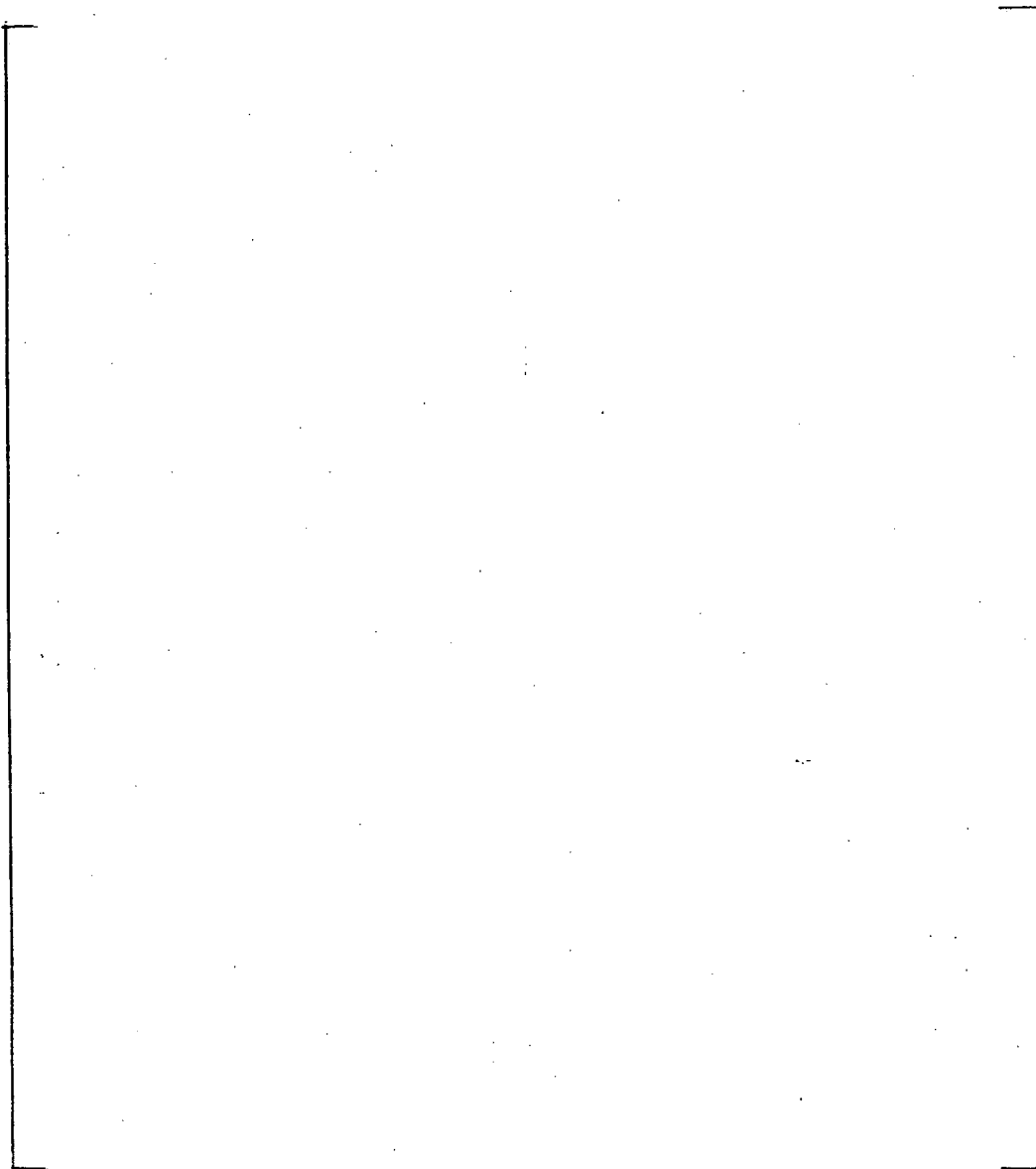
- Steam generator primary inlet and primary outlet nozzles
- Steam generator support feet
- Reactor coolant pump inlet and outlet nozzles
- Reactor coolant pump support feet

[] a,c



a,c

Figure 4-3. RHR Line Model X-Z Plane



a,c

Figure 4-4. RHR Line Model

[]

a,c

Because of the importance of the reactor vessel nozzles and support pads in this evaluation, a separate analysis was performed to demonstrate the adequacy of these components. The maximum applied loads were used to recalculate stresses at the most critical locations in the vessel inlet and outlet nozzles. []

[]

a,c

4-12. CONTROL ROD DRIVE MECHANISM

The control rod drive mechanism basically consists of six components, as shown in figure 4-5:

- rod travel housing
- latch assembly
- head adapter
- operating coil stack
- rod position indicator coils and
- drive rod assembly

The drive rod assembly consists of the control rods and the attached drive rod.

In order to determine the ability of the control rods to drop properly in the event of the postulated LOCA, a scram time analysis was performed which describes the motion of the control rod while falling into the core after release from the completely withdrawn position. An analysis was performed using the DAR13 program, a two-dimensional finite element dynamic analysis program which is the horizontal and rotational portion of the DARIWOSTAS program. []

[]

a,c

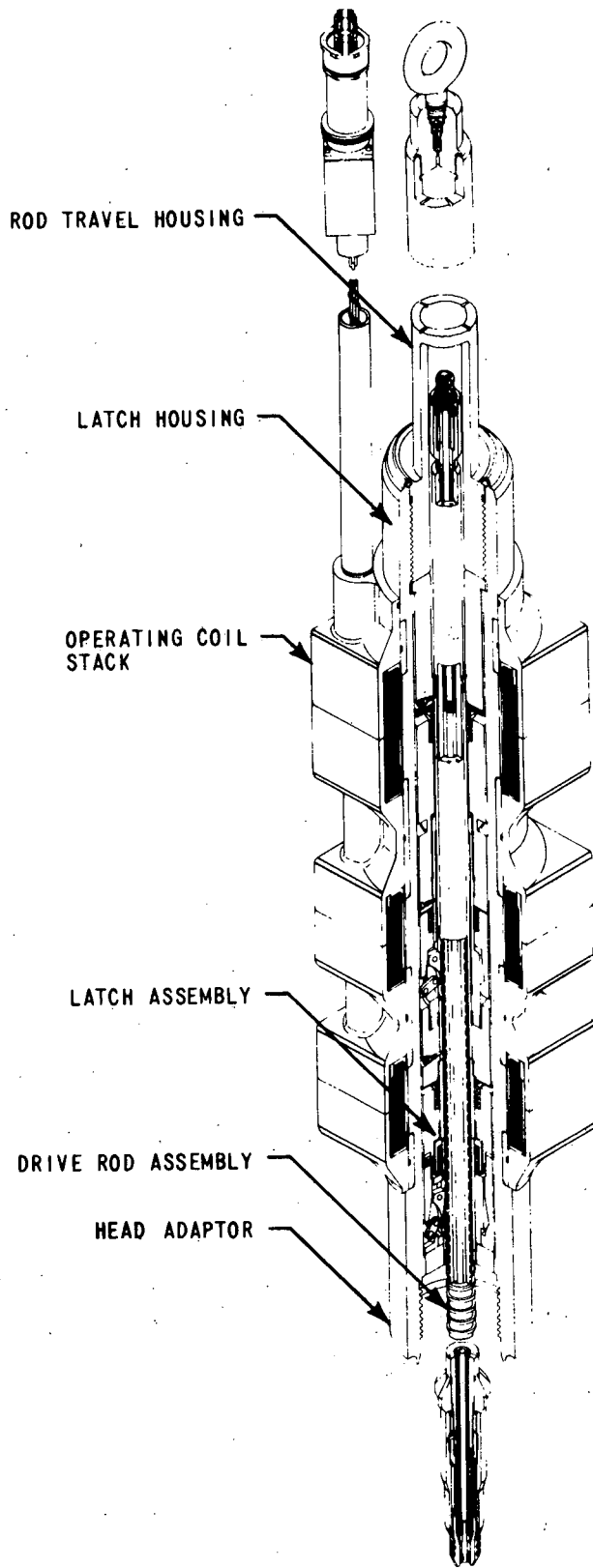
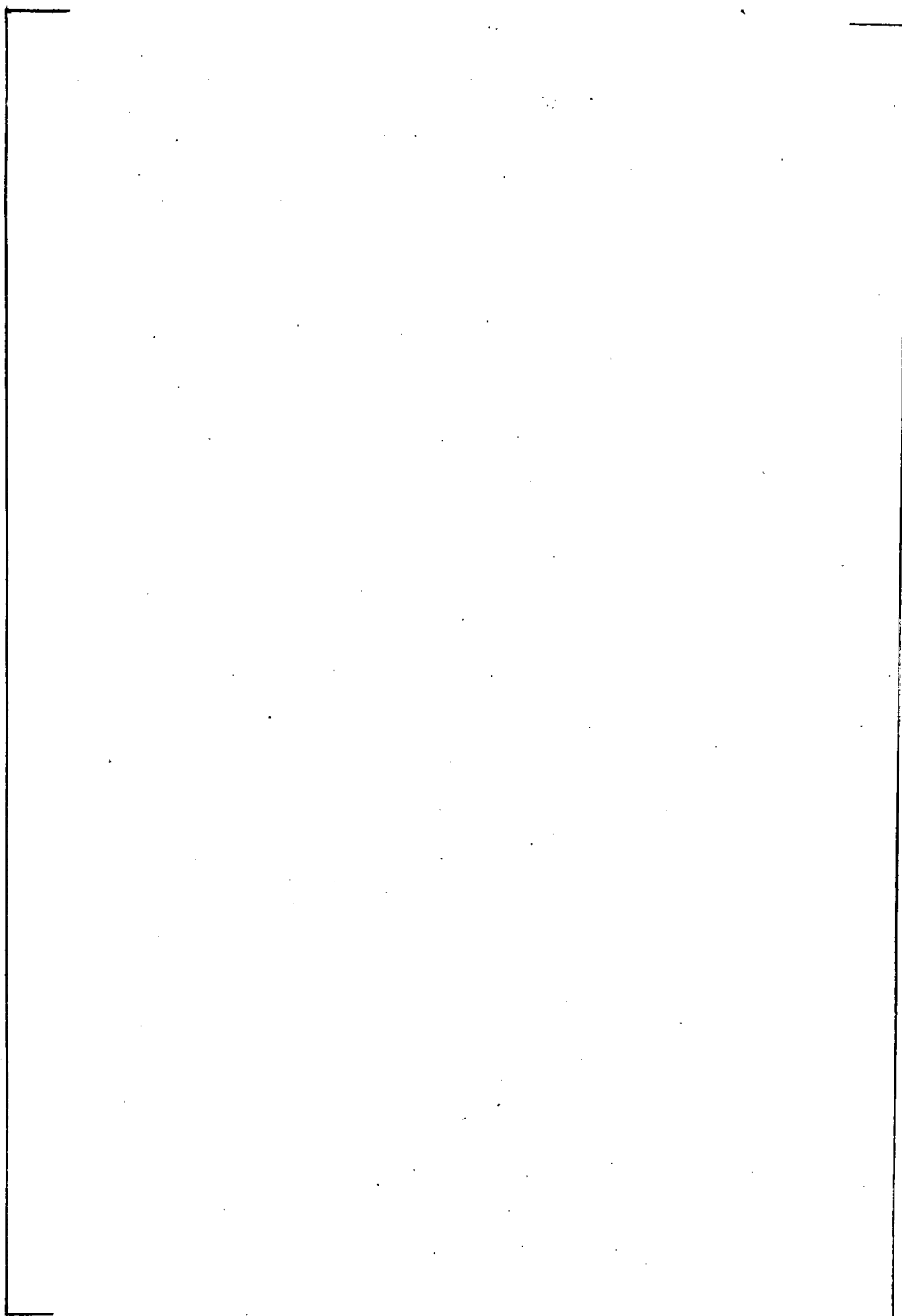
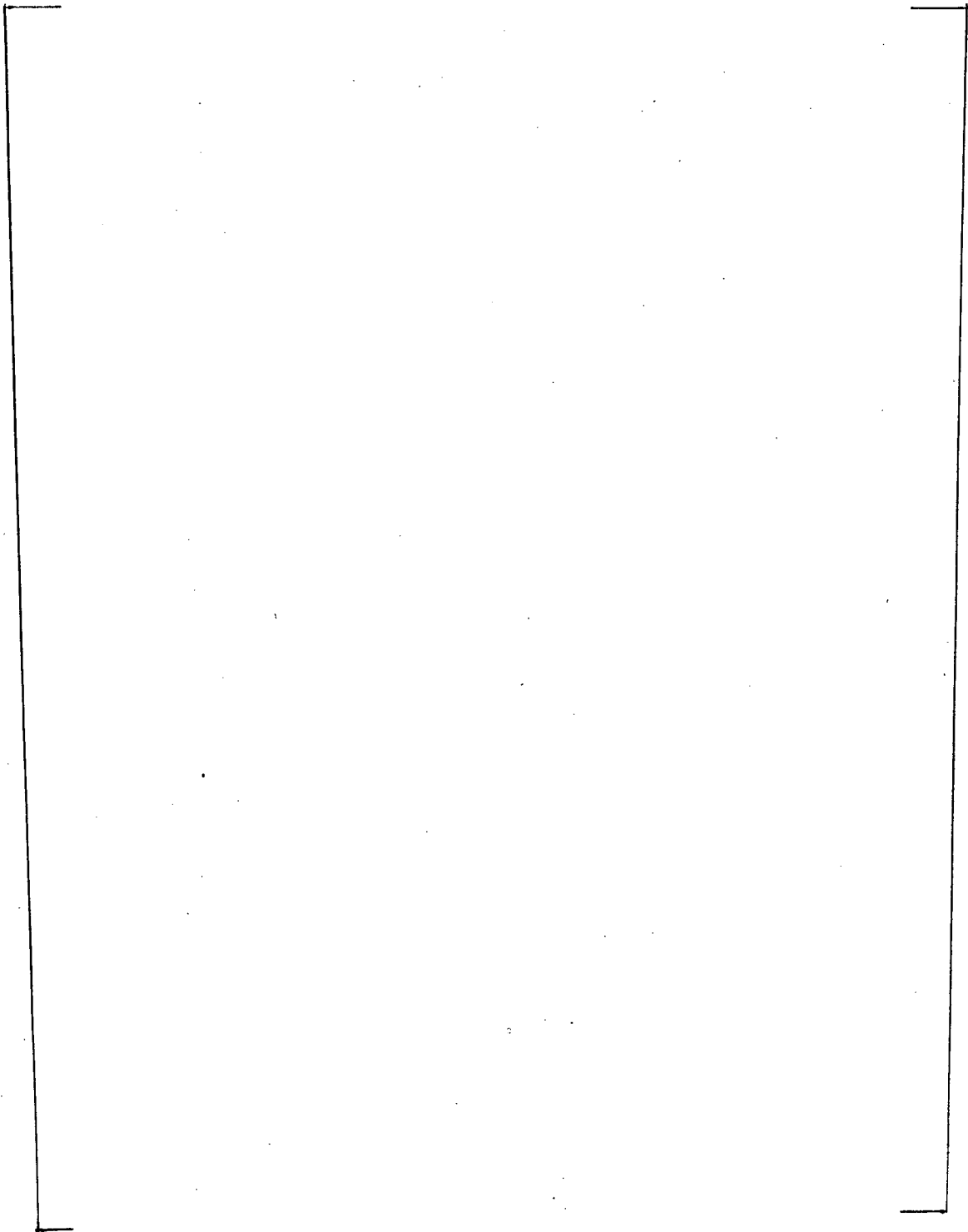


Figure 4-5. Detail of Control Rod Drive Mechanism



a,c

Figure 4-6. Nonlinear Model of the CRDM's Support Platform, Reactor Vessel, and Internals



a,c



Figure 4-7. Nonlinear Model of the CRDM's, Support Platform, Reactor Vessel, and Internals

a,c

[

a,c

The elapsed time for the rod to reach the dashpot is defined as the scramtime, and does not include the electrical signal time-caused tripping devices or the deceleration time while engaging the dashpot.

[

a,c

] The analysis

indicates an insignificant increase in scram time []

[] b,c

Additionally, the dynamic time-history motion of the reactor vessel were imposed on the model and a dynamic analysis was performed in order to evaluate loads and stresses in the mechanism. The most highly stressed section is at the head adapter. Table 4-3 presents the head adapter moment loads and ratios to allowable values. All the loads are acceptable.

TABLE 4-3 HEAD ADAPTER MOMENT LOADS		
	Moment (In-Kip)	% of Allowable
Longest CRDM	[]	[]
Shortest CRDM		

b,c

4-13. REACTOR CORE

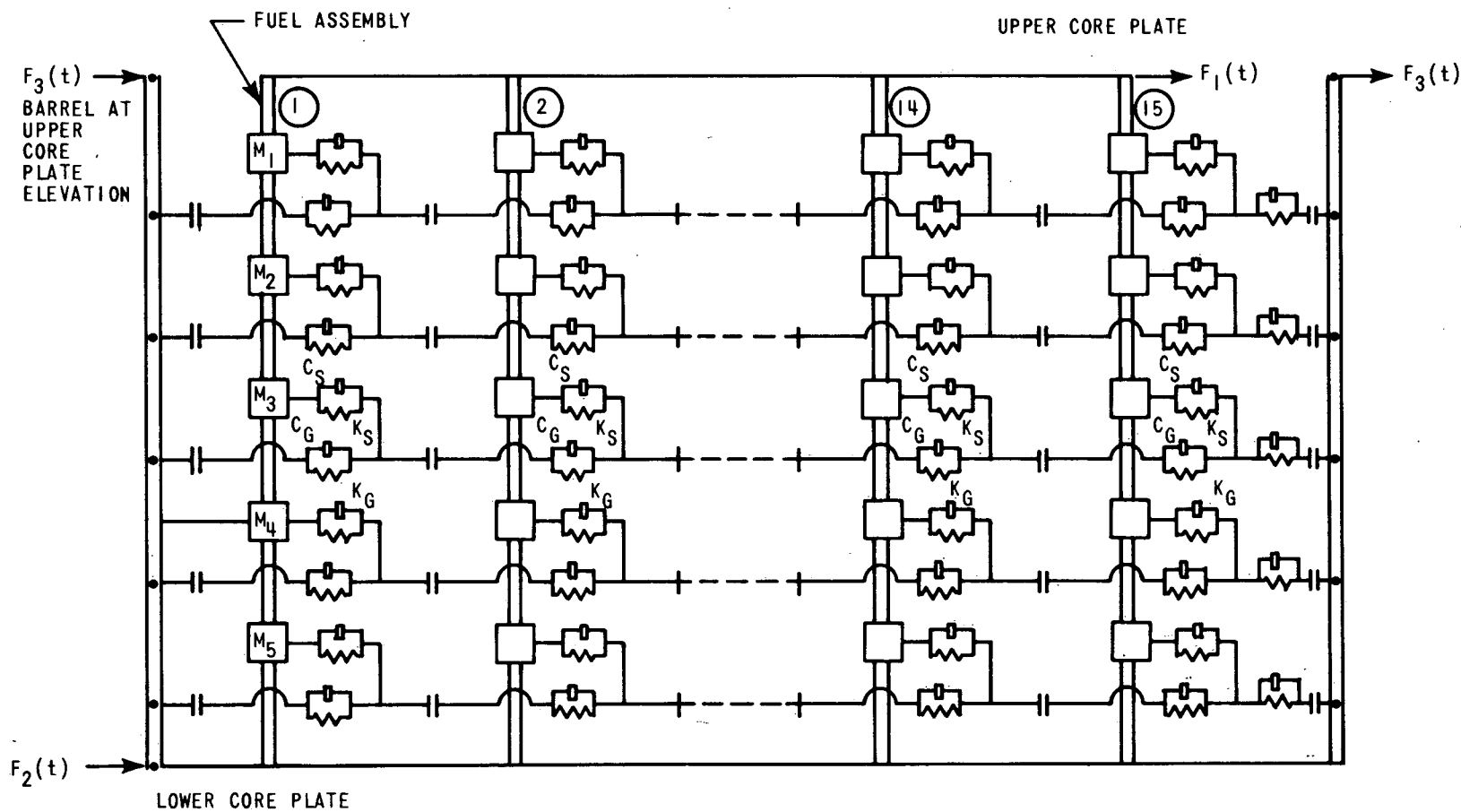
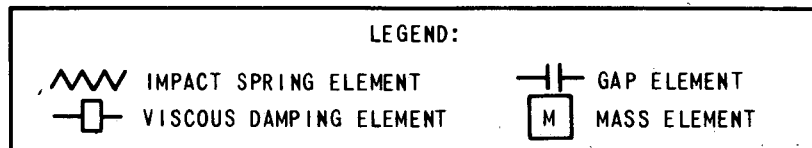
A series of fifteen fuel assembly elements was used to represent the core with the reactor baffle and support represented by a single beam element as indicated (figure 4-8). The Indian Point 3 fuel assembly is a 15 x 15 fuel rod pattern with 7 grids. The time history motions for the upper and lower core plates and the barrel at the upper core plate elevation were obtained from the DARIWOSTAS analysis of the reactor vessel and internals. []

[] a,c

The fuel assembly response, namely, displacements and grid impact forces, was obtained from the reactor core model using the core plate motions. []

[] b,c
] The fuel assembly stresses resulting from this deflection were evaluated and indicate substantial margins compared to the allowable values.

The fuel assembly grid impact forces were also obtained from the reactor core time-history response. The maximum impact force occurs at the peripheral fuel assembly location adjacent to the baffle wall directly opposite the pipe break. The grid impact forces are also rapidly attenuated for fuel assembly positions inward from the outer fuel assemblies. The grid impact force for the peripheral fuel assembly adjacent to the baffle on the pipe break side of the



4-20

Figure 4-8. Schematic Representation of Reactor Core Model

11,487-1

reactor were substantially lower than those on the opposite side of the core. Consequently, only a small portion of the core experiences substantial grid impact forces. []

[] b,c

The minimum load at which permanent deformation occurs was determined by tests performed on several 15 x 15 grids. Dynamic loads were applied to the grids in increasing magnitude until permanent deformation was noted. The grid minimum failure load from the test was [] pounds at room temperature. This must be reduced by [] to correspond to the high temperature environment. The minimum load at temperature is, therefore, approximately [] pounds. b,c

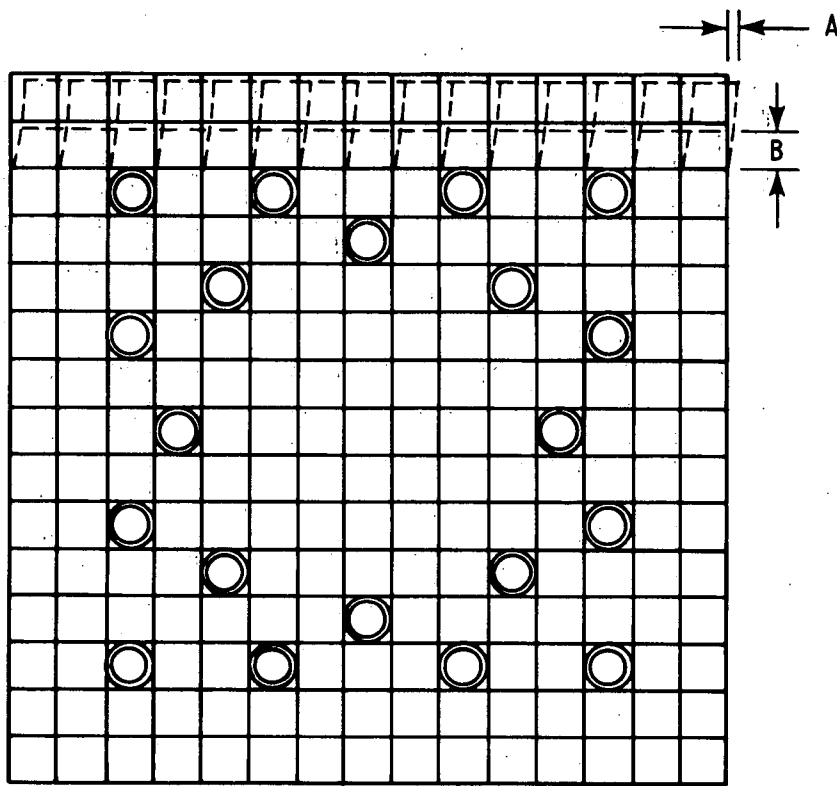
One complete row of the fuel was analyzed. No permanent deformation was experienced for the break at the reactor coolant pump discharge nozzle (maximum load approximately 1800 pounds). For the reactor vessel inlet break, the center grid in the outer assembly experienced an impact load of approximately [] percent greater than the minimum load at which permanent deformation would begin. The grids above and below the center grid in the outer assembly also experienced loads approximately [] percent over the minimum load. The center grid of the second row in from the periphery experienced an impact load approximately [] percent greater than the minimum load required to produce permanent distortion. b,c

All grids in the core except those noted above experienced analytical impact loads which were significantly less than [] pounds. The effect of exceeding [] pounds force on the four grids noted above has been evaluated. The typical deformed grid will have a configuration as shown in figure 4-9. The tests demonstrate that the deformation of the grid is confined to only one row. It has been determined that the maximum reduction in localized flow around the single deformed row will be approximately [] percent [] over the whole assembly). b,c

Further analyses beyond the elastic analysis (used to calculate the above loads) have been performed in which the elastic-plastic load deflection curve for the grids are inserted into the analysis. Results of these studies indicate that the buckling in the second row could most likely be eliminated by more detailed analyses. Although the grid impact loads were reduced, the deformation in the peripheral assemblies was not eliminated. However, the conservative results obtained from the elastic analysis are used in the evaluation of the core.

The effect of these distorted grids on ECCS performance has been evaluated using the October 1975 version of the Westinghouse Evaluation Model. Grid deformation in excess of the maximum observed to date in grid strength testing was postulated to occur in the hot assembly. Assuming that the fuel assembly experiencing permanent grid deformation is in the limiting fuel location in the entire core insures that the maximum peak clad temperature effect is

SCHEMATIC REPRESENTATION OF 15 x 15
TYPICAL GRID DEFORMATION PATTERN



--- INDICATES DEFORMED CONFIGURATION

Figure 4-9. Deformed Grid.

considered. In addition, the ECCS performance of the limiting LOCA break, a double-ended guillotine rupture, is analyzed rather than the 110 square-inches maximum break area at the vessel inlet nozzle. This approach has been adopted even though peak grid impact loads are calculated for the smaller break size (a lower PCT care) in order to upper bound the ECCS impact.

As previously reported⁶, the increase in peak clad temperature (PCT), assuming an upper bound to deformation, equals [] for the limiting discharge coefficient double-ended cold leg guillotine break in a 3-loop plant; a comparable calculation for a 4-loop plant showed a PCT increase of less than [] In light of the conservatism inherent in the above calculations, the effect of grid crushing on the PCT is not significant.

b,c

4-14. REACTOR INTERNALS

Following a LOCA, the plant must be capable of being shutdown and the core cooled in an orderly, safe fashion with the peak fuel cladding temperature kept within the required limits. This requires that following a LOCA, the deformation of the reactor internals be sufficiently small so that core cooling operations are assured. In addition, the allowable stress limits for the core support structures are limited to 2.4 Sm for primary stress intensity and 3.6 Sm for primary membrane plus bending stress intensity.

The evaluation of the reactor internals response following an inlet nozzle break consisted of two parts. The first part was an analysis of the in-plane response occurring in the vertical plane passing through the broken inlet nozzle. This was obtained from the DARIWOSTAS response analysis. The second part of this evaluation was to determine the core barrel shell response that consisted of the various $n = 0, 2, 3$, etc., ring mode responses occurring in the horizontal plane. These ring mode responses were generated as the inlet break rarefaction wave propagated to the core barrel at the inlet nozzle. This subjected the upper barrel to a non-axisymmetric expansion radial impulse that changed as the rarefaction wave propagated both around the barrel and down the outer flow annulus between the barrel and the vessel. From the resulting moment and shear force time-histories, the core barrel beam bending stresses and shear stresses were obtained. The barrel beam stresses were evaluated at the mid-barrel girth weld where the highest stresses in the barrel occur.

For the shell mode analysis of the core barrel, the differential pressures across the core barrel wall and those distributed around the circumference had to be determined. These pressure differences were directly obtained from the blowdown analysis and were applied to the core barrel. It is important to note that, unlike the beam analysis, the shell response of the barrel (the various horizontal ring modes 0, 2, 3, 4, etc.) is independent of the response of the

vessel on its supports, the response of the fuel, or any combination of these beam mode responses. Even though there are various phenomena that may affect vessel beam behavior, there is only one set of barrel shell results to be included in the stress combination. Also included in the core barrel stress evaluation, were the vertical response from the DARIWOSTAS analysis. To properly evaluate the total stress results in the core barrel, the horizontal beam, vertical, and shell modes were combined on a time-history basis.

The maximum stress intensities occurred, as mentioned, in the mid-barrel girth weld where there is a reduced section. The maximum membrane stress intensity was calculated to [] b,c psi and the maximum membrane plus bending stress intensity was [] psi. The allowable stresses based on $2.4 S_m$ and $3.6 S_m$ are 38,900 psi and 58,300 psi. Therefore, the core barrel responds in an acceptable manner for these applied loads.

4-15. PRIMARY SHIELD WALL EVALUATION

The primary shield wall structure was analyzed and was found to be capable of withstanding the loads induced due to the worst case pipe rupture. The loads applied to the structural model included the reactor vessel support reaction loads, tie rod loads and the reactor cavity pressurization loads. The tie rod loads were conservatively taken as the yield strength times the area of the tie rod. Reactor cavity pressurization loads for a 600-square-inch rupture at the reactor vessel inlet nozzle safe end location were used in the analysis. The loads included the nonuniform pressure distribution effect. The pressures for a 600-square-inch-break are more than twice those for the 110-square-inch break and are, therefore, conservative. The analysis was performed using the MARC-CDC computer code. A three dimensional model was used to represent the structure with only one-half of the shield wall modeled due to geometrical symmetry as shown in figure 4-10. The model consisted of 137 elements and 732 nodes. A portion of the 5' 1-1/2"-thick concrete slab at elevation 69' 1-1/2" was modeled. The bottom of the model was at elevation 46' 0" which is the top of the containment structure interior fill slab. The slab at elevation 69' 1-1/2" and the shield wall were modeled using 20 node isoparametric brick elements. For thick shell problems, one element through the thickness has been shown to give good results for both displacement and stress. A total of 96 of the 20 node bricks were used. The steel ring girder embedded on top of the shield wall was modeled using 4 and 8 node isoparametric membrane elements. A total of 37 of the 8 node membranes and 4 of the 4 node membranes were used. The concrete was assumed uncracked and no rebar was modeled. Frictional forces on the vertical bearing plane between the shield wall and ring girder were neglected. The separation of the steel and concrete along this bearing plane was also modeled. The base of the model and the outer edge of the slab were fixed. Along the assumed plane of symmetry either symmetric or antisymmetric boundary conditions were applied depending upon the load case.

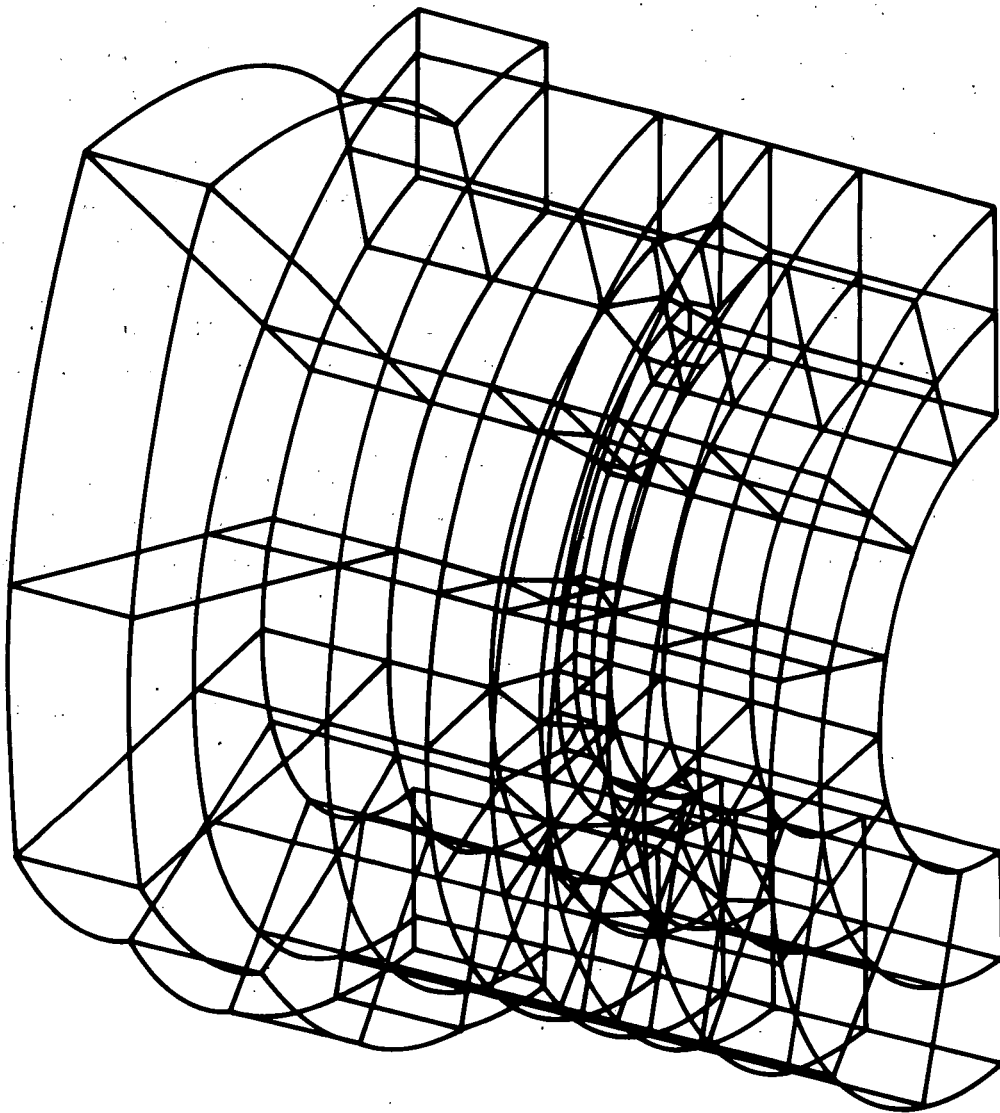


Figure 4-10. Primary Shield Wall Structural Model

The model does not include the primary coolant pipe opening in the primary shield wall since the results could be properly interpreted without this addition to the model.

The resulting membrane and bending loads in the hoop direction were evaluated and found to be well within the capacity of the primary shield wall structure assuming that the rebar absorbs the entire load. It is expected that local yielding would occur near the piping annulus due to the resulting stress concentrations; however, this effect would not significantly alter the overall load carrying capability of the shield wall. The analysis results indicate that the major portion of the pressure load is resisted by membrane and bending action in the hoop direction. The effect of modeling the pipe annulus openings would be to interrupt this load path and cause more load to be resisted in the vertical direction. Therefore, the resulting hoop loads from the analysis are conservative.

Calculations were performed assuming that all pressure loads would be resisted by a concrete beam between the pipe annulus openings. This technique is very conservative since the hoop direction would resist a large portion of the load. The shear from the pressure load and tie rod reaction was checked and found to be within the capacity of the concrete structure. Bending is not a consideration due to the very small span to depth ratio of the assumed vertical beam.

The reactor vessel support reaction loads were included with the pressure and tie rod loads and found to have negligible effect on the primary shield wall stress resultants. The effects of the reaction loads are local in nature. The load carrying capacity of the reactor vessel support structure is higher than the reaction loads; therefore, the reaction loads transmitted by the reactor vessel support shoes are acceptable.

These analyses verify the structural integrity of the primary shield wall for loads and pressures induced by postulated pipe ruptures.

SECTION 5 PLANT MODIFICATIONS

5-1. PLANT MODIFICATION

The following sections discuss proposed modifications to the Indian Point 3 Plant.

5-2. Primary Shield Wall Pipe Restraints

A system of reactor coolant loop pipe restraints has been designed for Indian Point to insure safe shutdown of the plant following a postulated pipe break at a reactor vessel nozzle. These restraints are located on both the hot and cold legs in the primary shield wall annuli. The pipe restraints serve a dual purpose: 1) they minimize the pipe break opening area which also limits pressure buildup on the reactor cavity; [

c,f

]

The pipe restraint (figure 5-1) consists of several bars parallel to the pipe centerline held by a sleeve that fits on the reactor coolant piping. These bars bear against the shield wall pipe liner sleeve to prevent large displacements of the reactor coolant piping. The pipe displacement restraint design will be finalized after field measurements are obtained.

5-3. Reactor Vessel Nozzle Inspection Openings

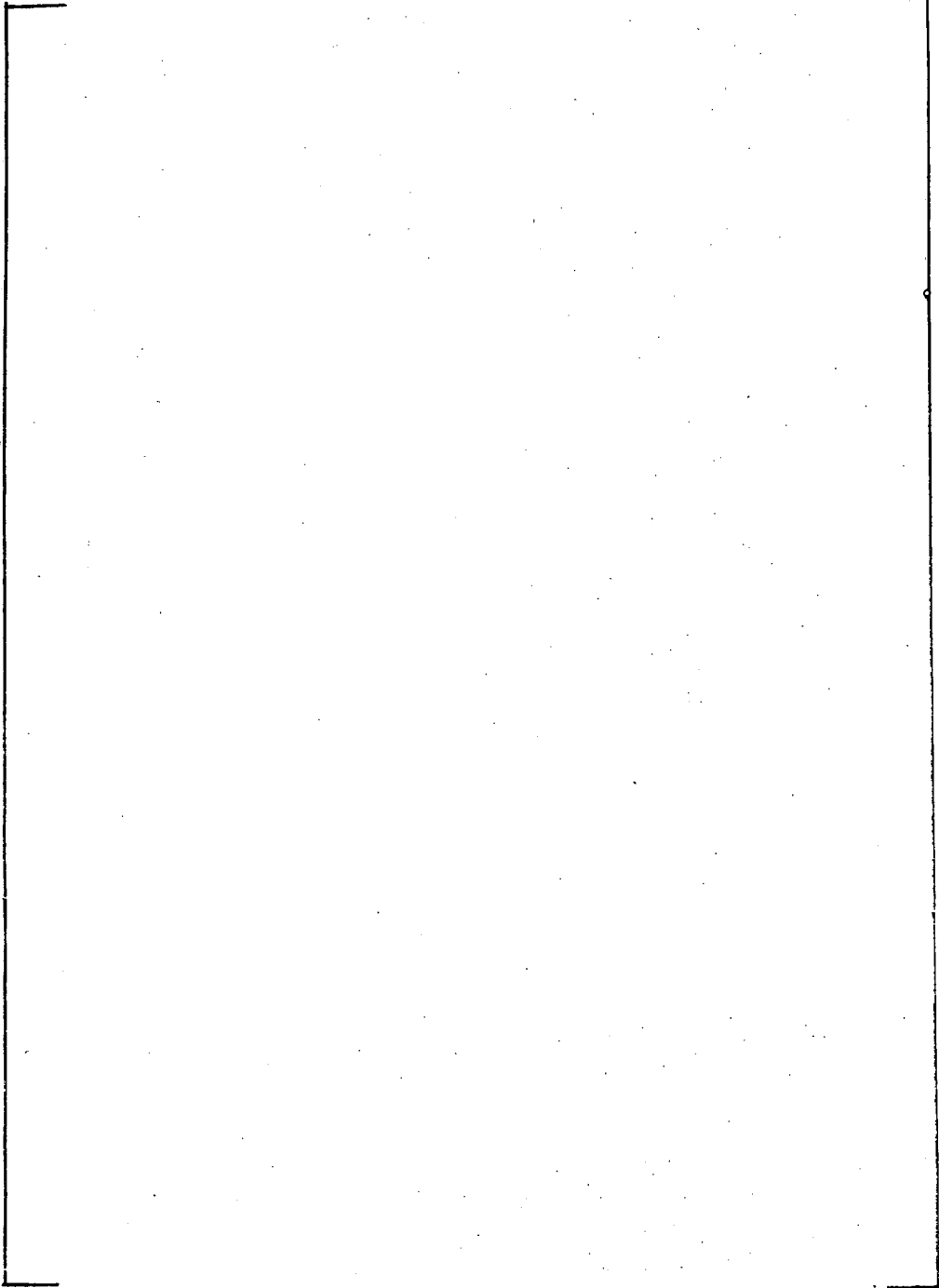
Openings are located in the primary shield wall concrete above each of the reactor vessel nozzle safe ends. The purpose of these openings is twofold: 1) to allow a path to visually inspect the reactor vessel safe end welds; 2) to provide venting for the fluid pressure in the event of a pipe rupture near the openings. Radiation shielding material is placed in the openings to prevent excessive radiation streaming to the containment. The design must be such that the flow path can be developed by the fluid pressure created by a pipe rupture. [

c,f

[

]

]



c,f

Figure 5-1. Pipe Displacement Restraints

SECTION 6 REFERENCES

1. Takeuchi, K., et al., "MULTIFLEX: A FORTRAN-IV Computer Program for Analyzing Thermal-Hydraulic-Structure System Dynamics," WCAP-8708, February 1976. (Westinghouse Proprietary)

Letter NS-CE-1076 from C. Eicheldinger, Westinghouse NES, to D. B. Vassallo, NRC (May 14, 1976).

Letter NS-CE-1099 from C. Eicheldinger, Westinghouse NES, to D. B. Vassallo, NRC (June 9, 1976).

Letter NS-CE-1324 from C. Eicheldinger, Westinghouse NES, to J. F. Stolz, NRC (December 31, 1976).

Letter NS-CE-1308 from C. Eicheldinger, Westinghouse NES, to J. F. Stolz, NRC (December 13, 1976).

Letter NS-CE-1086 from C. Eicheldinger, Westinghouse NES, to D. B. Vassallo, NRC (May 24, 1976).

Letter NS-CE-1140 from C. Eicheldinger, Westinghouse NES, to J. F. Stolz, NRC (July 21, 1976).

Letter NS-CE-1279 from C. Eicheldinger, Westinghouse NES, to J. F. Stolz, NRC (November 12, 1976).

Letter NS-CE-1258 from C. Eicheldinger, Westinghouse NES, to J. F. Stolz, NRC (October 28, 1976).

2. "Documentation of Selected Westinghouse Structural Analysis Computer Codes," WCAP-8252, April 1974.
3. "Ice Condenser Containment Pressure Transient Analysis Methods," WCAP-8077, March 1973. (Westinghouse Proprietary)

4. "Bench Mark Problem Solutions Employed for Verification of WECAN Computer Program," WCAP-8929, June 1977.
5. Appendix F of ASME Boiler and Pressure Vessel Code, Section III, Division 1, Subsection NA, "Rules for Evaluation of Faulted Conditions," American Society of Mechanical Engineers, New York, 1974.
6. Letter NS-CE-1452 from C. Eicheldinger, Westinghouse-NES, to D. F. Ross, NRC (June 10, 1977), Proprietary.

APPENDIX A

BREAK OPENING AREA CALCULATION

APPENDIX A BREAK OPENING AREA DETERMINATION

The break opening area for pipe ruptures postulated at the reactor vessel safe end locations was calculated considering the motion limiting effects of the pipe restraints installed in the primary shield wall pipe annulus. The area first chosen for the generation of the hydraulic loads on the system was based on scoping analyses for this plant. Once the loads resulting from this break opening area were applied to the final model for this plant, the vessel motion was known and the break opening area could be calculated more accurately. This area was the area used in the final analysis.

In determining the area, the movement of the piping and equipment is assumed to be in a worst case configuration. That is, the reactor coolant pump (or steam generator for the vessel outlet nozzle break) is at its maximum displacement away from the reactor vessel, the broken pipe has moved through the gap and into the pipe restraint with the maximum load in the restraint, and the reactor vessel is at its maximum displacement away from the break and at its maximum vertical displacement. The result of this configuration is that the two broken pipe ends are separated the most they could be at any time. This leads to a larger break opening area than realistically anticipated.

Once the motion of the piping and equipment is known, the axial and lateral separations of the broken pipe ends can be calculated by using the geometry of the system. These axial and lateral relative displacements can then be used in calculating the break opening area. The formula for calculating the area of two cylinders displaced axially and laterally from each other is:

$$\text{Area} = 2 \pi R_i \Delta_A + 2 \Delta_A \Delta_L$$

where

R_i = inside pipe radius

Δ_A = axial separation

Δ_L = lateral separation

This formula is applicable only when the lateral separation, Δ_L , is less than the thickness of the pipe, which is true in this case.

The calculation described above resulted in a maximum break opening area for the vessel inlet break and the vessel outlet break of 110 square inches.

The actual displacements of the piping and equipment from the structural analyses are as follows:

RPV Inlet Break

Reactor coolant pump displacement	=	[]	
Pipe displacement at break	=		
Reactor vessel horizontal displacement	=		
Reactor vessel vertical displacement	=		b,c

RPV Outlet Break

Steam generator displacement	=	[]
Pipe displacement at break	=	
Reactor vessel horizontal displacement	=	
Reactor vessel vertical displacement	=	

The axial and lateral separations resulting from the component motion given above are as follows:

RPV Inlet Break

Axial separation	=	[]	b,c
Lateral separation	=	[]	

RPV Outlet Break

Axial separation	=	[]	b,c
Lateral separation	=	[]	

These displacements lead to a break opening area of approximately [] square inches for both the vessel inlet and outlet rupture. Since this area is less than the area used to generate the applied loads, the adequacy of the analysis is verified.

APPENDIX B

REACTOR SUPPORT TEST REPORT

APPENDIX B
INDIAN POINT REACTOR SUPPORT SHOE TEST

A structural test of a one-eighth scale model of the reactor support shoe was undertaken to establish the ultimate load of the shoe assembly, to determine the failure mechanism, and to determine the horizontal stiffness. Both static and dynamic loads were included in the test program. Results indicate that the failure mechanism is shearing of the leveling screws on a plane between the bottom of the reactor shoe and the top cooling plate. The ultimate capacity for the one-eighth scale model, for the same bolt heat treatment, as specified for in the full size bolts used at the site, is [] lbs. The horizontal stiffnesses are obtained from measurements of the force-displacement curves between appropriate points on the test specimen. b,c

Eight complete and separate test specimens were used for the test program. Each specimen included a one-eighth scale structure of the reactor shoe, leveling screws, shim plates, cooling plate, and a portion of the support girder. In addition, a test support structure was designed to provide a stiffness similar to the full support girder. Figure B-2 shows the general arrangement of the test specimen. Materials for the test specimens were selected to match those specified on the drawings.

Table B-1 lists the result of the tests. As shown on the table, several parameters, such as temperature, vertical preload, leveling screw strength were included for the test. The values presented on the table are for the one-eighth scale model. To convert to equivalent full scale values the loads are multiplied by 64.

The tests were run to determine the failure mode, failure load, and horizontal stiffness under various conditions of temperature, preload, load rate, and bolt strength. [

] Temperatures were applied through the reactor pad, and the horizontal load applied after thermal equilibrium occurred. A static preload was applied to the test specimen to account for the system deadweight and vertical component of dynamic loading. Vertical loads were applied to the shoe prior to application of the horizontal load and maintained until failure of the test specimen. [

]



b,c

In addition to the basic testing, a substantial number of supportive tests were made to determine material stress relationships, hardness, friction and bolt shear strength. Results of these tests were used to confirm material specifications.

Figure B-3 shows a typical load-displacement (P- δ) curve. This curve indicates the displacement at the location of the top of the shoe on the loaded side of the pad. Stiffness in pounds/inches determined from the (P- δ) curve are multiplied by eight to obtain an equivalent full scale stiffness.

The test results for the shear failure load agree closely with the ultimate load as determined by static analysis for bolt shear failure. The calculated failure load, based on actual hardened material strength is [] lbs. versus a measured test failure load of [] psi. The load deflection curve, figure B-3, is used to [

a,b,c

a,c

**TABLE B-1
TEST CONDITIONS AND RESULTS**

Test	Temperature	Horizontal Preload Lbs.	Level Screw Ultimate Tensile Stress psi	Horizontal Load & Application	Ultimate Load (lbs)
1	RT	[]
2	RT				
3	500°F				
4	500°F				
5	500°F				
6	500°F				
7	500°F				
8	500°F				

[] b,c

b,c

B-4

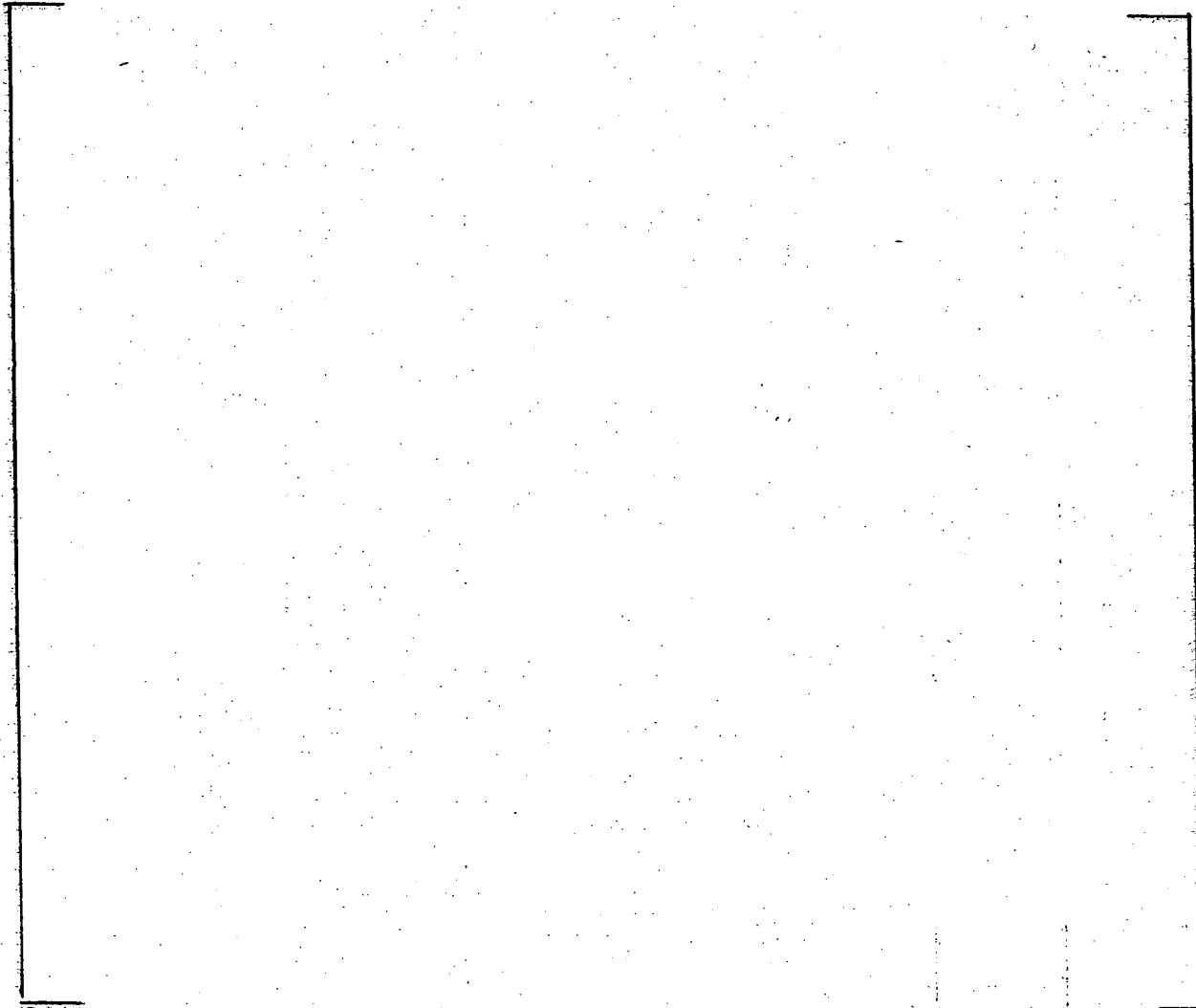
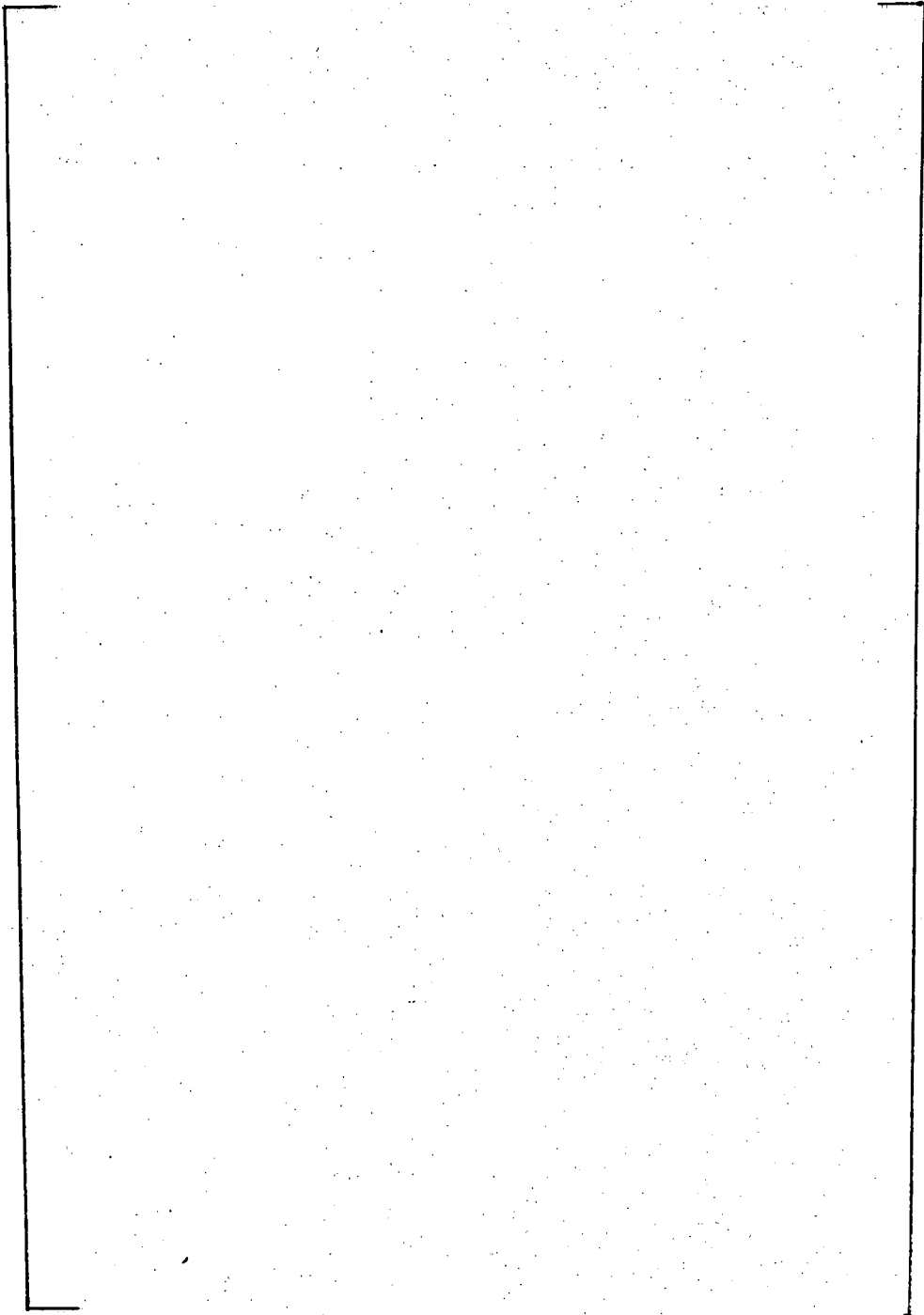


Figure B-1. Test Support Structure



b,c

Figure B-2 Horizontal Load - Horizontal Displacement Curve (LVDT No. 3) RVSS Test of B-7 Specimen with Vertical Preload of 20,000 Lbs. at 550°F Pad Temperature

B-8



b,c

Figure B-3. Fracture of Shoe – Test B-8



APPENDIX C

PLANT GENERAL ARRANGEMENT DRAWINGS

APPENDIX C
PLANT GENERAL ARRANGEMENT DRAWINGS

The following drawings show the reactor coolant system and surrounding concrete general arrangement of Indian Point 3 Nuclear Power Plant.

(The drawings of the reactor coolant system and surrounding concrete general arrangement of Indian Point 3 Nuclear Power Plant are proprietary and have been deleted from this version of the report.)

a,b,c

APPENDIX D
DISCUSSION OF PROCEDURE USED FOR REACTOR
COOLANT LOOP EVALUATION

APPENDIX D
DISCUSSION OF PROCEDURE USED FOR REACTOR
COOLANT LOOP EVALUATION

The material in Appendix D has been deleted, as it is
proprietary.

a,c